UNITED STATES
DEPARTMENT OF THE INTERIOR
GEOLOGICAL SURVEY

CHANGES IN TIDAL FLOW, CIRCULATION, AND FLUSHING CAUSED BY DREDGE AND FILL IN TAMPA BAY, FLORIDA

By Carl R. Goodwin

Open-File Report 84-447

Prepared in cooperation with the
U.S. ARMY CORPS OF ENGINEERS
and the TAMPA PORT AUTHORITY

Tallahassee, Florida
1984

UNITED STATES DEPARTMENT OF THE INTERIOR

WILLIAM P. CLARK, Secretary

GEOLOGICAL SURVEY

Dallas L. Peck, Director

For additional information write to:

District Chief
U.S. Geological Survey
Suite 3015
227 North Bronough Street
Tallahassee, Florida 32301

Copies of this report can be purchased from:

Open-File Services Section
Western Distribution Branch
U.S. Geological Survey
Box 25425, Federal Center
Denver, Colorado 80225
(Telephone: (303) 236-7476)

CONTENTS

ILLUSTRATIONS

TABLES

TABLES--Continued

ABBREVIATIONS AND CONVERSION FACTORS

Factors for converting inch-pound units to International System of Units (SI) and abbreviation of units

Multiply	By	To obtain
foot (ft)	0.3048	meter (m)
mile (mi)	1.609	kilometer (km)
square mile (mi^2)	2.590	square kilometer (km^2)
cubic foot (ft^3)	0.02832	cubic meter (m^3)
cubic yard (yd^3)	0.7646	cubic meter (m^3)
foot per second (ft/s)	0.3048	meter per second (m/s)
mile per hour (mi/h)	1.609	kilometer per hour (km/h)
pound per second (lb/s)	0.4536	kilogram per second (kg/s)
pound per day (lb/d)	0.4536	kilogram per day (kg/d)
square foot per second (ft^2/s)	0.09290	square meter per second (m^2/s)
cubic foot per second (ft^3/s)	0.02832	cubic meter per second (m^3/s)
foot per square second (ft/s^2)	0.3048	meter per square second (m/s^2)
pound per square foot (lb/ft^2)	4.882	kilogram per square meter (kg/m^2)
slug (lb s^2/ft4)	14.59	kilogram (kg)
micromho per centimeter at 25°C (umho/cm)	1.000	microseimens per centimeter at 25°C (uS/cm)

* * * * * * * * * * * * *

National Geodetic Vertical Datum of 1929 (NGVD of 1929).--A geodetic datum derived from a general adjustment of the first-order level nets of both the United States and Canada, formerly called mean sea level.

* * * * * * * * * * * * *

CHANGES IN TIDAL FLOW, CIRCULATION, AND FLUSHING CAUSED BY DREDGE AND FILL IN TAMPA BAY, FLORIDA

By Carl R. Goodwin

ABSTRACT

Tampa Bay, Florida, has undergone extensive physical changes between 1880 and 1972 due to construction of causeways, islands, channels, and shoreline fill. These changes have caused a progressive reduction in the quantity of water that enters and leaves the bay due to tidal action. Dredged and filled areas have also changed the magnitude and direction of tidal flows in large parts of the bay.

A two-dimensional, finite-difference, hydrodynamic model was used to simulate changes in both tidal and residual water and constituent transport caused by physical changes to the bay between 1880 and 1972. The calibrated and verified model was also used to simulate changes that will result from a major Federal dredging project that is scheduled for completion in 1985.

Computed transport changes due to the Federal dredging project were much less areally extensive than corresponding transport changes due to construction in Tampa Bay between 1880 and 1972. Changes of more than 50 percent in computed flood and ebb transports, due to the Federal dredging project, were found over only 8 square miles of the bay's 390-square-mile surface area. Similar changes, due to construction between 1880 and 1972, were computed to occur over 58 square miles of the bay. Changes of more than 50 percent in computed residual transport, due to the Federal dredging project, were found over 57 square miles of the bay. Similar changes, due to construction between 1880 and 1972, were computed over 167 square miles.

Computations reveal historical tide-induced circulation patterns consisting of a series of about 20 interconnected circulatory features that range in diameter from 1 to 6 miles. Changes in size, position, shape, and intensity of these features, caused by dredge and fill construction, were found to increase tide-induced circulation and flushing throughout most or the bay. As a result of past and projected physical changes, the bay can and will more rapidly transfer waterborne constituents that have landward sources to the Gulf of Mexico. Conversely, the bay can and will more rapidly transfer constituents that have their source in the Gulf into the upper parts of the bay.

The bay was subdivided into eight zones based on circulation characteristics. Zones near the entrances to Tampa Bay and the major bay subunits, Hillsborough Bay and Old Tampa Bay, were found to have several times greater average circulation than adjacent and more landward zones. Circulation generally decreased from the Gulf of Mexico to the head of Hillsborough and Old Tampa Bays with a striking exception in mid-Tampa Bay. A 9-mile section of the bay was found to have significantly lower average circulation than that of adjacent zones, particularly for conditions in 1880. This section of the bay is thought to have been a circulation constriction that reduced the potential transport of dissolved and suspended constituents.

Circulation in the constricted section was computed to increase 6 percent due to dredge and fill construction between 1880 and 1972. Another 21 percent increase due to the Federal dredging project was also computed. With these increases, the zone acts as less of a constriction than it did in 1880. This and other circulation increases may have contributed to increased bay salinity and more rapid flushing of constituents from the bay to the Gulf of Mexico.

INTRODUCTION

Dredge, fill, and other construction activities have created many physical features in Tampa Bay that were not present prior to about 1880. These features include tens of miles of ship channels, many square miles of islands and submerged dredged-material disposal sites, four major bridges and causeways that span the bay, and numerous residential and commercial shoreline landfills. Most construction occurred between 1880 and 1972 with peak activity in the 1950's and 60's. Prior to this study, the cumulative impacts that these features have had on movement of water and waterborne constituents in the bay were not well understood, and impacts of proposed future physical changes could not be anticipated or compared with past changes.

A Federal dredging project to widen and deepen the main ship channel in Tampa Bay was started in 1976. By 1985, the anticipated end of the project, approximately 70 million cubic yards of bay bottom will have been moved and deposited as large islands or in submerged disposal areas along the 35-mile channel. Prior to the start of dredging, the magnitude of the project and lack of information regarding possible changes in tidal flow, circulation, and flushing caused considerable concern regarding potential adverse environmental effects. A need for predictive and comparative information on flow, circulation, and flushing was recognized.

Changes in water circulation can have an impact on the health and well-being of estuaries. In general, increases in estuarine circulation result in more rapid net movement of

dissolved and suspended constituents from regions of high concentration to regions of low concentration. Changes in circulation in an estuary, therefore, can cause long-term changes to the distribution and concentration levels of all waterborne material.

Long-term changes in many physical, chemical, and biological properties of estuarine water can induce ecological shifts that may destroy natural checks and balances within estuaries that have evolved over many hundreds or thousands of years. Recognition of potential ecological shifts due to unknown circulation changes caused by dredge and fill led to this study. The study was undertaken by the U.S. Geological Survey, initially in cooperation with the Tampa Port Authority and subsequently in cooperation with the U.S. Army Corps of Engineers.

Purpose and Scope

The effects of dredge and fill on tidal flow, circulation, and flushing in Tampa Bay are addressed in this study.

The objectives were:

1. To develop methods by which changes in tidal flow, circulation, and flushing due to physical changes to estuaries can be quantified and compared;
2. To determine tidal flow, circulation, and flushing changes caused by the cumulative impact of construction in Tampa Bay from 1880 to 1972, prior to a large Federal dredging project to widen and deepen the main ship channel in Tampa Bay;
3. To determine tidal flow, circulation, and flushing changes between 1972 and 1985 caused by the Federal dredging project; and
4. To compare and evaluate tidal flow, circulation, and flushing changes caused by the Federal dredging project and all prior construction in Tampa Bay.

The circulation mechanism investigated in this report is a tidal "pumping" action caused by interaction between tidal flow and irregular bottom configuration (Fischer and others, 1979). If tidal inflow (flood) and tidal outflow (ebb) patterns in an estuary are exactly the same and other flow-inducing mechanisms are not operating, a water parcel would return to the same position after a tidal cycle that it occupied at the start of the cycle. If flood and ebb patterns differ, the water parcel would not return to its initial position, but be displaced by some distance from its starting position. The net displacement of every water parcel over successive tidal cycles is a result of

circulation caused by tidal "pumping." Different flood and ebb-flow patterns are caused by irregular physical dimensions of an estuary that include its general shape and bottom configuration and the size and shape of islands, peninsulas, channels, shoals, and marshes.

Circulation and flushing in estuaries can be influenced by physical alterations created by channels, islands, causeways, and shoreline dredge and fill areas. The nature and extent of this influence can be investigated by application of computer simulation techniques.

This report is intended to convey information on:

1. Computer simulation modeling of tidal flow, circulation, and flushing in estuaries, and
2. Tidal flow, circulation, and flushing changes in Tampa Bay due to dredge and fill.

Methodology

To meet study objectives, detailed hydrodynamic simulation models of water and constituent motion were created for three levels of development in Tampa Bay. The levels represent (1) conditions that existed in 1880 before any significant alterations were made to the bay, (2) conditions that existed in 1972 before start of the recent ship-channel dredging, and (3) conditions that are expected to exist in 1985 after completion of ship-channel dredging. Results from the models were analyzed and compared by using vector maps, vector change maps, and circulation and flushing summary diagrams to determine the nature and degree of changes in tidal flow, circulation, and flushing between the 1880, 1972, and 1985 levels of development.

Because study conclusions depend on numerical simulations of water and constituent motion in Tampa Bay, effort was directed to develop a close match between (1) measured physical dimensions of the bay and their numerical representation in the model and (2) other measurable phenomena and corresponding model computations. Bathymetric field measurements were made to supplement available depth information. Measurements of water levels were made at many sites along the bay's shoreline. The magnitude and direction of tidal currents were measured at several sites within the bay. Constituent motion, in the form of turbidity plumes, was obtained from satellite imagery.

Description of Study Area

Tampa Bay is a shallow, Y-shaped embayment along the west-central coast of peninsular Florida (fig. 1), one of the most rapidly growing regions of the State. The bay occupies parts of Hillsborough, Manatee, and Pinellas Counties and is bordered by the major cities of Tampa, St. Petersburg, Clearwater, and Bradenton. The population of the three-county area in 1982 was approximately 1.6 million with a growth rate of about 42,000 residents yearly since 1970 (Thompson, 1980).

Tampa Bay has a total surface area of about 390 mi^2 (Lewis and Whitman, in press) and is the largest estuary in Florida. Its average depth is about 12 feet. The maximum depth, about 90 feet, is off the northern tip of Egmont Key at the mouth of Tampa Bay.

The Tampa Bay area has a subtropical climate that is characterized by long, warm, humid summers and mild winters. Total rainfall averages about 53 inches per year (Heath and Conover, 1981). More than half of the rainfall occurs from June through September, primarily from thunderstorms.

Tributary inflow to Tampa Bay averages about 1,900 ft^3/s mainly from the Hillsborough, Alafia, Little Manatee, and Manatee Rivers. Tributary inflow, municipal and industrial discharge, and runoff from adjacent urban and agricultural basins into the bay contain a variety of dissolved and suspended organic and inorganic constituents. Many constituents settle to the bottom of the bay and are subject to benthic processes. Some constituents, however, remain dissolved and are distributed by tide-induced water circulation throughout the bay. The dissolved constituents undergo various chemical and biological processes before they are flushed into the Gulf of Mexico.

Seasonal variations in freshwater runoff cause measurable changes in the concentration and distribution of salinity and other constituents in bay waters (Goetz and Goodwin, 1980, p. 20). However, tide and wind actions combine to inhibit formation of salinity differences with depth under most conditions. The bay is predominantly vertically well mixed and has little density stratification.

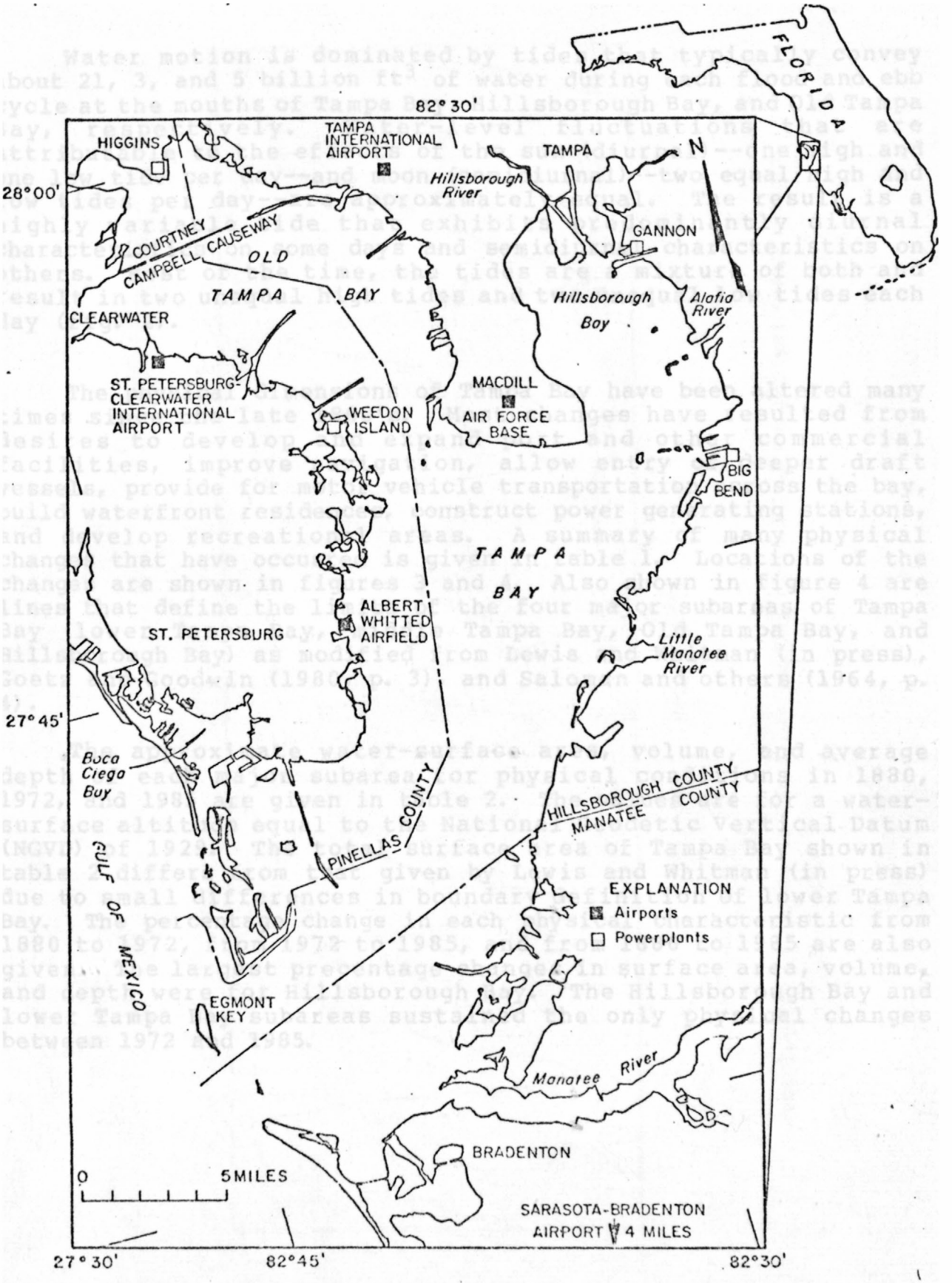

Figure 1.--Location of Tampa Bay study area.

Water motion is dominated by tides that typically convey about 21, 3, and 5 billion ft^3 of water during each flood and ebb cycle at the mouths of Tampa Bay, Hillsborough Bay, and Old Tampa Bay, respectively. Water-level fluctuations that are attributable to the effects of the sun (diurnal)--one high and one low tide per day--and moon (semidiurnal)--two equal high and low tides per day--are approximately equal. The result is a highly variable tide that exhibits predominantly diurnal characteristics on some days and semidiurnal characteristics on others. Most of the time, the tides are a mixture of both and result in two unequal high tides and two unequal low tides each day (fig. 2).

The physical dimensions of Tampa Bay have been altered many times since the late 1800's. Most changes have resulted from desires to develop and expand port and other commercial facilities, improve navigation, allow entry of deeper draft vessels, provide for motor vehicle transportation across the bay, build waterfront residences, construct power generating stations, and develop recreational areas. A summary of many physical changes that have occurred is given in table 1. Locations of the changes are shown in figures 3 and 4. Also shown in figure 4 are lines that define the limits of the four major subareas of Tampa Bay (lower Tampa Bay, middle Tampa Bay, Old Tampa Bay, and Hillsborough Bay) as modified from Lewis and Whitman (in press), Goetz and Goodwin (1980, p. 3), and Saloman and others (1964, p. 4).

The approximate water-surface area, volume, and average depth of each major subarea for physical conditions in 1880, 1972, and 1985 are given in table 2. The values are for a water-surface altitude equal to the National Geodetic Vertical Datum (NGVD) of 1929. The total surface area of Tampa Bay shown in table 2 differs from that given by Lewis and Whitman (in press) due to small differences in boundary definition of lower Tampa Bay. The percentage change in each physical characteristic from 1880 to 1972, from 1972 to 1985, and from 1880 to 1985 are also given. The largest precentage changes in surface area, volume, and depth were for Hillsborough Bay. The Hillsborough Bay and lower Tampa Bay subareas sustained the only physical changes between 1972 and 1985.

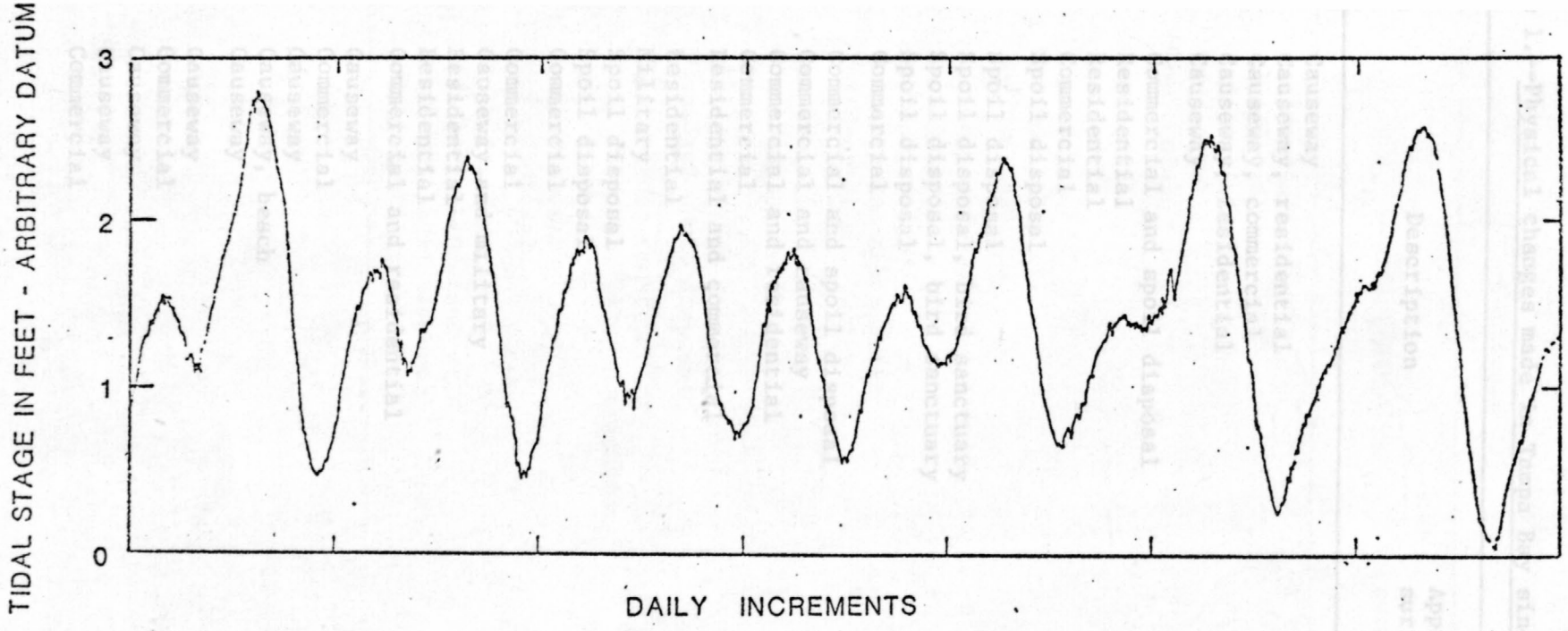

Figure 2.--Typical tides in Tampa Bay showing diurnal and semidiurnal characteristics.

Table 1.--Physical changes made in Tampa Bay since 1880

Index No. (figs. 3 and 4)	Description	Approximate surface area (mi^2)
1	Causeway	0.04
2	Causeway, residential	.07
3	Causeway, commercial	.13
4	Causeway, residential	.14
5	Causeway	.22
6	Commercial and spoil disposal	.15
7	Residential	.14
8	Residential	.59
9	Commercial	.76
10	Spoil disposal	.11
11	Spoil disposal	.06
12	Spoil disposal, bird sanctuary	.02
13	Spoil disposal, bird sanctuary	.04
14	Spoil disposal	.05
15	Commercial	.05
16	Commercial and spoil disposal	.23
17	Commercial and causeway	.86
18	Commercial and residential	1.56
19	Commercial	.23
20	Residential and commercial	.30
21	Residential	1.18
22	Military	.12
23	Spoil disposal	.24
24	Spoil disposal	.03
25	Commercial	.08
26	Commercial	.23
27	Causeway and military	.11
28	Residential	.18
29	Residential	.25
30	Commercial and residential	.03
31	Causeway	.13
32	Commercial	.06
33	Causeway	.02
34	Causeway, beach	.19
35	Causeway	.17
36	Causeway	.09
37	Commercial	.15
38	Causeway	.54
39	Causeway	.20
40	Commercial	.27

Table 1.--Physical changes made in Tampa Bay since 1880
--Continued

Index No. (figs. 3 and 4)	Description	Approximate surface area (mi^2)
41	Residential	0.12
42	Residential	.12
43	Residential	.10
44	Commercial	.08
45	Commercial	.23
46	Commercial	.03
47	Residential	.09
48	Causeway	.13
49	Residential	.43
50	Residential	.40
51	Causeway and residential	.40
52	Residential	.39
53	Residential	.36
54	Causeway and residential	.29
55	Residential	.21
56	Residential	.04
57	Causeway and residential	.79
58	Causeway	.19
59	Causeway	.19
60	Submerged spoil disposal	8.59
61	Ship-channel construction	4.69
62	Spoil disposal, beach nourishment	.16
63	Spoil disposal	.81
64	Spoil disposal	.02
65	Spoil disposal	.02
66	Spoil disposal	.98
67	Circulation-inducing cuts	.47
68	Submerged spoil disposal	3.12
69	Ship-channel widening	.94

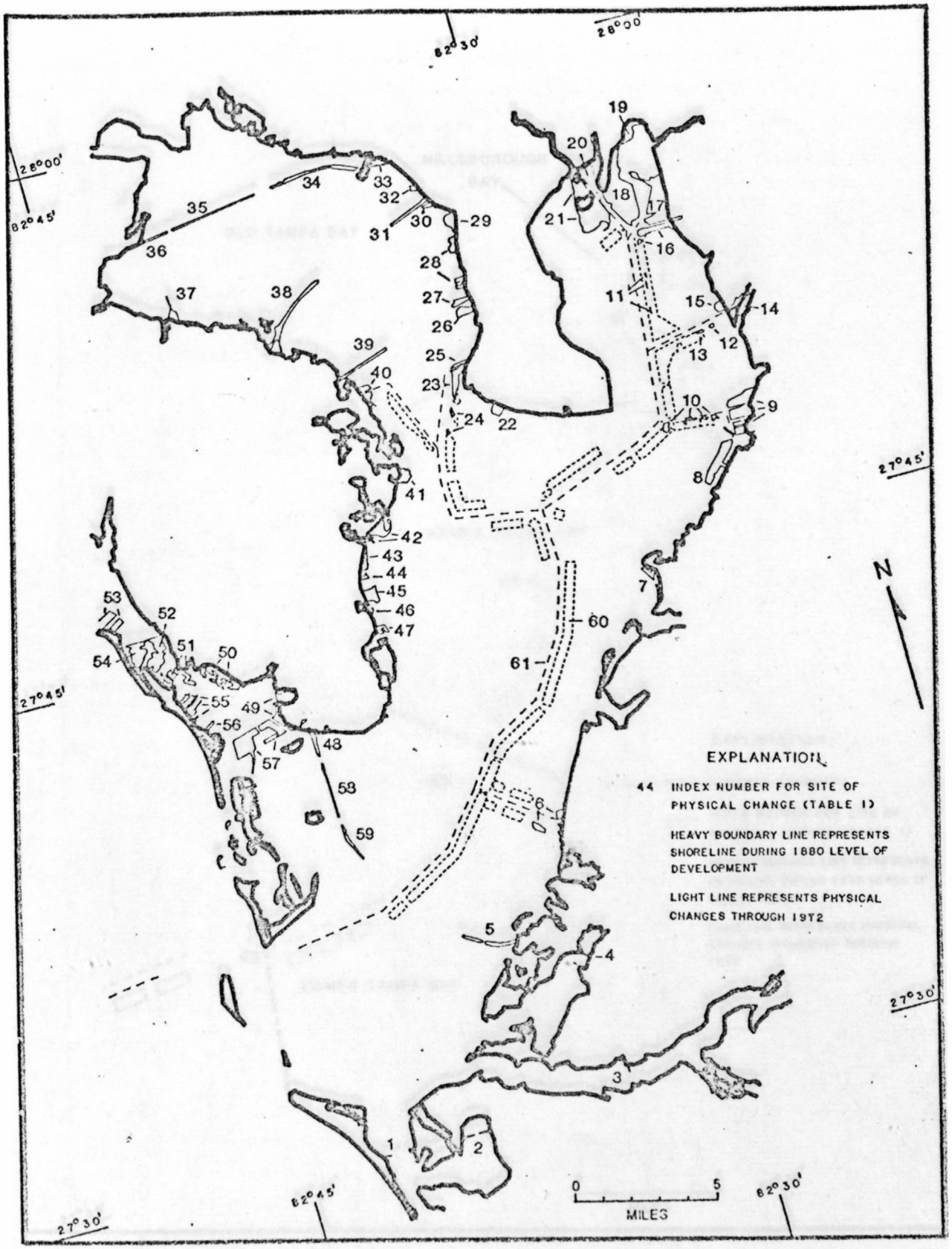

Figure 3.--Locations where physical changes have been made to Tampa Bay between 1880 and 1972.

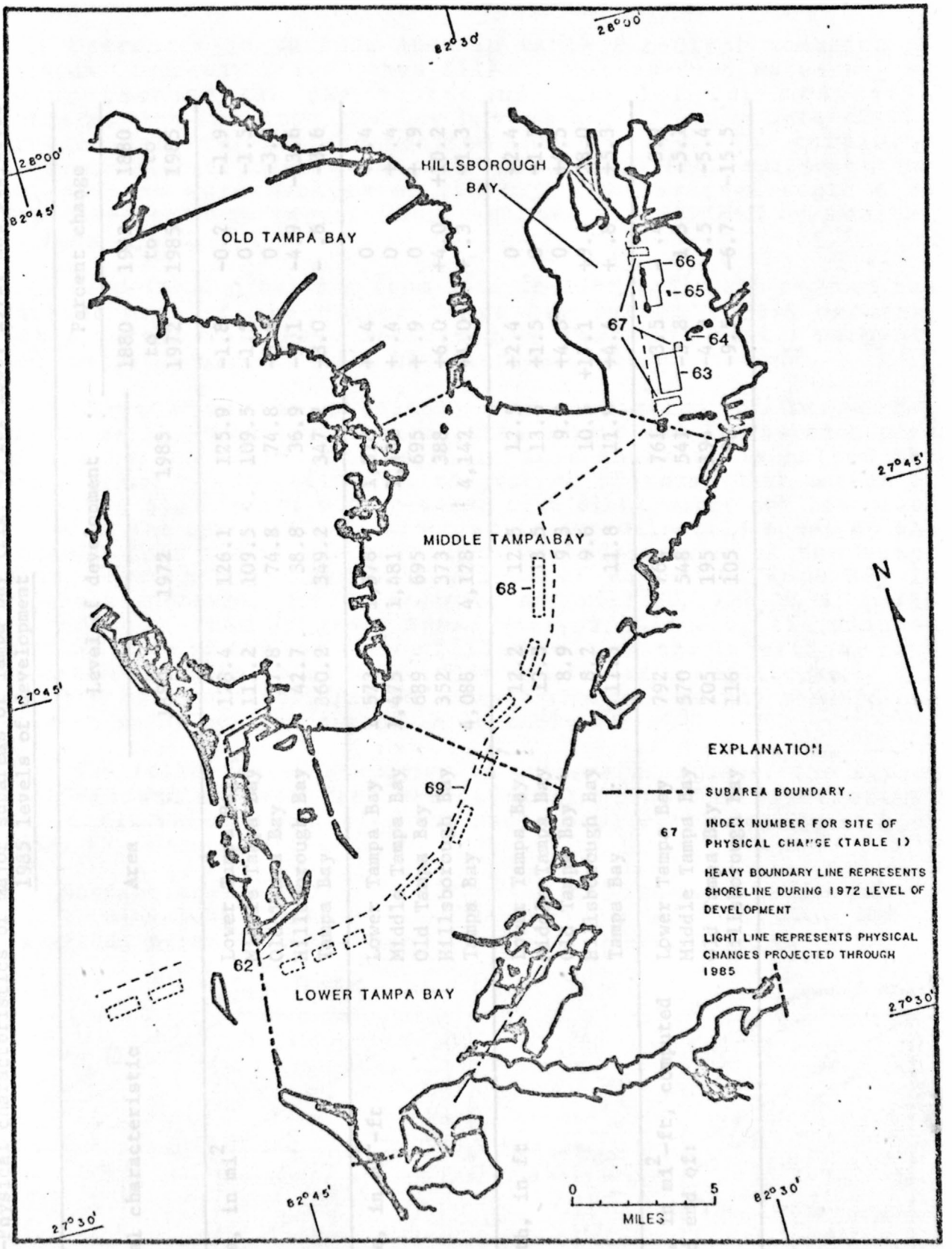

Figure 4.--Locations of major subareas and areas of physical change projected for Tampa Bay between 1972 and 1985.

Table 2.--Physical characteristics of major subareas of Tampa Bay (fig. 4) for 1880, 1972, and projected 1985 levels of development

Physical characteristic	Area	Level of development			Percent change		
		1880	1972	1985	1880 to 1972	1972 to 1985	1880 to 1985
Surface area, in mi^2	Lower Tampa Bay	128.4	126.1	125.9	-1.8	-0.2	-1.9
	Middle Tampa Bay	111.2	109.5	109.5	-1.5	0	-1.5
	Old Tampa Bay	77.8	74.8	74.8	-3.8	0	-3.8
	Hillsborough Bay	42.7	38.8	36.9	-9.1	-4.9	-13.6
	Tampa Bay	360.2	349.2	347.2	-3.0	- .6	-3.6
Water volume, in mi^2-ft	Lower Tampa Bay	1,572	1,578	1,578	+ .4	0	+ .4
	Middle Tampa Bay	1,475	1,481	1,481	+ .4	0	+ .4
	Old Tampa Bay	689	695	695	+ .9	0	+ .9
	Hillsborough Bay	352	373	388	+6.0	+4.0	+10.2
	Tampa Bay	4,088	4,128	4,142	+1.0	+ .3	+1.3
Average depth, in ft	Lower Tampa Bay	12.2	12.5	12.5	+2.4	0	+2.4
	Middle Tampa Bay	13.3	13.5	13.5	+1.5	0	+1.5
	Old Tampa Bay	8.9	9.3	9.3	+4.5	0	+4.5
	Hillsborough Bay	8.2	9.6	10.5	+17.1	+9.4	+28.0
	Tampa Bay	11.3	11.8	11.9	+4.4	+ .8	+5.3
Tidal prism, in mi^2-ft, computed at seaward end of:	Lower Tampa Bay	792	764	761	-3.5	- .4	-3.9
	Middle Tampa Bay	570	548	541	-3.8	-1.3	-5.1
	Old Tampa Bay	205	195	194	-4.9	- .5	-5.4
	Hillsborough Bay	116	105	98	-9.5	-6.7	-15.5

Decreases in surface area in table 2 reflect creation of islands, causeways, and other fills. Increases in water volume occur because (1) the source of material for most fill construction was from the bay bottom and (2) only part of the dredged material was redeposited into the bay. The remaining dredged material became new emergent upland and represents the net gain in water volume of the bay. The average depth also increased because larger water volumes are divided by smaller surface areas.

Dredging and filling from 1880 to 1985 will have reduced the surface area of the entire Tampa Bay system by 3.6 percent. Water volume will have increased in Tampa Bay by 1.3 percent, and the average depth will have increased by 5.3 percent.

Changes to the physical characteristics of Tampa Bay influence the quantity of water that enters and leaves each part of the bay on every tidal cycle. This quantity is called the tidal prism and is defined as the volume of water that enters or leaves a tidal water body between high slack water and low slack water at the entrance. Tidal prism is approximately equal to the surface area times a representative tidal range of the water body. Even though the total volume of water in Tampa Bay is slightly increased due to dredging and filling, the tidal prism is reduced. This apparent anomaly is explained by the reduced surface area of the bay due to filling within the intertidal zone (between the limits of high tide and low tide altitudes). The tidal prism and associated percentage changes at the seaward end of each major subarea are given in table 2.

The following sketch shows an extreme example of the impact that reduced surface area has on tidal prism for hypothetical prismatic estuaries having the same total water volume at high tide.

Surface area = 2AC
Total volume = ABC
Tidal prism = 2aAC

Surface area = AC
Total volume = ABC
Tidal prism = aAC

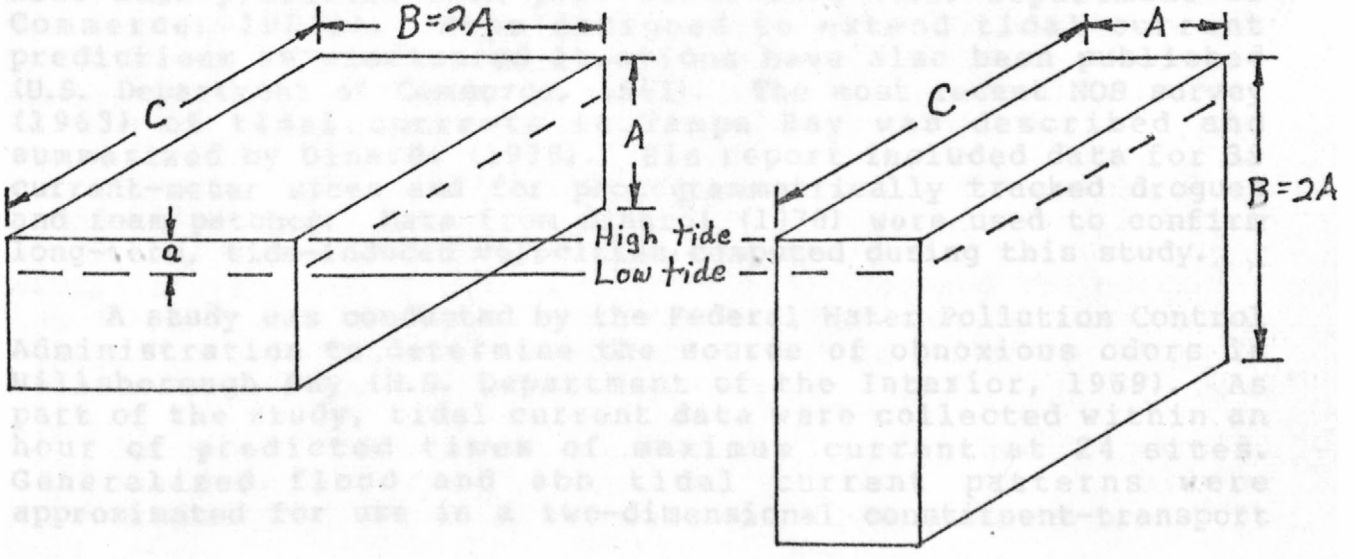

Tidal prism reductions from 1880 to 1985 are expected to be 3.9 percent at the seaward end of lower Tampa Bay, 5.1 percent at the seaward end of middle Tampa Bay, 5.4 percent for Old Tampa Bay, and 15.5 percent for Hillsborough Bay. These changes mean that one effect of dredge and fill construction is that overall tidal exchange throughout the bay is reduced, and consequently, there is less potential for tidal mixing and flushing. Modeling results from this study will show that dredge and fill also cause circulation increases that more than overcome the effects of reduced flushing potential in most parts of Tampa Bay.

Previous Studies

This report follows a series of previous investigations that were either directly or indirectly concerned with tidal effects in Tampa Bay. As background and reference information, many of these studies are briefly described and discussed herein.

Studies of tidal motion in Tampa Bay were first undertaken by the National Ocean Service (NOS), formerly the U.S. Coast and Geodetic Survey, as part of its mission to chart the coastline of the United States. Because water depths are measured from a constantly changing water surface, it is essential to the chart-making process to reference water-surface altitudes to a meaningful navigational datum, normally mean lower low water (MLLW). MLLW is defined as the average of the lowest low-water height of each tidal day observed over a tidal epoch of 18.6 years. Shorter periods of observation must be corrected by comparison with simultaneous observations at a long-term control station. Tidal stage data were first collected by NOS in Tampa Bay in 1878. A continuous recording tide gage has been operating at St. Petersburg since 1947.

Analyzing tide data in terms of its harmonic constituents, the NOS has predicted tides (U.S. Department of Commerce, 1982a) each year since 1939. Tidal currents at selected locations have also been predicted each year since 1950 (U.S. Department of Commerce, 1982b). Maps designed to extend tidal current predictions to unmeasured locations have also been published (U.S. Department of Commerce, 1951). The most recent NOS survey (1963) of tidal currents in Tampa Bay was described and summarized by Dinardi (1978). His report included data for 39 current-meter sites and for photogrammetrically tracked drogues and foam patches. Data from Dinardi (1978) were used to confirm long-term, tide-induced velocities computed during this study.

A study was conducted by the Federal Water Pollution Control Administration to determine the source of obnoxious odors in Hillsborough Bay (U.S. Department of the Interior, 1969). As part of the study, tidal current data were collected within an hour of predicted times of maximum current at 24 sites. Generalized flood and ebb tidal current patterns were approximated for use in a two-dimensional constituent-transport

model having 40 segments or cells. Little information was given regarding tidal circulation and flushing in Hillsborough Bay.

In two master's theses done at the University of South Florida, R. D. Ghioto (written commun., March, 1978) and D. H. Cote (written commun., June, 1973) developed and applied a two-dimensional, hydrodynamic model of tidal flow in Tampa Bay that was based on an algorithm by Reid and Bodine (1968). Residual tidal current patterns were determined by Cote by integrating tidal currents at each 1/2-mile grid site over a 14-day lunar tidal cycle. The resulting vector map indicated that several gyres or net rotational features existed in the bay that appeared to contribute to bay circulation and flushing characteristics. Results from a similar model reported by Ross (1973) showed a different gyre pattern than that computed by Cote. Such differences confirm that circulation and residual tidal current computations are sensitive to one or more of the following items.

1. Choice of hydrodynamic model;
2. Schematization of bottom configuration;
3. Grid size;
4. Location of seaward boundary; and
5. Choice of tidal boundary function.

It is important to note that there are no fixed patterns of circulation in any estuary. Fischer and others (1979) point out that circulation is an ever-changing quantity that evolves in response to changing tide, wind, and other driving forces. Determination of a truly representative or average circulation pattern must be deferred until exhaustive measurements and computations are undertaken. Until then, reasonable estimates of representative conditions will differ because of computational sensitivity to the above items.

This study extends the work of Ghioto (written commun., 1973), Cote (written commun., 1973), and Ross (1973) in several ways. Special emphasis is given to model calibration and verification. Observed and computed data are closely matched to assure that model computations represent conditions in the real system. The modeled area in this study is significantly larger so that interactions between Tampa Bay and the Gulf of Mexico can be studied. Also, the entire bay is modeled at a finer grid size to provide greater resolution of circulation features.

Computer studies of tidal mixing in upper Old Tampa Bay were conducted at the University of South Florida by Ross and Anderson (1972). A two-dimensional, hydrodynamic model was developed having a grid size of 1/4 mile. The model covered the northerly two-thirds of the bay. A novel method was used to measure changes in flushing characteristics caused by various alteration options to the Courtney Campbell Causeway.

Goodwin (1977) compared computed residual tidal currents in Hillsborough Bay for islands of various configurations constructed from materials dredged from the ship channel. He

concluded that circulation patterns could be modified by changes in island configurations, but that little potential existed for improving overall circulation between waters of Hillsborough Bay and Tampa Bay. Preliminary circulation results from a detailed model of Hillsborough Bay (Goodwin, 1980) showed complex net tidal currents that had not been previously detected. Comparisons were made between computed flow and circulation patterns for conditions both before and after proposed dredging of the ship channel.

Giovannelli (1981) used the results of Goodwin (1980) as input to a salt-transport model to analyze specific conductance changes in Hillsborough Bay off the mouth of the Alafia River. He found that a 17-fold increase in river discharge (40 to 680 ft^3/s) produced a 25 percent reduction in the specific conductance (40,000 to 30,000 umho/cm) of bay water near the river mouth. Specific conductance at the river mouth was reduced by more than 70 percent. This indicates significant mixing of river water with Hillsborough Bay water near the Alafia River.

Acknowledgments

We are grateful to the Tampa Port Authority, particularly Delmar Drawdy, for initiation and cooperative financing of this study from 1971 to 1973. We are also grateful to the U.S. Army Corps of Engineers, Jacksonville District, for continuation of the study and financial support through 1984.

Large computer simulation runs that culminated this study were made possible by the Defense Communications Agency (DCA) Hybrid Simulation Facility at Reston, Va. Without assistance from DCA, a full-scale study could not have been made.

Initial model calibration by Jan Leendertse of the Rand Corporation and Robert Baltzer of the U.S. Geological Survey research staff on a precursor of the models described in this report is gratefully acknowledged. Enhancement of satellite imagery by Gerald Moore of the Earth Resources Observation Systems (EROS) Data Center is also appreciated.

DESCRIPTION OF COMPUTER SIMULATION SYSTEM

The model used in this study has the capability to simulate water and constituent motion in well-mixed estuaries, embayments, and other coastal areas. Equations that describe the physical laws governing water and constituent motion in two dimensions are applied between every location where simulated information is desired. These equations are solved at successive small time steps to provide a close approximation of the time history of water level, water transport, and constituent transport at each corresponding location in the real system.

The following sections describe the equations, numerical procedures, input requirements, and operational aspects of the simulation system.

Governing Equations

Water motion in estuaries is governed by the physical laws of conservation of momentum and conservation of mass. The two-dimensional estuarine simulation system (SIMSYS2D), applied in this study, uses vertically integrated forms of equations that describe conservation of mass and momentum, as given by Leendertse (1970, p. 8).

$$\frac{\partial \zeta}{\partial t} + \frac{\partial (HU)}{\partial x} + \frac{\partial (HV)}{\partial y} = 0 \qquad (1)$$

$$\frac{\partial U}{\partial t} + U\frac{\partial U}{\partial x} + V\frac{\partial U}{\partial y} - fV + g\frac{\partial \zeta}{\partial x} + g\frac{U(U^2 + V^2)^{1/2}}{C^2 H} - \frac{1}{\rho H}\tau^s_x = 0 \qquad (2)$$

$$\frac{\partial V}{\partial t} + U\frac{\partial V}{\partial x} + V\frac{\partial V}{\partial y} + fU + g\frac{\partial \zeta}{\partial y} + g\frac{V(U^2 + V^2)^{1/2}}{C^2 H} - \frac{1}{\rho H}\tau^s_y = 0 \qquad (3)$$

where

f = the Coriolis parameter, $2w \sin\phi$, (s^{-1}); where w = the angular velocity of the earth around its axis (radians per second), and ϕ = geographical latitude (degrees),

g = acceleration of gravity, in foot per second squared,

ρ = water density, in pound · second^2 per foot^4,

ζ = water-level altitude with respect to the reference plane, in feet,

h = distance from the reference plane to the embayment bottom, in feet,

$H = h + \zeta$ = water depth, in feet,

C = Chezy roughness coefficient, in foot$^{1/2}$ per second,

τ_x^s = surface wind-stress component in the x-direction, in pound per square foot,

τ_y^s = surface wind-stress component in the y-direction, in pound per square foot, and

t = time, in seconds.

The variables U and V are the vertically averaged velocities of flow defined as

$$U = \frac{1}{H} \int_{-h}^{\zeta} u \, dz \tag{4}$$

$$V = \frac{1}{H} \int_{-h}^{\zeta} v \, dz \tag{5}$$

where u and v are the point-flow velocities in the positive x and y directions, respectively. The wind-stress components are given by Dronkers (1964, p. 188) as

$$\tau_x^s = \theta \rho_a w^2 \sin\alpha \tag{6}$$

and

$$\tau_y^s = \theta \rho_a w^2 \cos \varkappa \qquad (7)$$

where

θ = wind-stress coefficient 0.0026, from Leendertse and Gritton (1971, p. 9), nondimensional,

ρ_a = air density, in pound · second^2 per foot^4,

w = wind velocity, in foot per second, and

$\varkappa$ = angle between wind vector and y axis, in degrees.

Equation 1 expresses continuity of mass in two dimensions. Equations 2 and 3 express continuity of momentum in the x and y Cartesian coordinate directions, respectively. These equations assume that water density is constant both horizontally and vertically, that vertical flow components do not exist, and that horizontal flow components do not vary vertically. The model is limited in application to areas that are vertically and horizontally well mixed. However, this type of model has been successfully applied where gradually varying horizontal density gradients occur.

Transport of dissolved constituents is governed by large scale advective or translatory motion of water and by fine scale dispersive or mixing action caused by presence of turbulence superimposed on the average flow. Transport of dissolved constituents is governed by the conservation of solute mass incorporating advective and dispersive concepts and allowing for constituent sources and sinks as given by Leendertse and Gritton (1971, p. 4) for two-dimensional flow (equation 8).

$$\frac{\partial (HP)}{\partial t} + \frac{\partial (HUP)}{\partial x} + \frac{\partial (HVP)}{\partial y} - \frac{\partial \left(HD_x \frac{\partial P}{\partial x}\right)}{\partial x} - \frac{\partial \left(HD_y \frac{\partial P}{\partial y}\right)}{\partial y} - HS_A = 0 \qquad (8)$$

where

D_x = dispersion coefficient, flow in the x-direction, in square foot per second,

D_y = dispersion coefficient, flow in the y-direction, in square foot per second, and

S_A = source and sink function, including the rate of injection of constituent A.

As with the velocities U and V, P is the integrated average mass concentration of the constituent in the vertical given by

$$P = \frac{1}{H} \int_{-h}^{\zeta} p_A \, dz \qquad (9)$$

where p_A is the local mass concentration of a particular constituent substance, A.

Holley (1969, p. 628) noted that, except in regions of large constituent concentration gradients, mass transport by longitudinal dispersion is often very small compared with mass transport by advection. Leendertse (1970, p. 13) reasoned that, if this were true, small errors in assigning values to the longitudinal dispersion coefficient would not substantially change the solutions obtained. He then assumed that dispersion could be adequately defined by two components, an isotropic component representing the effect of lateral mixing and a directional component approximating longitudinal effects. The dispersion coefficients, D_x and D_y, used in SIMSYS2D are given by Leendertse (1970, p. 14) as:

$$D_x = dHUg^{1/2}C^{-1} + D_w \qquad (10)$$

$$D_y = dHVg^{1/2}C^{-1} + D_w \qquad (11)$$

where

D_w = a diffusion coefficient representing wave, wind, and lateral mixing effects (square foot per second), and

d = an empirical dimensionless constant similar to that presented by Elder (1959).

Numerical Procedures

Partial differential equations 1, 2, 3, and 8 describe general relations that exist between the many forces that control water and solute motion. Because the equations cannot be solved analytically for most real-world conditions, procedures have been devised that provide approximate solutions by using computers to rapidly perform an enormous quantity of numerical computations.

The numerical procedure used in SIMSYS2D is summarized below and is presented in detail by Leendertse and Gritton (1971, p. 15). Equations 1, 2, 3, and 8 can be approximated over a region in time and space by a large number of difference equations. Each difference equation is similar in form to the parent differential equation, but is applicable at only one point in time and space and is separated from all other points by finite time and space increments. The value of a finite-difference approximation is that a differential equation is reduced to multiple interrelated algebraic equations involving quantities at defined locations.

Each difference equation contains known and unknown terms. As long as the number of equations equals the number of unknown terms, the system is solvable. The method of solution for the unknown terms involves a point to point, repeating, stepwise procedure that incorporates previously computed values and input data as appropriate.

A space-staggered grid scheme (fig. 5) is used in the SIMSYS2D model. Water levels (ζ) and solute mass density (P) are defined at integer values of m and n. Water depths (h), measured from the National Geodetic Vertical Datum of 1929, are defined at points midway between integer values of both m and n. Velocities in the y-direction (V) are defined at points midway between integer values of n and at integer values of m. Velocities in the x-direction (U) are defined at points midway between integer values of m and at integer values of n.

The grid extends to the boundaries of the modeled area in the positive and negative x and y directions. On land areas, water depths (h) are replaced by land altitudes (-h) and water velocities are computed only at times when water levels exceed land elevations. Time is also simulated in a stepwise manner with computational elements defined at integer points and midway between integer points. Simulation time extends from the beginning to the end of each period of interest.

Leendertse and Gritton (1971, p. 11) give a complete description of how equations 1, 2, 3, and 8 are structured at each (x, y, t) point and how unknowns in each equation are solved. An overview of the solution scheme is also given by Cheng and Casulli (1982, p. 1,655).

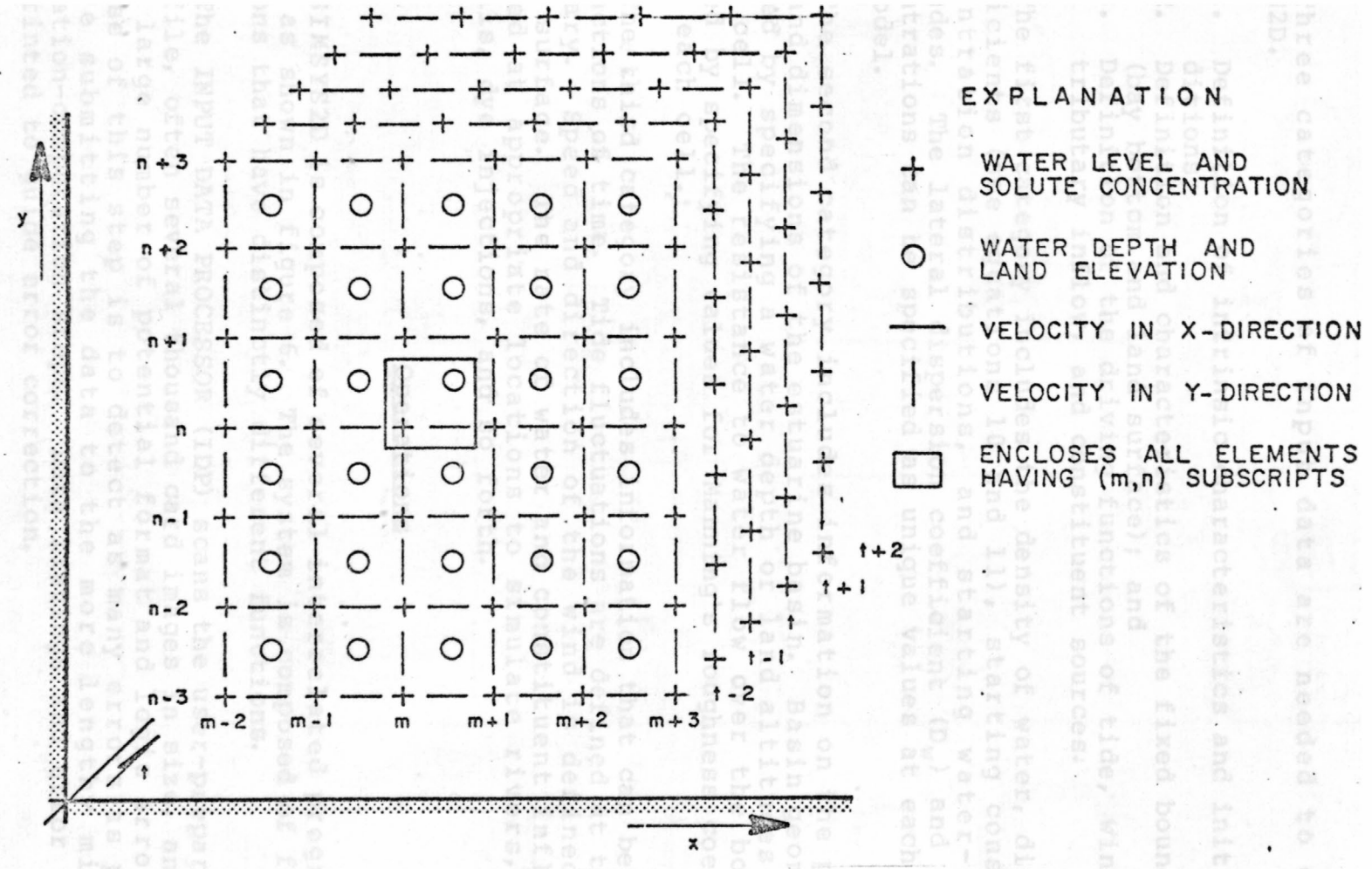

Figure 5.--Finite-difference scheme for computer simulation model (modified from Leendertse and Gritton, 1971).

Input Requirements

Three categories of input data are needed to operate SIMSYS2D.

1. Definition of intrinsic characteristics and initial conditions;
2. Definition and characteristics of the fixed boundary (bay bottom and land surface); and
3. Definition of the driving functions of tide, wind, tributary inflow, and constituent sources.

The first category includes the density of water, dispersion coefficients (see equations 10 and 11), starting constituent concentration distributions, and starting water-surface altitudes. The lateral dispersion coefficient (D_W) and starting concentrations can be specified as unique values at each cell in the model.

The second category includes information on the physical size and dimensions of the estuarine basin. Basin geometry is defined by specifying a water depth or land altitudes at each model cell. The resistance to water flow over the bottom is defined by specifying values for Manning's roughness coefficient (n) at each cell.

The third category includes information that can be entered as functions of time. Tide fluctuations are defined at the ocean boundary. Speed and direction of the wind is defined at the water surface. The rate of water and constituent inflows are defined at appropriate locations to simulate rivers, sewage outfalls, dye injections, and so forth.

Operations

SIMSYS2D is composed of several interrelated programs and files as shown in figure 6. The system is composed of four main sections that have distinctly different functions.

The INPUT DATA PROCESSOR (IDP) scans the user-prepared input data file, often several thousand card images in size, and checks for a large number of potential format and logic errors. The purpose of this step is to detect as many errors as possible before submitting the data to the more lengthy mixer and simulation-computation steps. Data listings and error messages are printed to guide error correction.

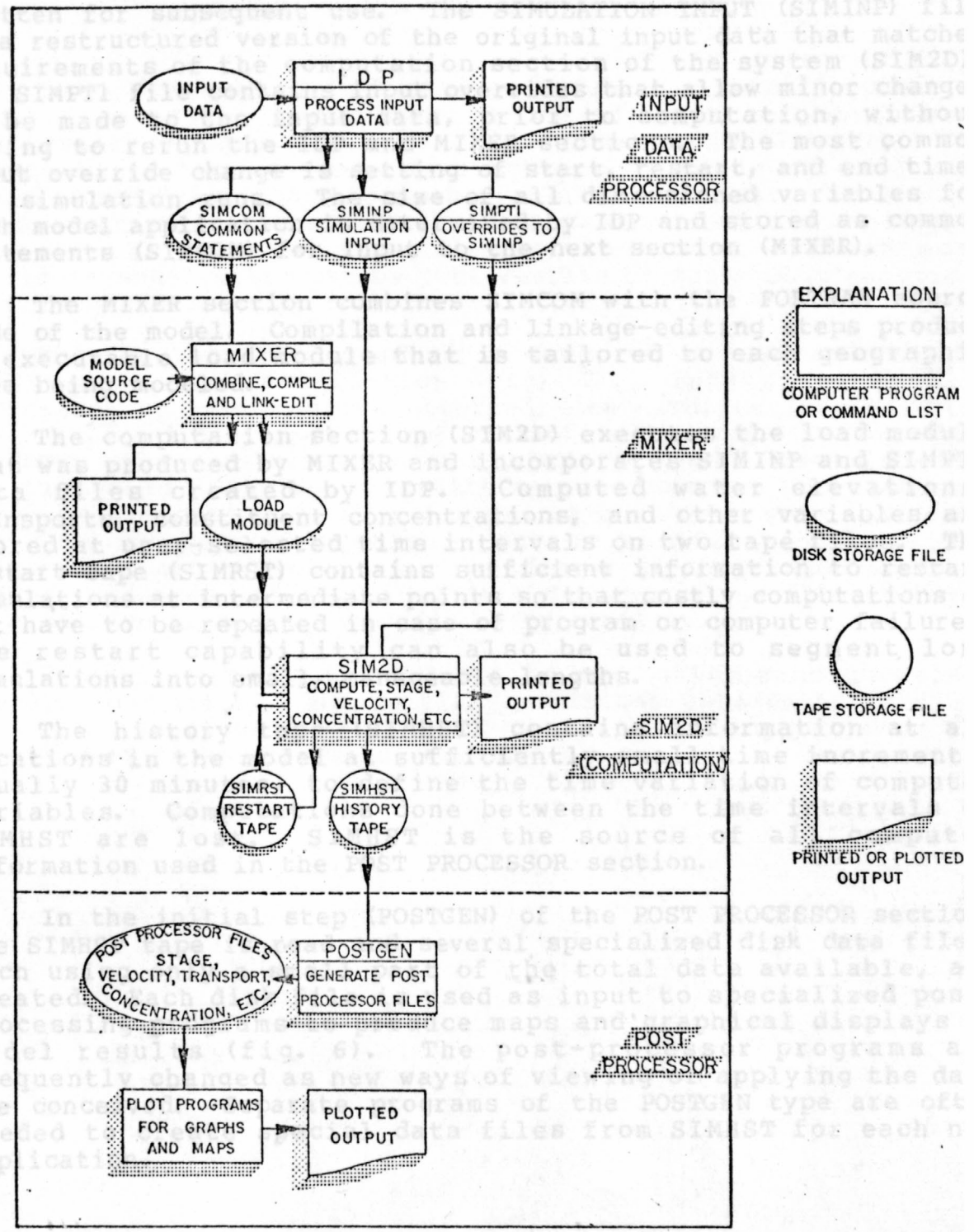

Figure 6.--Relation of programs, files, input, and output for the simulation modeling system.

With successful completion of IDP, three disk files are written for subsequent use. The SIMULATION INPUT (SIMINP) file is a restructured version of the original input data that matches requirements of the computation section of the system (SIM2D). The SIMPT1 file contains input overrides that allow minor changes to be made to the input data, prior to computation, without having to rerun the IDP and MIXER sections. The most common input override change is setting of start, restart, and end times for simulation runs. The size of all dimensioned variables for each model application is determined by IDP and stored as common statements (SIMCOM) for input to the next section (MIXER).

The MIXER section combines SIMCOM with the FORTRAN source code of the model. Compilation and linkage-editing steps produce an executable load module that is tailored to each geographic area being modeled.

The computation section (SIM2D) executes the load module that was produced by MIXER and incorporates SIMINP and SIMPTI data files created by IDP. Computed water elevations, transports, constituent concentrations, and other variables are stored at user-selected time intervals on two tape files. The restart tape (SIMRST) contains sufficient information to restart simulations at intermediate points so that costly computations do not have to be repeated in case of program or computer failures. The restart capability can also be used to segment long simulations into small, manageable lengths.

The history tape (SIMHST) contains information at all locations in the model at sufficiently small time increments, usually 30 minutes, to define the time variation of computed variables. Computations done between the time intervals of SIMHST are lost. SIMHST is the source of all computed information used in the POST PROCESSOR section.

In the initial step (POSTGEN) of the POST PROCESSOR section, the SIMHST tape is read and several specialized disk data files, each using only a small part of the total data available, are created. Each disk file is used as input to specialized post-processing programs to produce maps and graphical displays of model results (fig. 6). The post-processor programs are frequently changed as new ways of viewing or applying the data are conceived. Separate programs of the POSTGEN type are often needed to create special data files from SIMHST for each new application.

MODEL DEVELOPMENT AND APPLICATION

Model development is a process by which a general estuarine simulation system is structured and adjusted to represent a particular estuary, embayment, or other coastal area. The objective of the process is to achieve as close agreement as possible and practicable between simulated and observed values of tidal stage, tidal currents, constituent distributions, and other measureable factors. The closer the agreement, the more confident model users can be that results of subsequent numerical experiments accurately reflect real conditions.

The development procedure is composed of two basic steps, calibration and verification (fig. 7). Both steps involve comparison of computed and observed data. The calibration step has a feedback loop that is not present in the verification step. Feedback allows adjustments to imprecisely known input data for the purpose of improving the match between observed and simulated data. Verification is done for one or more data sets that were not used during calibration. During verification, further adjustments are not allowed. The degree of comparison achieved between observed and simulated data during the verification step is a measure of model accuracy and reliability.

The following sections describe how bottom configuration, boundary conditions, and initial conditions were determined and show results of calibration and verification comparisons for development of the Tampa Bay model.

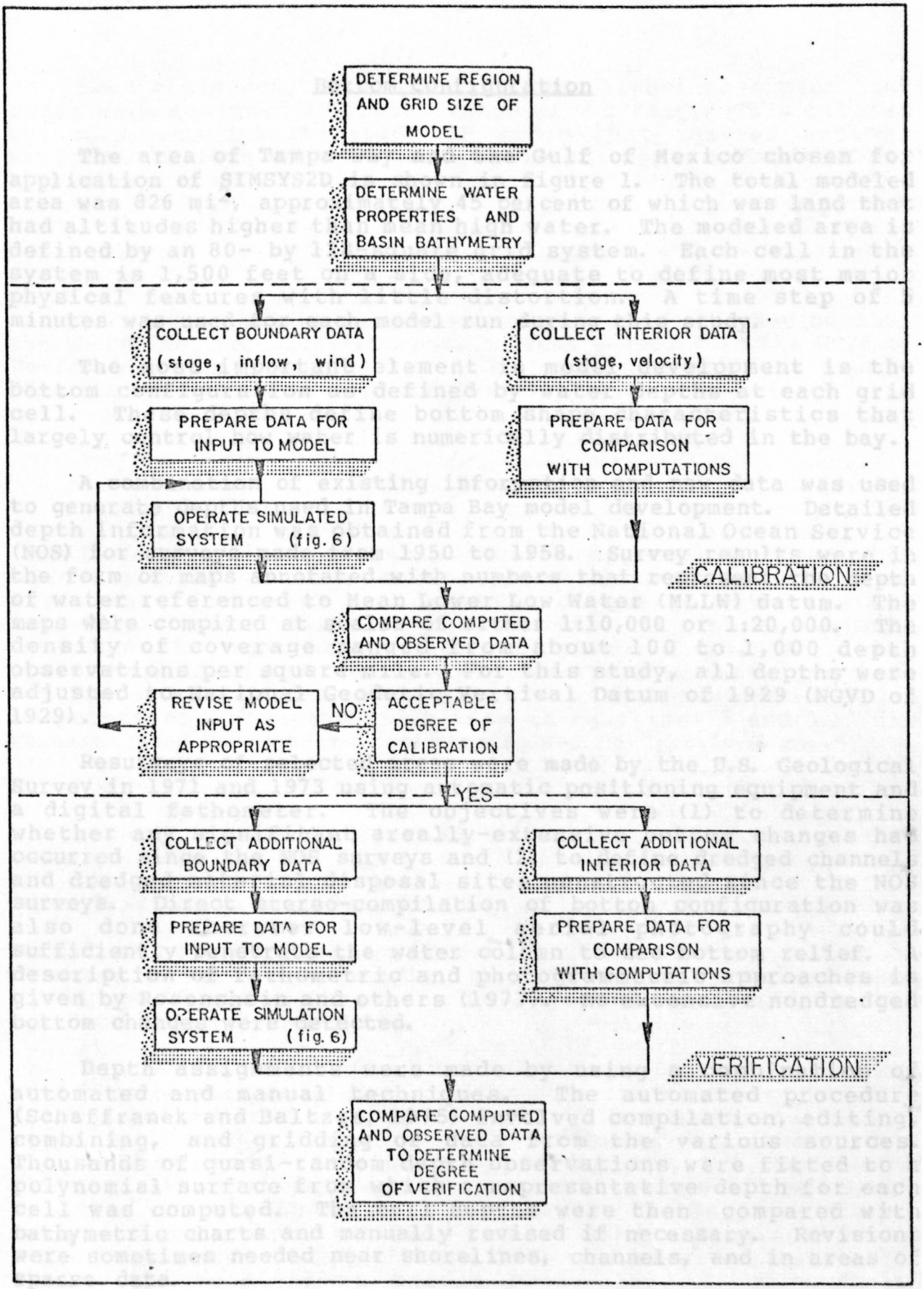

Figure 7.--Calibration and verification steps in model development.

Bottom Configuration

The area of Tampa Bay and the Gulf of Mexico chosen for application of SIMSYS2D is shown in figure 1. The total modeled area was 826 mi^2, approximately 45 percent of which was land that had altitudes higher than mean high water. The modeled area is defined by an 80- by 128-square grid system. Each cell in the system is 1,500 feet on a side, adequate to define most major physical features with little distortion. A time step of 5 minutes was used for each model run during this study.

The most important element in model development is the bottom configuration as defined by water depths at each grid cell. These depths define bottom shape characteristics that largely control how water is numerically distributed in the bay.

A combination of existing information and new data was used to generate depths used in Tampa Bay model development. Detailed depth information was obtained from the National Ocean Service (NOS) for surveys made from 1950 to 1958. Survey results were in the form of maps annotated with numbers that represent the depth of water referenced to Mean Lower Low Water (MLLW) datum. The maps were compiled at scales of either 1:10,000 or 1:20,000. The density of coverage ranged from about 100 to 1,000 depth observations per square mile. For this study, all depths were adjusted to National Geodetic Vertical Datum of 1929 (NGVD of 1929).

Resurveys of selected areas were made by the U.S. Geological Survey in 1971 and 1973 using automatic positioning equipment and a digital fathometer. The objectives were (1) to determine whether any significant areally-extensive bottom changes had occurred since the NOS surveys and (2) to define dredged channels and dredged material disposal sites constructed since the NOS surveys. Direct stereo-compilation of bottom configuration was also done wherever low-level aerial photography could sufficiently penetrate the water column to see bottom relief. A description of fathometric and photogrammetric approaches is given by Rosenshein and others (1977). No extensive nondredged bottom changes were detected.

Depth assignments were made by using a combination of automated and manual techniques. The automated procedure (Schaffranek and Baltzer, 1975) involved compilation, editing, combining, and gridding of data from the various sources. Thousands of quasi-random depth observations were fitted to a polynomial surface from which a representative depth for each cell was computed. The cell depths were then compared with bathymetric charts and manually revised if necessary. Revisions were sometimes needed near shorelines, channels, and in areas of sparse data.

Land altitudes for cells that were higher than mean high water were assigned a default value of 3.0 feet. This limited the model to investigation of tides that reached maximum altitudes of less than 3.0 feet. This was not a constraint for this study.

Boundary Conditions

Boundaries of the Tampa Bay model include the bay bottom, the shoreline, tributary streams, a tidal boundary in the Gulf of Mexico, and the water surface. A description of the data used to describe conditions at each boundary follows.

Bottom Boundary

The bay bottom is treated as an impermeable, immovable boundary that causes resistance to free flow of water. Resistance increases as roughness of the bottom material increases. Values of the roughness coefficient, "n" in Manning's equation, were assigned to each cell of the model. A related open-channel flow equation by Chezy incorporates another bottom-roughness coefficient, "C", that is actually used in model computations. (See the sixth term in equations 2 and 3.) The relation used to convert from Manning's n to Chezy's C is:

$$C = \frac{1.49}{n} H^{1/6} \qquad (12)$$

where H is the water depth, in feet.

Manning's n is an empirical coefficient that cannot be measured directly. By varying the coefficient, model-computed tidal stage and current can be adjusted to closely match corresponding measured data.

Manning's n values used in simulation of other estuaries and bays have been reported in the literature and were used to guide initial values used in this study. It is recognized that n-values are somewhat dependent on the particular algorithm used in model computations. In a study of Jamaica Bay, N.Y., Leendertse (1972, p. 11) used n-values that ranged between 0.026 and 0.034. In areas of corresponding depths in the St. Lawrence River, Prandle and Crookshank (1974, p. 523) used a Mannings "n" of 0.028. April and others (1975, p. 769) used n-values that ranged from 0.010 to 0.018 in Mobile Bay, Ala. In a study of Masonborough Inlet, N.C., Masch and Brandes (1975, p. 230) used n-values that ranged from 0.018 to 0.035 for depths from 4 to 30

feet. Beauchamp and Spaulding (1978, p. 525) used an n-value of 0.028 in the Long Island Sound, Block Island Sound, Rhode Island Sound, and Buzzards Bay area of New England. Wang (1978, p. 505) used an n-value of 0.025 in South Biscayne Bay, Fla.

An initial n-value of 0.025 was chosen for this study based on the most comparable conditions reported in the literature. Other n-values, as low as 0.022, were used in the model calibration process. A uniform value of 0.0235 was chosen as providing the best fit to prototype data. Whenever water depth in any cell became less than 1 foot, however, the model automatically reassigned an n-value of 0.040 to simulate the increased importance of bottom friction.

Shoreline and Tributary Streams

The shoreline is defined as a no-flow boundary except where tributary streams enter the bay. A flooding and drying feature of the model simulates landward or seaward movement of the shoreline with changes in tidal stage. This feature is of lesser significance in Tampa Bay in comparison with other coastal plain estuaries that have extensive areas of tidal flats.

Freshwater inflow of streams tributary to Tampa Bay (fig. 1) was determined from data published by the U.S. Geological Survey. The freshwater inflow used (table 3) is the annual average computed from long-term records at the most downstream gaging station on each river (U.S. Geological Survey, 1977). The inflow contribution from ungaged areas was approximated by a proportionate increase based on drainage area ratios. Inflow was entered at appropriate cells near the shoreline of the model.

Once-through cooling-water systems of power-generating stations were handled in a similar way. Cooling-water intakes were simulated as negative discharges at cells close to the locations of intake structures. Cooling-water discharges were simulated as positive values at cells close to the discharge sites. A representative of the Tampa Electric Company (oral commun., 1975) indicated that typical cooling-water discharge rates for both the Big Bend and Gannon stations (fig. 1) are 1,960 ft^3/s. Information from a Florida Power Company representative (oral commun., 1975) indicated typical cooling-water discharge rates were 1,000 ft^3/s for both the Higgins and Weedon Island stations (fig. 1).

Table 3.--Average annual discharge of streams tributary to Tampa Bay (U.S. Geological Survey, 1977)

Tampa Bay subarea	Stream	Average annual discharge (ft^3/s)[1/]
Hillsborough Bay	Hillsborough River	636
	Alafia River	459
	Total of several small streams	99
Old Tampa Bay	Total of several small streams	117
Middle Tampa Bay	Little Manatee River	240
Lower Tampa Bay	Manatee River	353
Total		1,904

[1/] All values linearly adjusted to include effect of ungaged drainage area.

Seaward Boundary

Fluctuations in tidal stage, the primary force causing time-dependent water motion, were applied at the seaward boundary of the model. The model distributed water to and from sections of the estuary by solving equations 1, 2, and 3 for each designated time and space increment. At the seaward boundary, velocities are computed using simplified linearized equations that do not require any information outside the boundary. This procedure produces less precise computations at and near the seaward boundary than at other locations.

Because of less precise velocity computations and increased susceptibility of the simplified equations to numerical instability, it is desirable for the seaward boundary to be located some distance from areas where model results could be important and where large depth changes could induce instability. Location of the seaward boundary approximately 4 miles offshore from Egmont Key accomplished these two objectives.

To generate offshore tidal conditions, a cross-spectral analysis technique described by Leendertse and Liu (1974) and used by Van der Ree and others (1978) was applied to transfer tidal-stage, time-series data at Fort De Soto (site 22, fig. 8) to the seaward boundary at location WC-154 (site 24). The technique required concurrent time-series data at each location to define cross-spectral relations. Once established, these relations could then be used to generate time-series data at site 24 for any period for which data were available at Fort De Soto.

Concurrent time-series data were available for the period January 25 to February 11, 1979, when offshore pressure recordings were obtained by Woodward-Clyde Consultants (1979) and the Fort De Soto gage was in operation. A part of the concurrent data (fig. 9) shows significant amplitude and phase differences. The computed data at site 24, after cross-spectral adjustments were made to the Fort De Soto record, are shown in figure 10 and compared with measured data. The standard error between measured and computed data is about 0.1 foot.

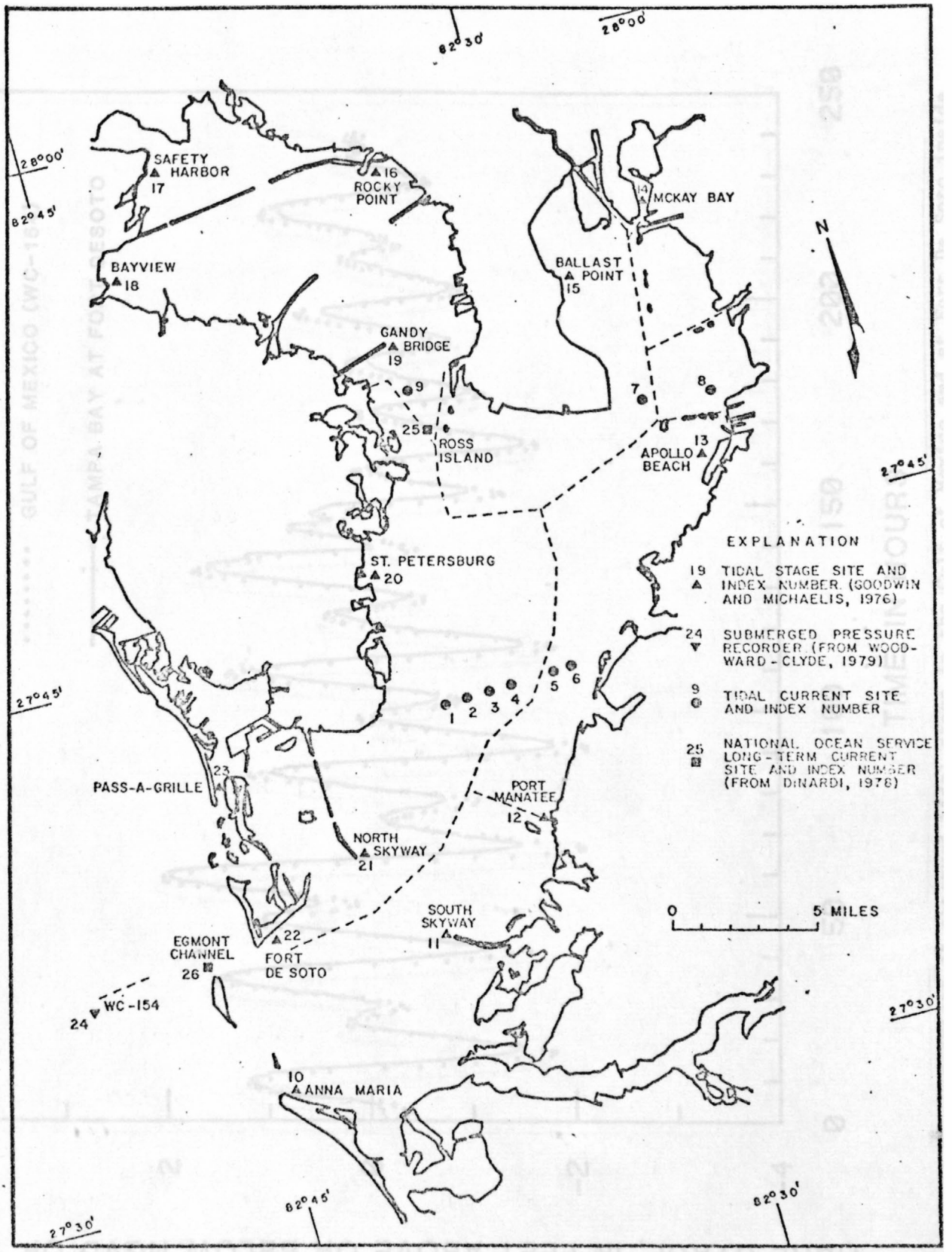

Figure 8.--Location of tidal stage and tidal current measuring sites.

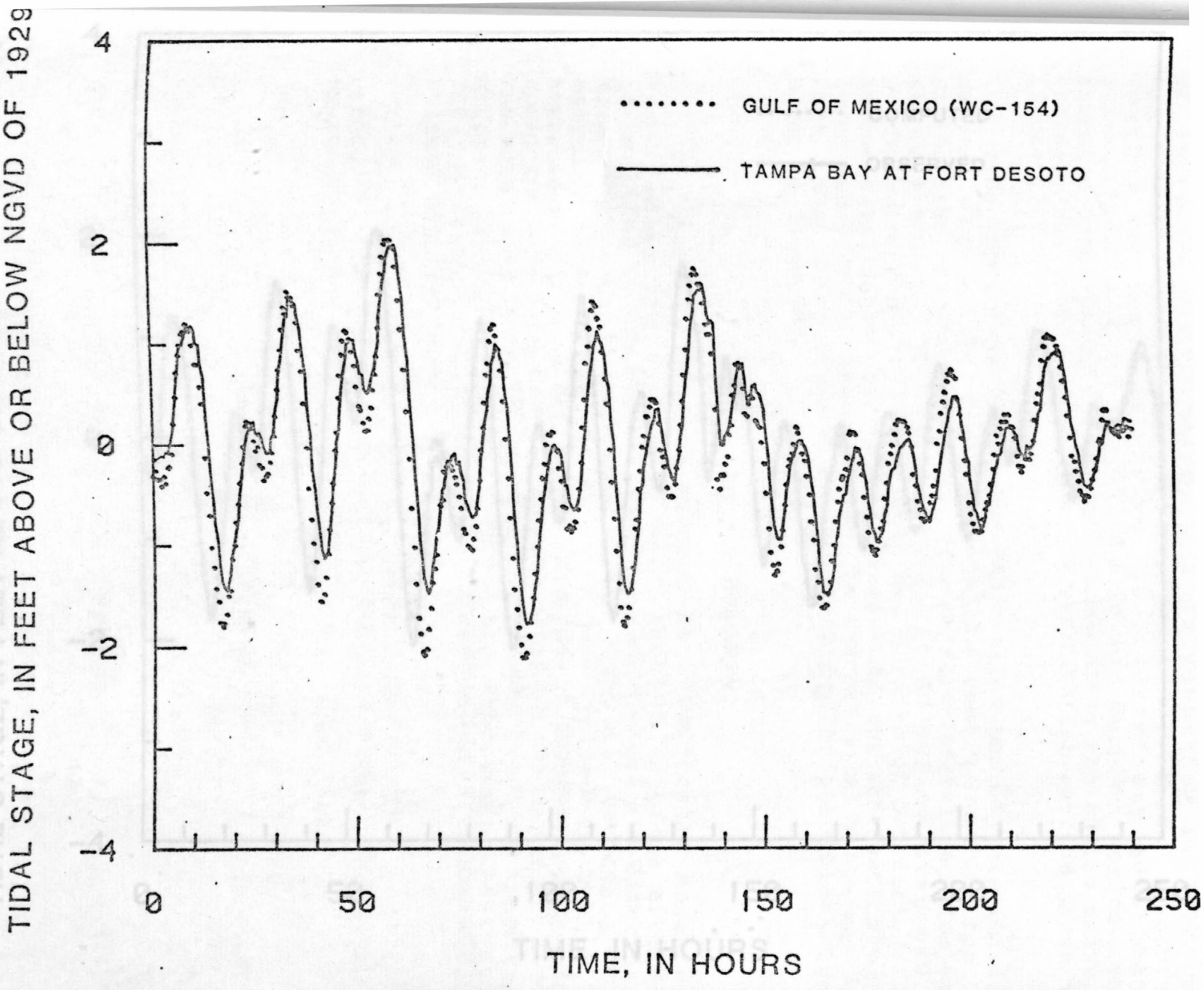

Figure 9.--Comparison of observed tidal stage in the Gulf of Mexico and at Fort De Soto inside the mouth of Tampa Bay. (Locations of sites are shown in figure 8.)

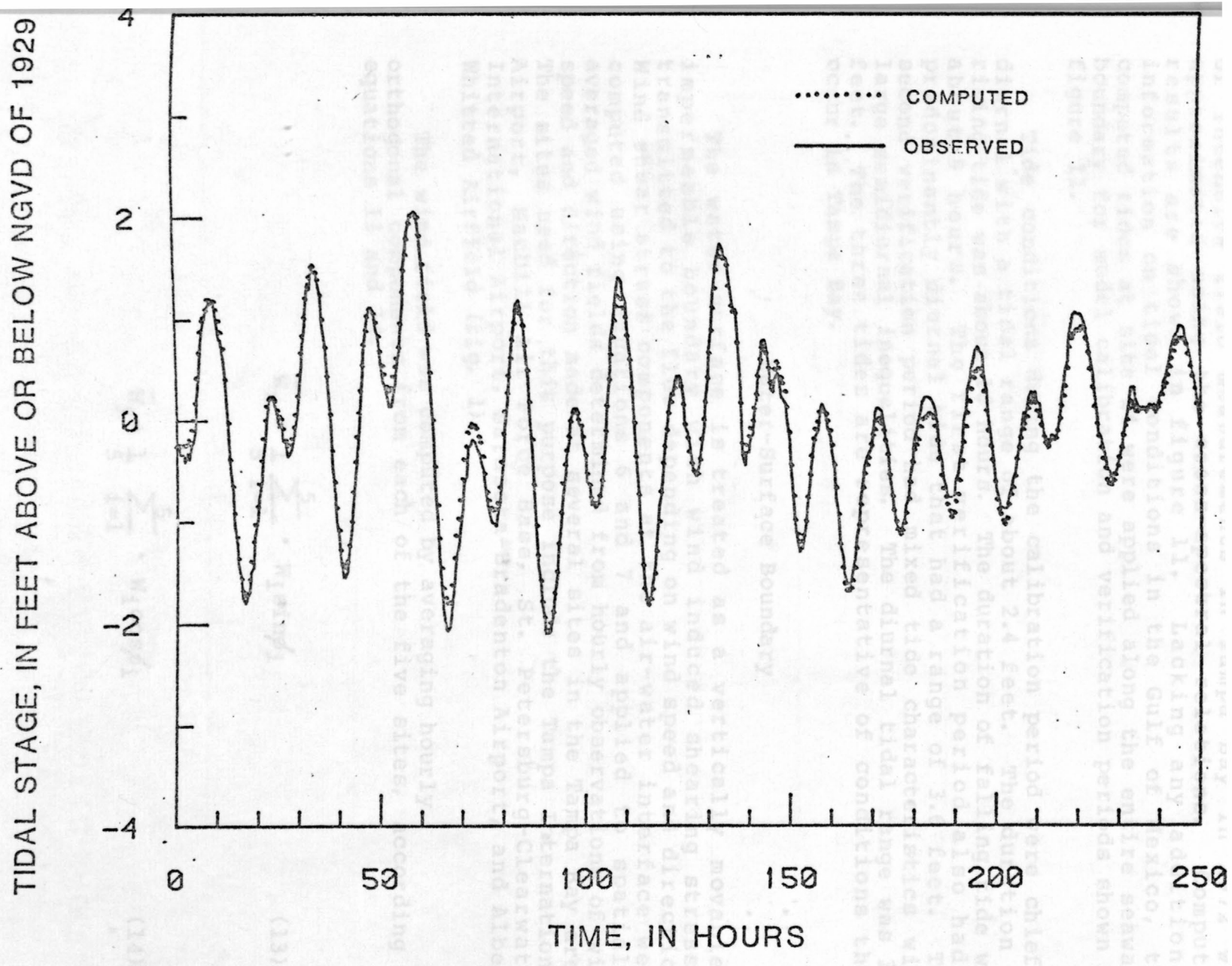

Figure 10.--Comparison of observed tidal stage in the Gulf of Mexico and tidal stage computed using cross-spectral procedure (described by Leendertse and Liu, 1974).

The tide that existed in the Gulf of Mexico during a period of intensive field measurements in Tampa Bay in 1972 was approximated using the cross-spectral relations. Computed results are shown in figure 11. Lacking any additional information on tidal conditions in the Gulf of Mexico, the computed tides at site 24 were applied along the entire seaward boundary for model calibration and verification periods shown in figure 11.

Tide conditions during the calibration period were chiefly diurnal with a tidal range of about 2.4 feet. The duration of rising tide was about 16 hours. The duration of falling tide was about 9 hours. The first verification period also had a predominantly diurnal tide that had a range of 3.6 feet. The second verification period had mixed tide characteristics with large semidiurnal inequalities. The diurnal tidal range was 3.0 feet. The three tides are representative of conditions that occur in Tampa Bay.

Water-Surface Boundary

The water surface is treated as a vertically movable, impermeable boundary with wind induced shearing stresses transmitted to the flow depending on wind speed and direction. Wind shear stress components at the air-water interface were computed using equations 6 and 7 and applied to spatially averaged wind fields determined from hourly observations of wind speed and direction made at several sites in the Tampa Bay area. The sites used for this purpose include the Tampa International Airport, MacDill Air Force Base, St. Petersburg-Clearwater International Airport, Sarasota-Bradenton Airport, and Albert Whitted Airfield (fig. 1).

The wind field was computed by averaging hourly orthogonal components from each of the five sites, according to equations 13 and 14.

$$\bar{W}_x = \frac{1}{5} \sum_{i=1}^{5} \cdot W_i \sin\phi_i \qquad (13)$$

$$\bar{W}_y = \frac{1}{5} \sum_{i=1}^{5} \cdot W_i \cos\phi_i \qquad (14)$$

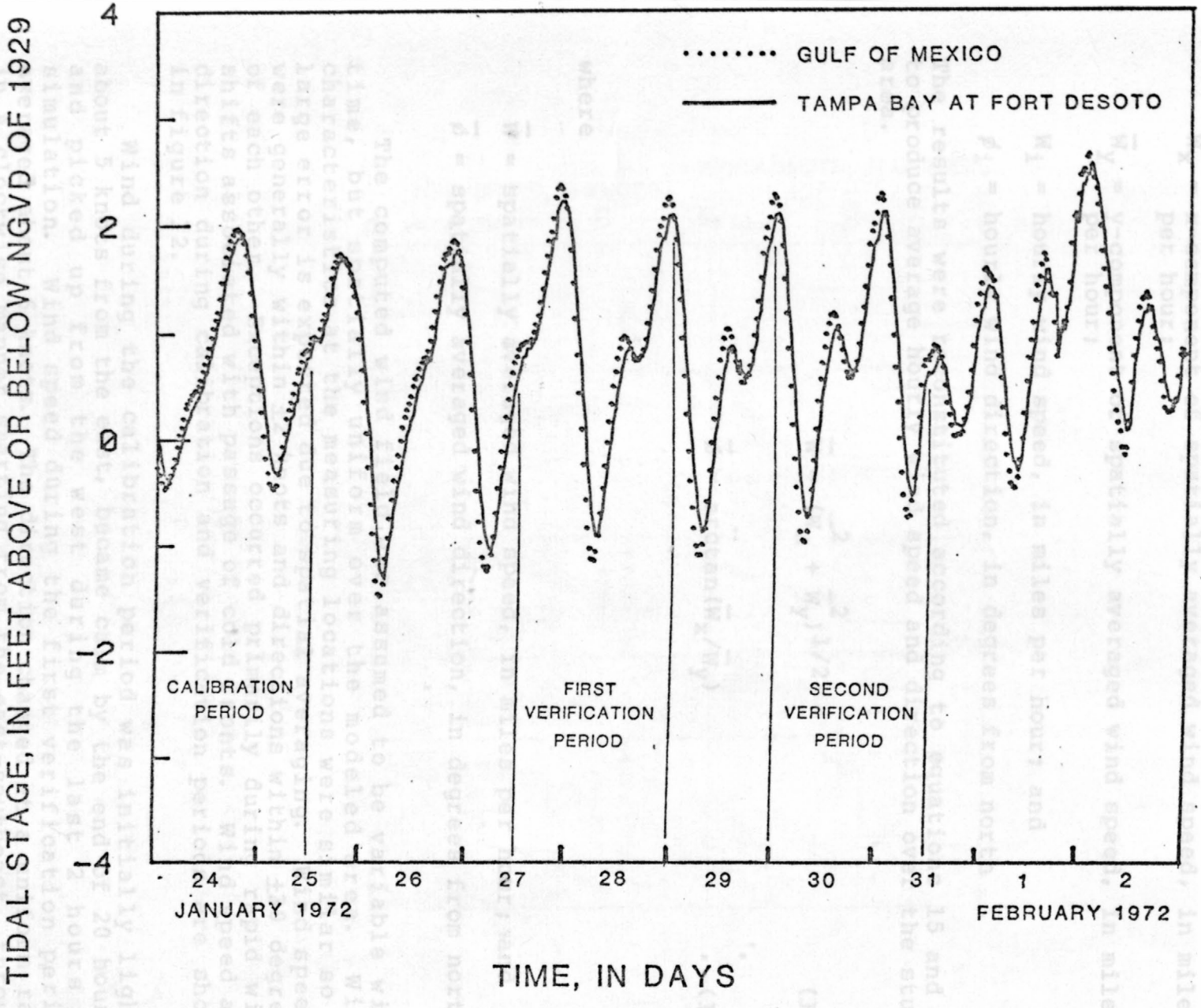

Figure 11.--Comparison of computed tidal stage in the Gulf of Mexico with observed tides at Fort De Soto during model calibration and verification periods.

where

$\bar{W}_x$ = x-component of spatially averaged wind speed, in miles per hour;

$\bar{W}_y$ = y-component of spatially averaged wind speed, in miles per hour;

W_i = hourly wind speed, in miles per hour; and

ϕ_i = hourly wind direction, in degrees from north

The results were reconstituted according to equations 15 and 16 to produce average hourly wind speed and direction over the study area.

$$\bar{W} = (\bar{W}_x^2 + \bar{W}_y^2)^{1/2} \tag{15}$$

$$\bar{\phi} = \arctan(\bar{W}_x/\bar{W}_y) \tag{16}$$

where

$\bar{W}$ = spatially averaged wind speed, in miles per hour; and

$\bar{\phi}$ = spatially averaged wind direction, in degrees from north.

The computed wind field was assumed to be variable with time, but spatially uniform over the modeled area. Wind characteristics at the measuring locations were similar so no large error is expected due to spatial averaging. Wind speeds were generally within ±2 knots and directions within ±30 degrees of each other. Exceptions occurred primarily during rapid wind shifts associated with passage of cold fronts. Wind speed and direction during calibration and verification periods are shown in figure 12.

Wind during the calibration period was initially light, about 5 knots from the east, became calm by the end of 20 hours, and picked up from the west during the last 2 hours of simulation. Wind speed during the first verification period averaged about 6 knots. The direction changed at a uniform rate in a clockwise manner starting from the east-southeast, through north, and around the points of the compass to reach north a second time. Wind during the second verification period started off calm, then averaged about 7 knots from the south-southwest for most of the period.

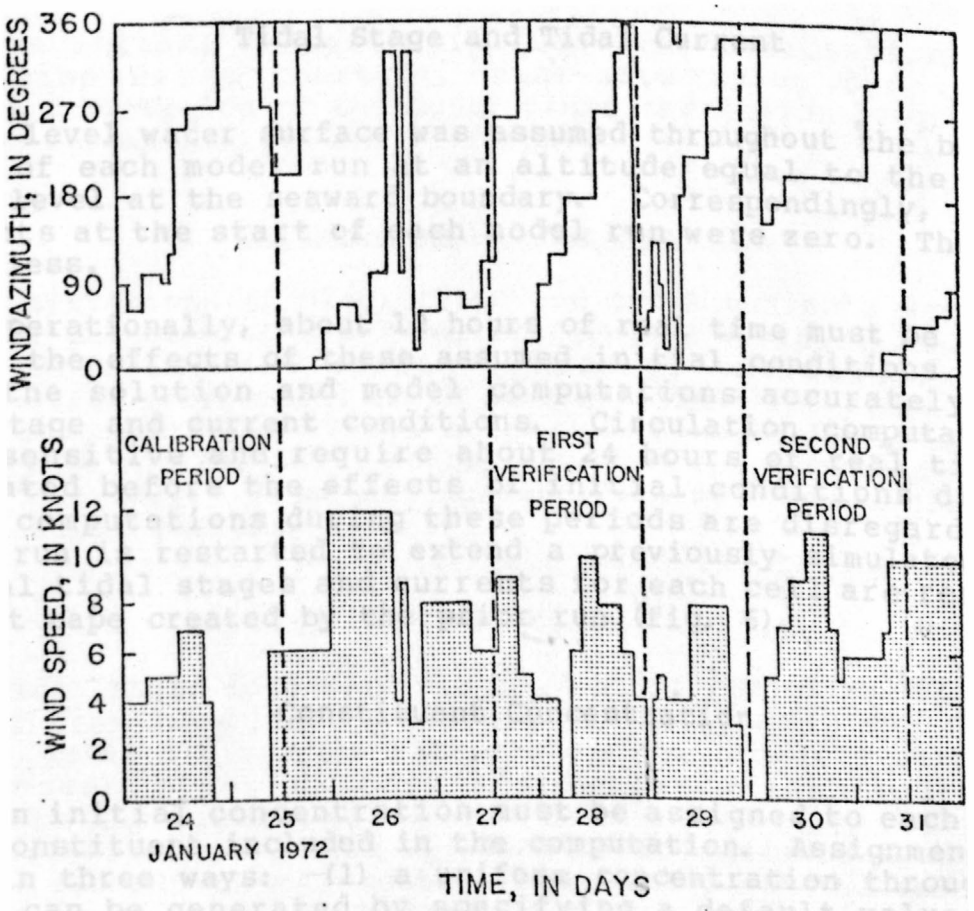

Figure 12.--Wind speed and direction during calibration and verification periods.

Initial Conditions

Initial conditions are necessary to define three time-varying parameters: tidal stage, tidal current, and constituent concentration when starting model computation. The following sections describe how these initial conditions are assigned and how they affect simulation results.

Tidal Stage and Tidal Current

A level water surface was assumed throughout the bay at the start of each model run at an altitude equal to the starting water level at the seaward boundary. Correspondingly, all tidal currents at the start of each model run were zero. The bay was motionless.

Operationally, about 12 hours of real time must be simulated before the effects of these assumed initial conditions disappear from the solution and model computations accurately reflect real stage and current conditions. Circulation computations are more sensitive and require about 24 hours of real time to be simulated before the effects of initial conditions disappear. Model computations during these periods are disregarded. If a model run is restarted to extend a previously simulated period, initial tidal stages and currents for each cell are read from a restart tape created by the prior run (fig. 6).

Constituent Concentration

An initial concentration must be assigned to each cell for each constituent included in the computation. Assignments can be made in three ways: (1) a uniform concentration throughout the model can be generated by specifying a default value; (2) the default value can be changed at one or many cells by specifying values that override the default value; and (3) a complete array can be provided that defines the initial concentration at each cell.

A uniformly low initial background concentration is useful when simulating the spread of dye or other constituent injected at a point. Overrides can be used to advantage if one or more small subregions are known to have different concentrations than the rest of the simulated region. An array is normally provided if an accurate definition of constituent gradients is needed at the start of a model run.

Constituent concentrations at the seaward boundary of the model are computed from values at interior points during ebb flow. During flood flow, however, water with unassigned and

uncomputed constituent concentrations can be brought from outside the modeled area and cause rapid degeneration of computed concentrations near the seaward boundary. To avoid this, the model allows a gradual return of concentrations to an initially defined value. This procedure is approximate, but allows reasonable computation of concentrations to continue at the seaward boundary through all phases of the tide. This procedure is also considered to be more realistic than assignment of a constant concentration to all water crossing the seaward boundary during flood flows.

The initial concentration used for calibration of model dispersion was a constant, near-zero value for turbidity. Further description of turbidity plume simulation is given in the section on calibration and verification.

Calibration and Verification

Observations of tidal stage and tidal currents were made in 1972 for purposes of model calibration and verification. Table 4 shows starting and ending times for the calibration and verification periods and field data available for comparison with model computations. Tidal-current data were not available for January 24 and 25, 1972, so calibration was accomplished using stage data only. Stage and current data were available for both verification periods.

Tidal Stage

Tidal stage data were measured at 14 locations (sites 10-23, fig. 8) from June 1971 to December 1973 (Goodwin and Michaelis, 1976). Table 5 gives the site number, the complete station name, downstream order number, and latitude-longitude position progressing counterclockwise around the bay for the most southerly station. Each of the 14 stations were equipped with digital recording instruments that measured water-level altitudes every 5 or 15 minutes as controlled by crystal timers that were accurate to 5 seconds per month. Gages were referenced to NGVD of 1929 by spirit leveling to first-order benchmarks wherever possible. The location of gage WC-154, site 24, is also given in table 5.

Table 4.--Calibration and verification time periods and field data availability

Period	Start		End		Duration (hours)	Field data availability	
	Day	Hour	Day	Hour		Stage	Velocity
Calibration	1-24-72	0005	1-25-72	1200	36	Yes	No
First verification	1-27-72	1205	1-28-72	2400	36	Yes	Yes
Second verification	1-30-72	0005	1-31-72	1200	36	Yes	Yes

Table 5.--Summary of tidal stage stations in Tampa Bay

Site (fig. 8)	USGS downstream order No.	Station identification[1/]	North latitude	West longitude
10	02-3000.72	Tampa Bay at Anna Maria	27°32'03"	82°43'50"
11	02-3000.85	Tampa Bay near Terra Ceia (South Skyway)	27°35'30"	82°37'45"
12	02-3000.88	Tampa Bay near Piney Point (Port Manatee)	27°38'06"	82°33'32"
13	02-3005.60	Tampa Bay near Ruskin (Apollo Beach)	27°46'57"	82°25'53"
14	02-3017.61	McKay Bay at Tampa	27°54'54"	82°25'25"
15	02-3060.32	Hillsborough Bay at Ballast Point at Tampa	27°53'22"	82°28'47"
16	02-3061.00	Old Tampa Bay at Rocky Point at Tampa	27°57'59"	82°33'57"
17	02-3075.78	Old Tampa Bay at Safety Harbor	27°59'17"	82°41'07"
18	02-3077.69	Old Tampa Bay near Bayview	27°56'28"	82°43'15"
19	02-3079.30	Old Tampa Bay at Gandy Bridge near Tampa	27°52'46"	82°34'57"
20	02-3080.82	Tampa Bay at St. Petersburg	27°46'24"	82°37'25"
21	02-3084.26	Tampa Bay at Sunshine Skyway Bridge near St. Petersburg (North Skyway)	27°38'36"	82°40'12"
22	02-3086.00	Tampa Bay at Fort De Soto Park near Pass-a-Grille Beach	27°36'53"	82°43'33"
23	02-3086.50	Pass-a-Grille Channel near Pass-a-Grille Beach	27°41'30"	82°43'48"
24	----	Woodward-Clyde gage number 154 offshore of Egmont Key (WC-154)	27°36'12"	82°51'54"

[1/] Underlined name is shown in figure 8.

For the calibration period, the standard errors between computed and observed water levels at half-hour intervals during the last 24 hours of simulation ranged from 0.03 foot at South Skyway near the mouth of Tampa Bay, site 11, to 0.13 foot at Safety Harbor, site 17, and Bayview, site 18, in Old Tampa Bay (table 6). The average standard error for calibration was 0.07 foot. Graphical comparisons between observed and computed water levels for six stations from the mouth to the head of the bay are shown in figure 13. The time required for the effects of initial conditions to disappear can be seen during the first 12 hours of each graph.

The average standard error for both verification periods was 0.09 foot, and the range was from 0.04 to 0.15 foot (table 6). Graphical comparisons between observed and computed tidal stages for the first and second verification periods are shown in figures 14 and 15, respectively. Some difference between observed and computed stages is expected since all model adjustments were designed to make model computations match calibration period field observations as closely as possible. Adjustments were not made for verification periods. The fact that the standard errors are about the same for all three periods lends credibility to the model's capability to accurately simulate real conditions.

Table 6.--Standard error of tidal stage for calibration and verification periods

Site (fig. 8)	Station name	Standard error (feet)		
		Calibration	First verification	Second verification
10	Anna Maria	0.04	0.09	0.10
11	South Skyway	.03	.07	.08
12	Port Manatee	.04	.04	.04
15	Ballast Point	.06	.07	.11
16	Rocky Point	.11	.11	.07
17	Safety Harbor	.13	.15	.10
18	Bayview	.13	.15	.11
19	Gandy Bridge	.08	.13	.10
20	St. Petersburg	.05	.06	.09
21	North Skyway	.04	.06	.07
22	Fort De Soto	.04	.06	.07
	Average	.07	.09	.09

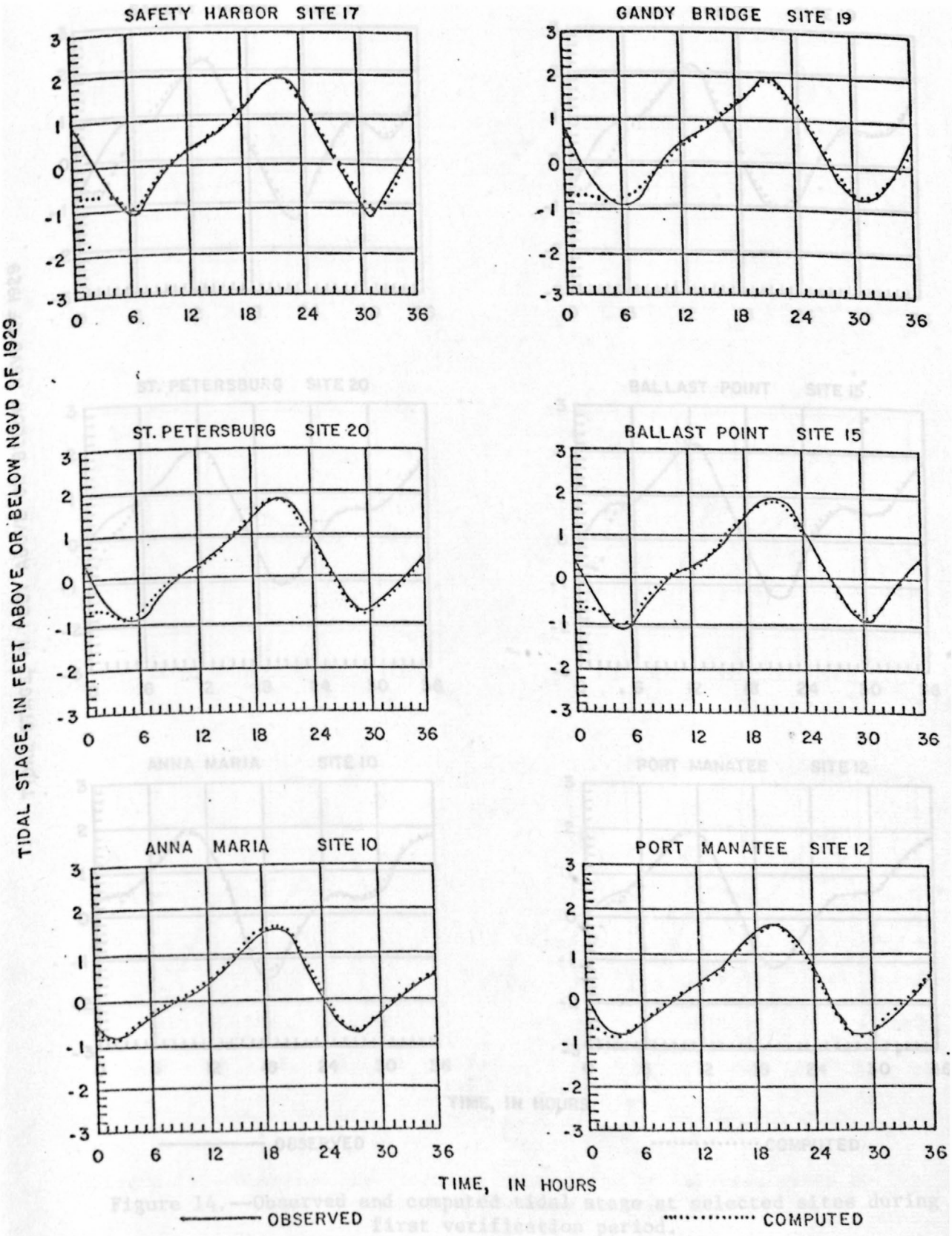

Figure 13.--Observed and computed tidal stage at selected sites during calibration period.

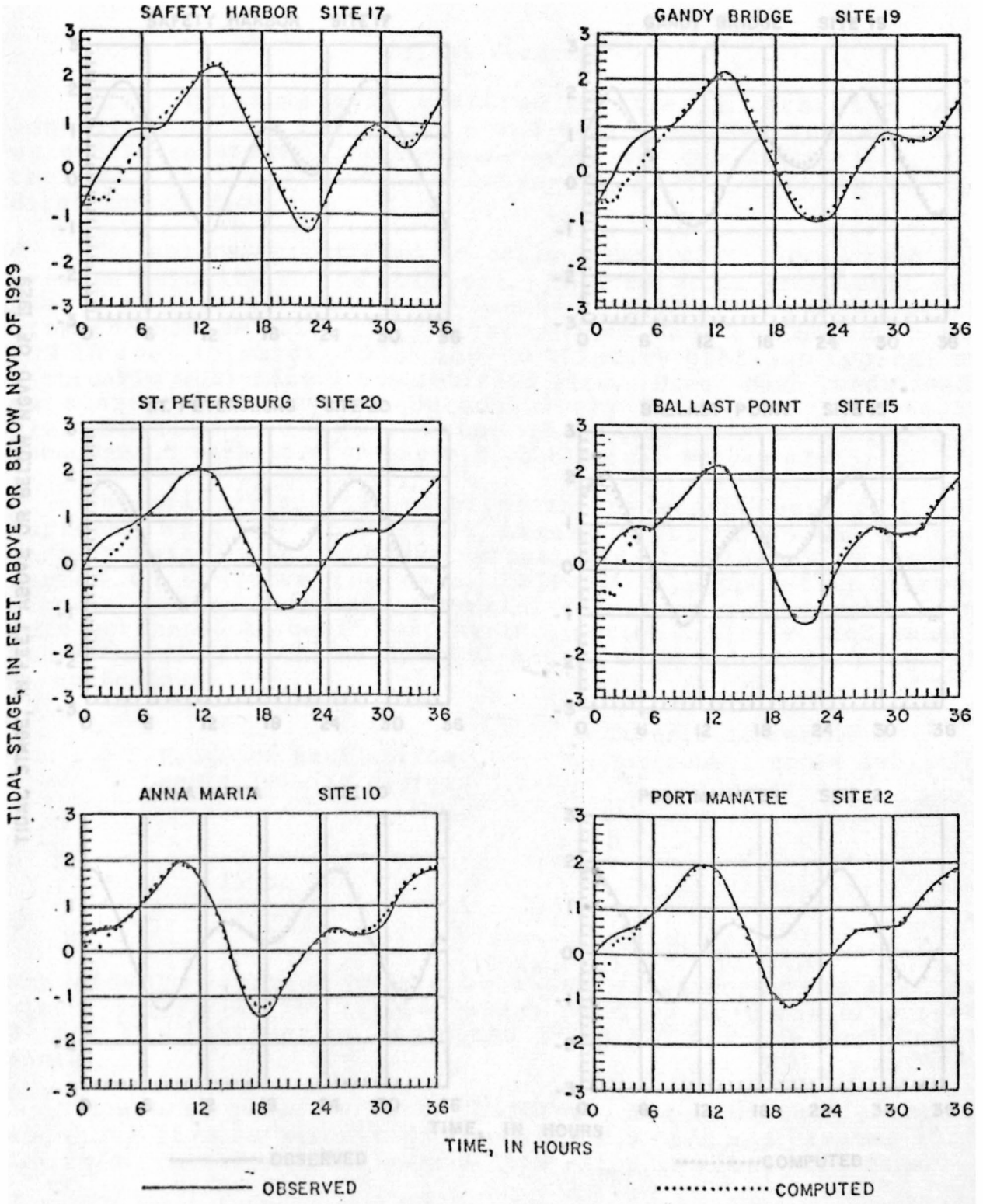

Figure 14.--Observed and computed tidal stage at selected sites during first verification period.

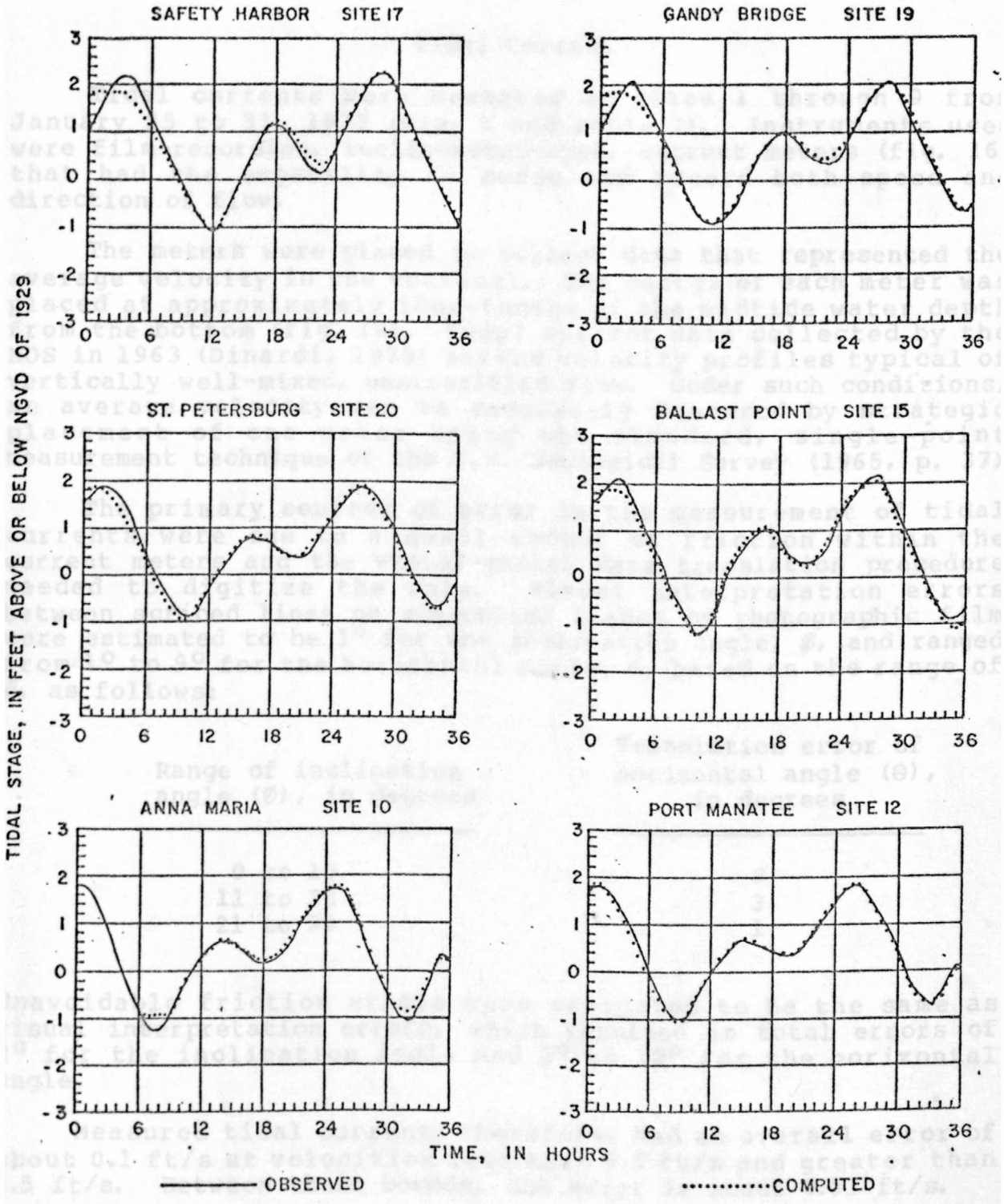

Figure 15.--Observed and computed tidal stage at selected sites during second verification period.

Tidal Current

Tidal currents were measured at sites 1 through 9 from January 25 to 31, 1972 (fig. 8 and table 7). Instruments used were film-recording, inclinometer-type, current meters (fig. 16) that had the capability to sense and record both speed and direction of flow.

The meters were placed to collect data that represented the average velocity in the vertical. The center of each meter was placed at approximately four-tenths of the midtide water depth from the bottom (fig. 16). Tidal current data collected by the NOS in 1963 (Dinardi, 1978) showed velocity profiles typical of vertically well-mixed, unstratified flow. Under such conditions, an average velocity can be adequately measured by strategic placement of one meter using the standard, single-point measurement technique of the U.S. Geological Survey (1965, p. 37).

The primary sources of error in the measurement of tidal currents were due to a small amount of friction within the current meters and the visual-manual data translation procedure needed to digitize the data. Visual interpretation errors between scribed lines on sequential frames of photographic film were estimated to be 1° for the inclination angle, $\emptyset$, and ranged from 1° to 9° for the horizontal angle, θ, based on the range of $\emptyset$, as follows:

Range of inclination angle ($\emptyset$), in degrees	Translation error of horizontal angle (θ), in degrees
0 to 10	9
11 to 20	3
21 to 90	1

Unavoidable friction errors were estimated to be the same as visual interpretation errors, which resulted in total errors of 2° for the inclination angle and 2° to 18° for the horizontal angle.

Measured tidal current, therefore, had an overall error of about 0.1 ft/s at velocities less than 0.5 ft/s and greater than 1.5 ft/s. Between these bounds, the error is about 0.03 ft/s.

Table 7.--Summary of tidal current measurement sites

Site (fig. 8)	North latitude	West longitude
1	27°43'01"	82°36'04"
2	27°42'54"	82°35'18"
3	27°42'59"	82°34'25"
4	27°42'46"	82°33'40"
5	27°42'42"	82°32'28"
6	27°42'39"	82°31'45"
7	27°49'20"	82°26'57"
8	27°49'16"	82°25'44"
9	27°50'57"	82°34'47"
25 Ross Island	27°36'32"	82°34'12"
26 Egmont Channel	27°36'32"	82°46'06"

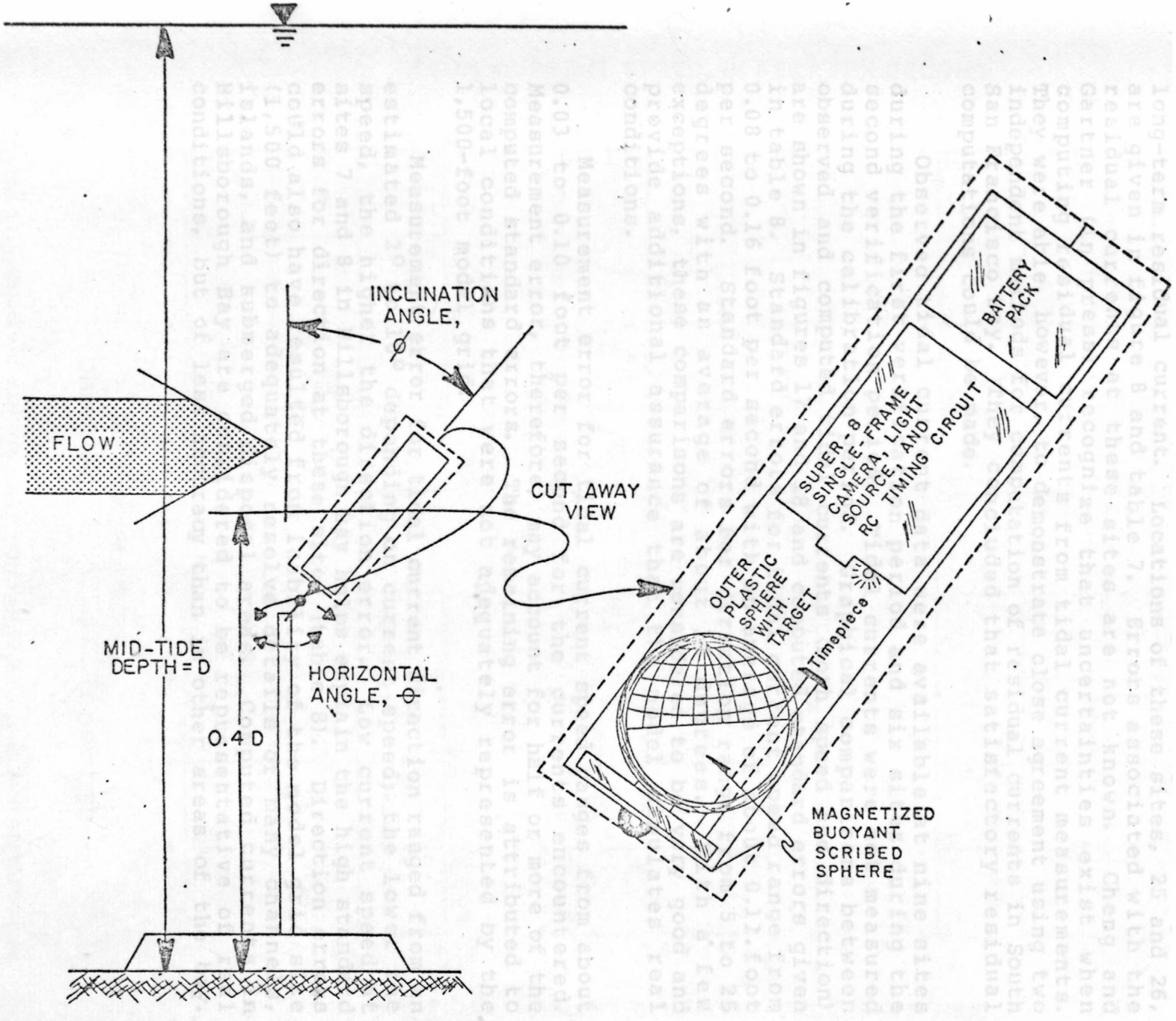

Figure 16.--Inclinometer current-meter placement and operation.

Tidal current data collected at two sites by the NOS in 1963 (Dinardi, 1978) were of sufficient length, 30 days, to compute a long-term residual current. Locations of these sites, 25 and 26, are given in figure 8 and table 7. Errors associated with the residual currents at these sites are not known. Cheng and Gartner (in press) recognize that uncertainties exist when computing residual currents from tidal current measurements. They were able, however, to demonstrate close agreement using two independent methods for computation of residual currents in South San Francisco Bay. They concluded that satisfactory residual computations could be made.

Observed tidal current data were available at nine sites during the first verification period and six sites during the second verification period. Tidal currents were not measured during the calibration period. Graphical comparisons between observed and computed tidal currents (both speed and direction) are shown in figures 17 and 18 and computed standard errors given in table 8. Standard errors for tidal current speed range from 0.08 to 0.16 foot per second with an average of about 0.11 foot per second. Standard errors for direction range from 5 to 25 degrees with an average of about 14 degrees. With a few exceptions, these comparisons are considered to be very good and provide additional assurance that the model simulates real conditions.

Measurement error for tidal current speed ranges from about 0.03 to 0.10 foot per second for the currents encountered. Measurement error, therefore, may account for half or more of the computed standard errors. The remaining error is attributed to local conditions that were not adequately represented by the 1,500-foot model grid.

Measurement error for tidal current direction ranged from an estimated 2° to 18° depending on current speed; the lower the speed, the higher the direction error. Low current speed at sites 7 and 8 in Hillsborough Bay helps explain the high standard errors for direction at these sites (table 8). Direction errors could also have resulted from inability of the model grid size (1,500 feet) to adequately resolve details of many channels, islands, and submerged disposal areas. Computed currents in Hillsborough Bay are considered to be representative of real conditions, but of less accuracy than in other areas of the bay.

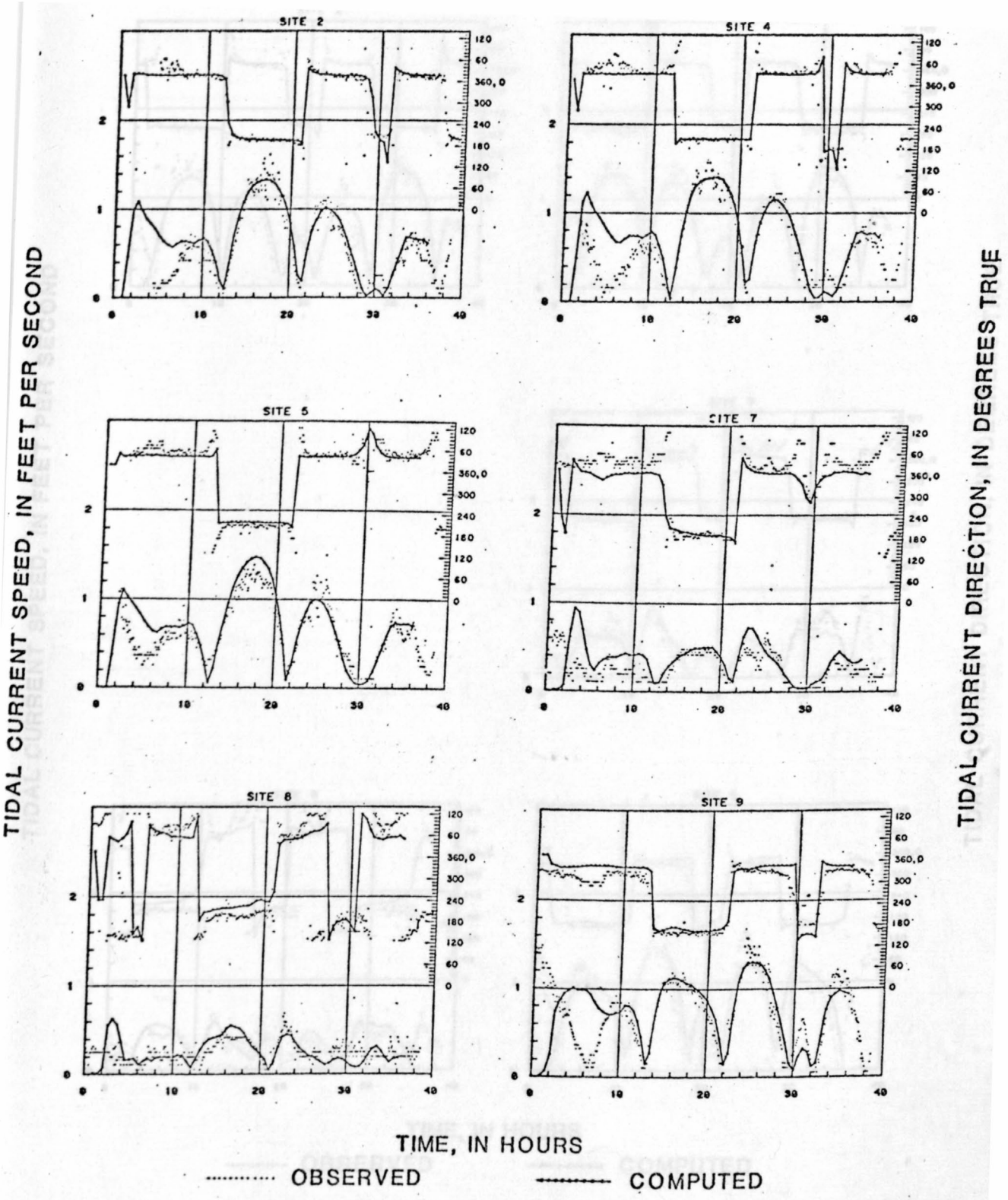

Figure 17.--Observed and computed tidal current speed and direction at selected sites during first verification period.

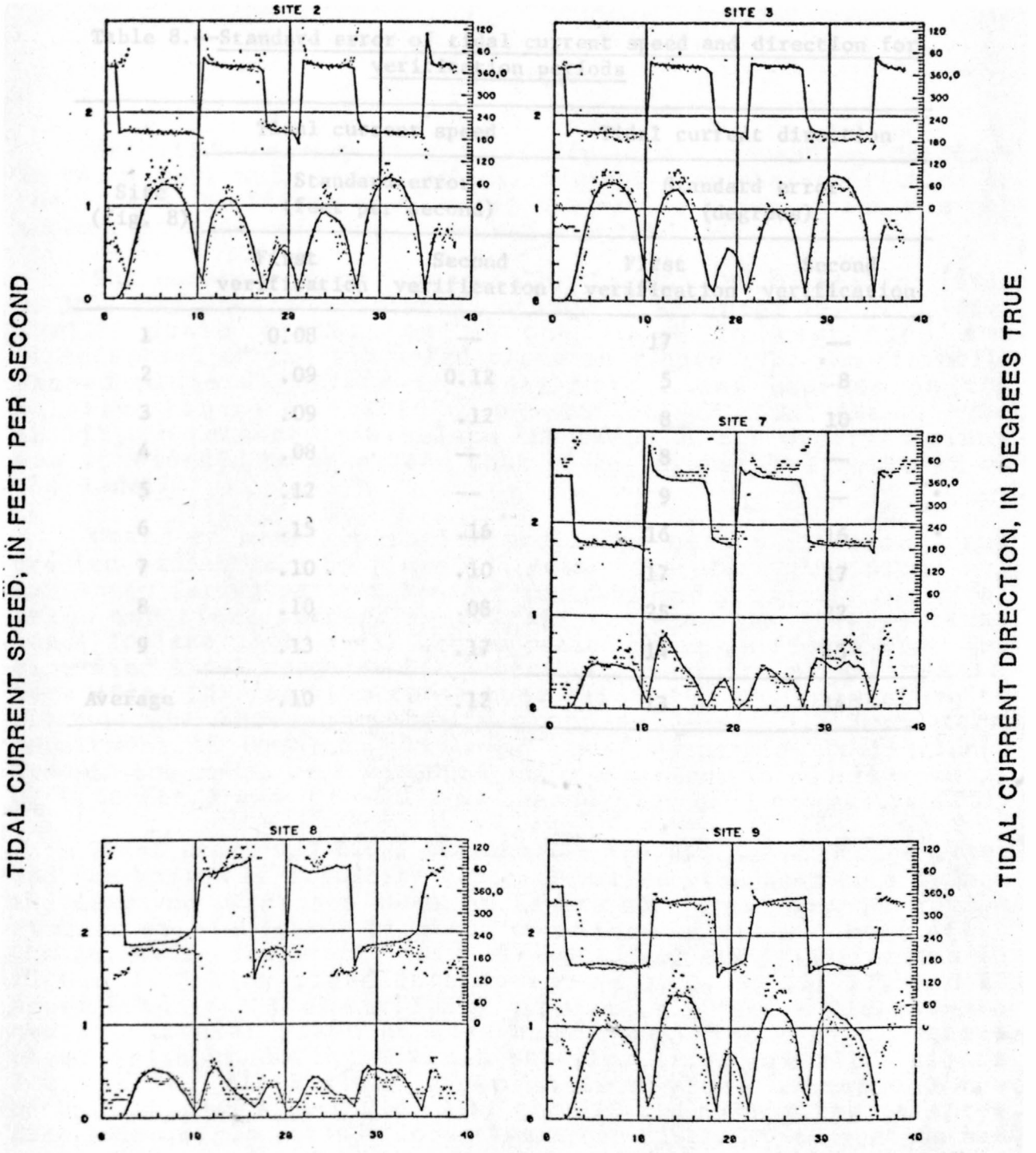

Figure 18.--Observed and computed tidal current speed and direction at selected sites during second verification period.

Table 8.--Standard error of tidal current speed and direction for verification periods

Site (fig. 8)	Tidal current speed		Tidal current direction	
	Standard error (feet per second)		Standard error (degrees)	
	First verification	Second verification	First verification	Second verification
1	0.08	--	17	--
2	.09	0.12	5	8
3	.09	.12	8	10
4	.08	--	8	--
5	.12	--	9	--
6	.15	.16	16	16
7	.10	.10	17	17
8	.10	.08	25	22
9	.13	.17	14	13
Average	.10	.12	13	14

Dispersion

Satellite imagery of a turbidity plume, caused by dredging in Tampa Bay, was used to calibrate dispersive characteristics of the model. Verification of model dispersive capabilities was not accomplished as only one plume was simulated.

The observed plume, reported by Goodwin and Michaelis (1981, p. 38), was created by a shell dredge on November 17, 1972 (fig. 19a). Scale distortion of the image is rectified and superimposed on the simulated plume in figure 19b. The "barbell" shaped plume is unique to tidal waters and depends on the relative timing of turbidity generation and tidal phase. The ability to reasonably simulate the shape of the observed plume was considered to be a good test of the dispersive features of the model.

Costs of model operation precluded making a separate run devoted exclusively to plume analysis. Therefore, the plume was simulated during part of a model run designed primarily for tidal stage and tidal current verification. (See the driving tidal stage for the first verification period shown in figure 11.) The simulated tidal range at St. Petersburg, near the plume, was 3.1 feet (fig. 14), and the range that existed at St. Petersburg to produce the observed plume was approximately 1.9 feet (U.S. Department of Commerce, 1971, p. 129). Dispersion coefficients used in the model were computed using equations 10 and 11 with $D_w = 50\ ft^2/s$ and $d = 25$ (J. J. Leendertse, oral commun., 1980).

Tidal stage and tidal current (at the simulated dredge site) and the period of turbidity generation that were used to simulate the observed plume are shown in figure 20. Turbidity generation started at high slack tide and continued to about 1 hour after the following low slack tide. The series of six illustrations in figure 21 follow plume development at 1, 5, 9, 13, 17, and 23 hours after start of turbidity generation. Figure 21a shows a nearly circular plume at near high slack tide. An elongated plume is shown during maximum ebb flow in figure 21b. Figure 21c, at low slack tide, shows maximum plume extent and the barbell shape. Figure 21d, 21e, and 21f show the plume at three succeeding times during flood flow after turbidity generation had stopped.

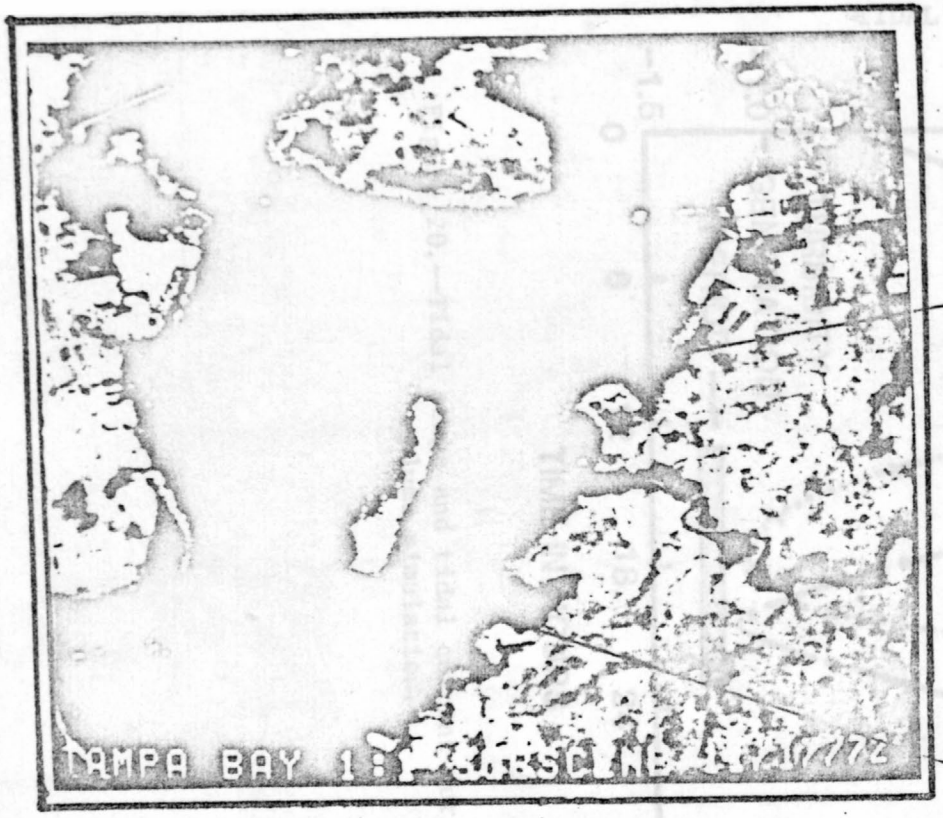

a. Satellite image

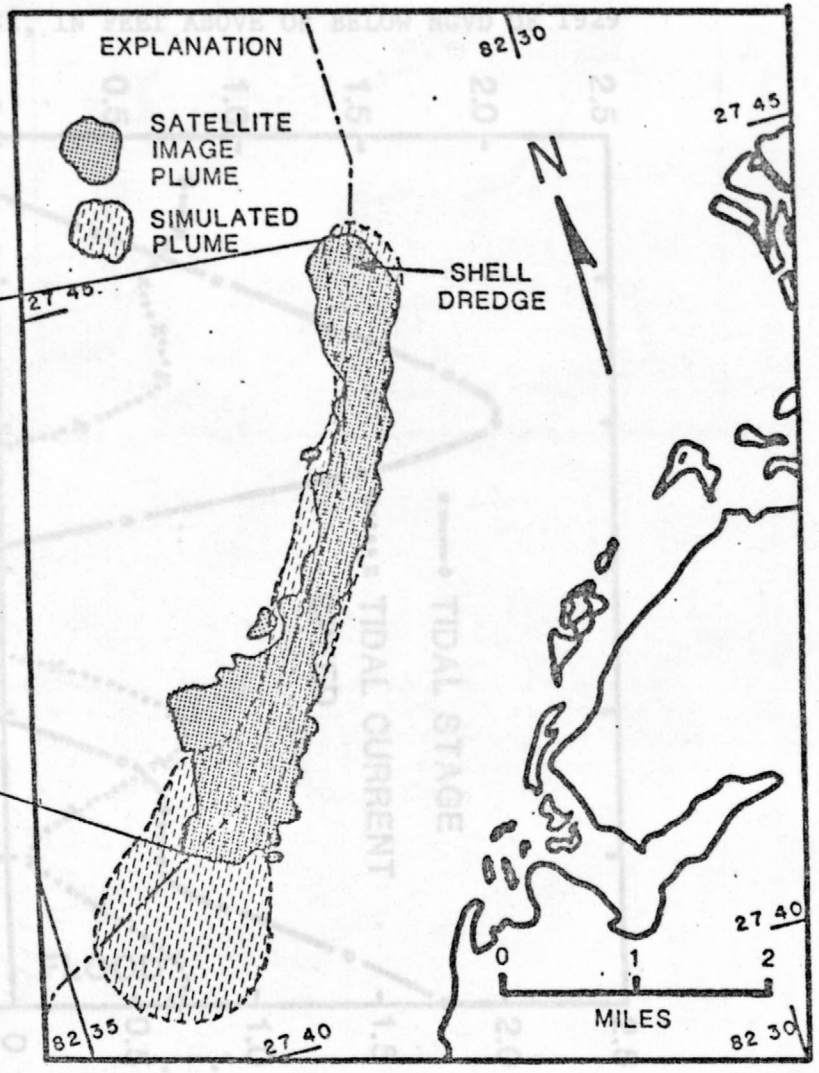

b. Comparison of satellite image and simulated turbidity plumes.

Figure 19.--Satellite image of turbidity plume in Tampa Bay and comparison with simulated plume.

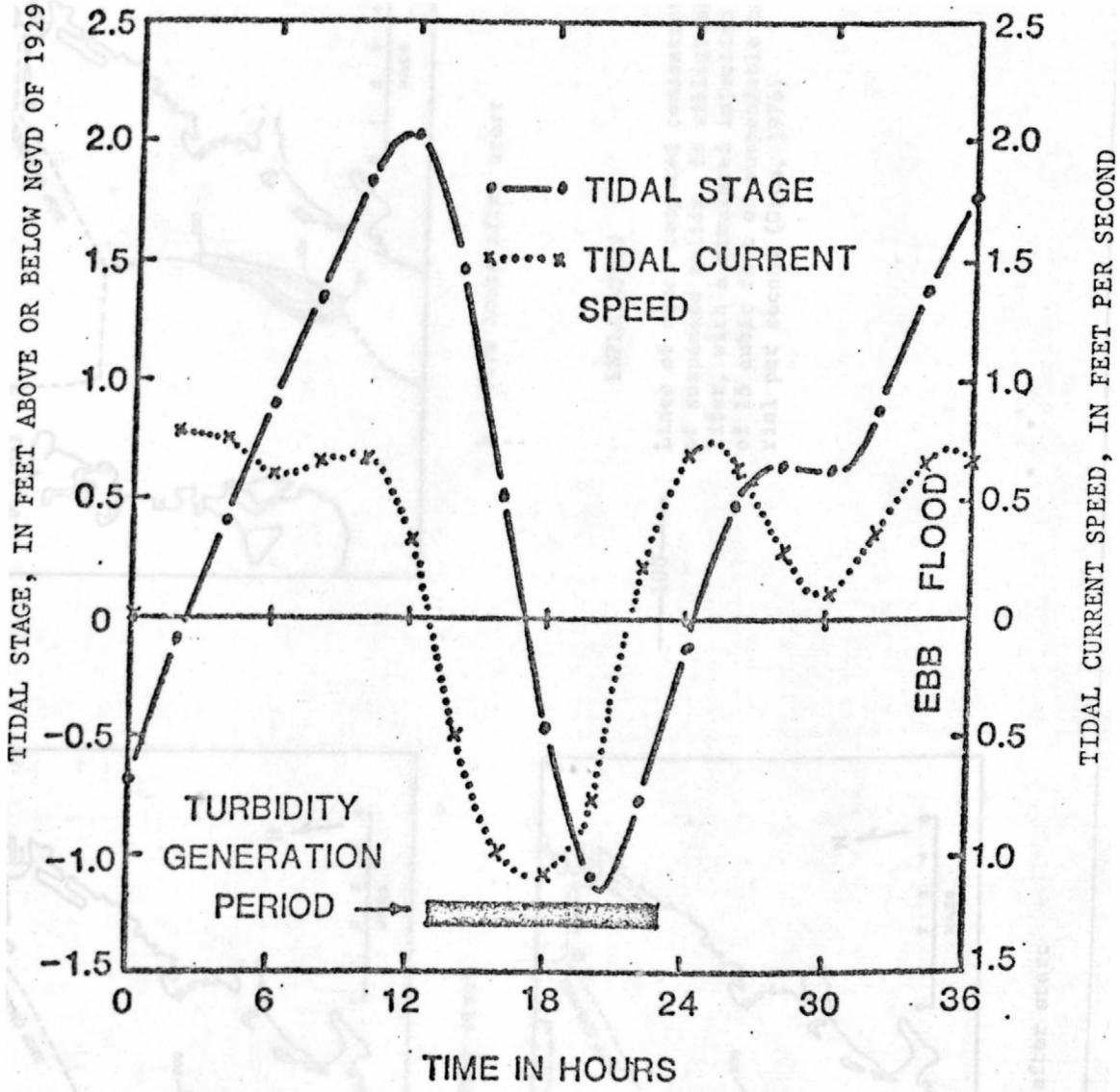

Figure 20.--Tidal stage and tidal current during turbidity plume simulation.

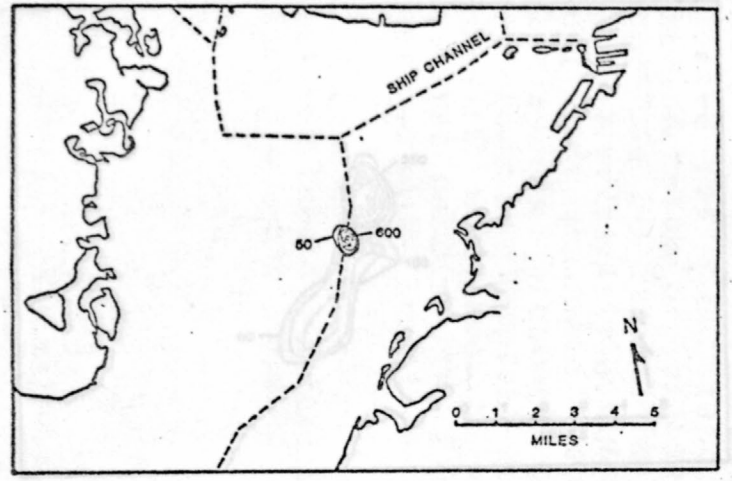

a. One hour after start

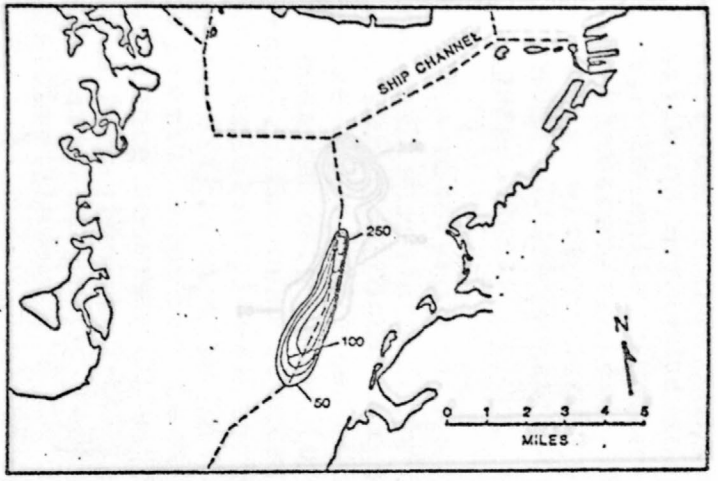

b. Five hours after start

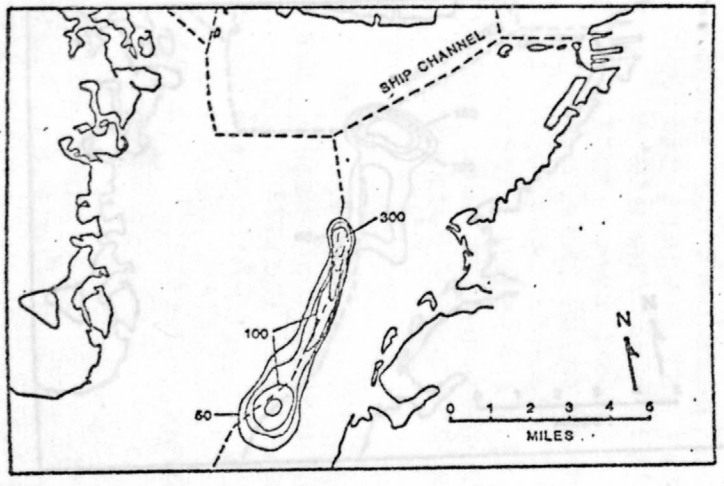

c. Nine hours after start

EXPLANATION

——100—— Lines of equal computed concentration of suspended solids, in milligrams per liter, with a simulated injection rate of 15 cubic feet of suspendable material per second (Gren, 1976)

Figure 21.--Shape of simulated turbidity plume at selected times following start of turbidity generation.

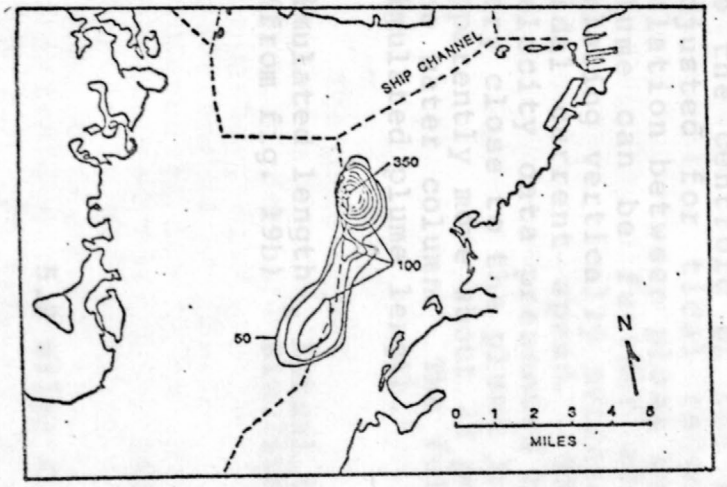

d. Thirteen hours after start

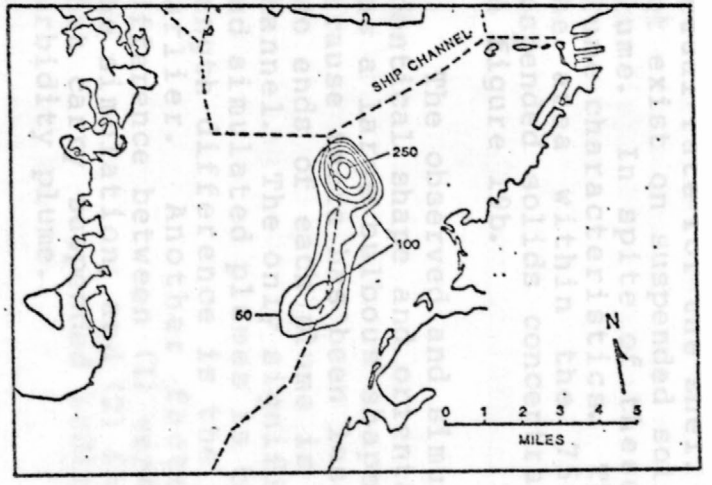

e. Seventeen hours after start

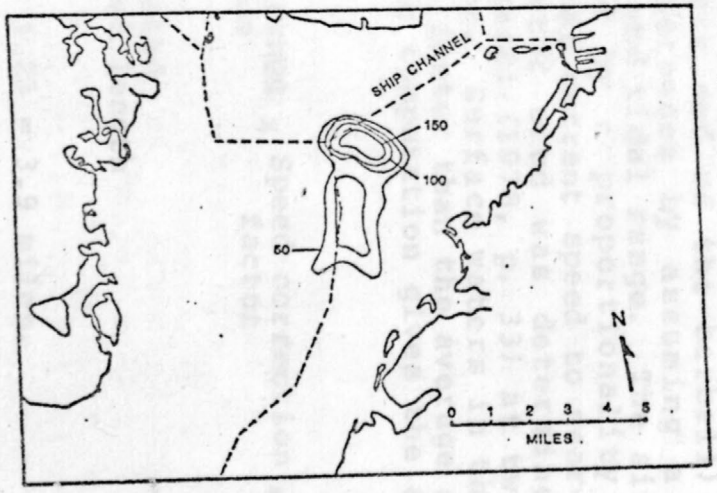

f. Twenty-three hours after start

EXPLANATION

——100—— Lines of equal computed concentration of suspended solids, in milligrams per liter, with a simulated injection rate of 15 cubic feet of suspendable material per second (Gren, 1976)

Figure 21.--Shape of simulated turbidity plume at selected times following start of turbidity generation--Continued.

A typical suspended solids discharge rate was used from the literature (Gren, 1976) to develop the simulated plume since the actual rate for the shell dredge was not known. Also, data did not exist on suspended solids concentrations within the observed plume. In spite of these drawbacks, the model did reproduce plume characteristics. The best visual comparison is shown by the area within the 75-milligram-per-liter line of equal suspended solids concentration in figure 21c that is reproduced in figure 19b.

The observed and simulated plumes in figure 19b show nearly identical shape and orientation. The southern end of each plume has a large bulbous shape. The northern ends show less bulge because there has been less time for dispersion. Connecting the two ends of each plume is a narrow section that follows the ship channel. The only significant difference between the observed and simulated plumes is their lengths. One factor causing the length difference is the inequality of tidal ranges mentioned earlier. Another factor affecting plume lengths is the difference between (1) vertically averaged tidal currents used in the simulation, and (2) faster near-surface currents in the bay that carry suspended sediment particles comprising the observed turbidity plume.

A comparison between simulated and observed plume lengths can be made by adjusting results shown in figure 19b for the effects of different tidal ranges and different current speeds. The length of the simulated plume (measured from the shell dredge to the centroid of the southern end of the barbell) can be adjusted for tidal range differences by assuming a linear relation between plume length and tidal range. The simulated plume can be further adjusted by a proportionality factor relating vertically averaged tidal current speed to near-surface tidal current speed. The factor used was determined from velocity data presented by Dinardi (1978, p. 33) at two sites very close to the plume location. Surface waters in this area apparently move about 23 percent faster than the average speed in the water column. The following computation gives the adjusted simulated plume length.

$$\text{Simulated length (from fig. 19b)} \times \frac{\text{Actual tidal range}}{\text{Simulated range}} \times \text{Speed correction factor} = \text{Adjusted simulated length} \qquad (17)$$

$$5.2 \text{ miles} \times \frac{1.9}{3.1} \times 1.23 = 3.9 \text{ miles.}$$

This compares very well with the length of the observed plume, 4.0 miles, as measured from figure 19b. The general agreement between observed and simulated turbidity plumes indicates that the dispersive features of the model adequately simulate real conditions.

Application to 1880, 1972, and 1985 Levels of Development

The model, following calibration and verification, was applied to determine flow, circulation, and flushing characteristics of Tampa Bay for historical (1880), predredging (1972), and postdredging (1985) levels of development. The following sections define the bottom configuration, boundary conditions, and initial conditions used for each application.

Bottom Configurations

The bay shorelines and areas of bottom changes for 1880, 1972, and 1985 are shown in figures 3 and 4. In 1880, the bottom configuration was characterized by gradually varying depths in most parts of the bay. Notable exceptions occur at the northern end of Egmont Key and at the mouth of Old Tampa Bay. Several islands existed near the mouth of Tampa Bay and at other locations around the bay periphery. The 1972 bottom configuration was characterized by broad areas of slowly changing depths interrupted by extensive manmade linear features, channels and islands, alined perpendicular and parallel to the major axis of the bay. In 1985, the bottom will have additional physical changes that include large disposal islands in Hillsborough Bay and more extensive submerged mounds along a deepened and widened ship channel.

Boundary Conditions

The same repeating tide was used as the open-water boundary condition for model application to the 1880, 1972, and 1985 levels of development. Of the three types of tides that occur in Tampa Bay, diurnal, semidiurnal, and mixed (fig. 2), the most prevalent is the mixed tide that has two unequal high tides and two unequal low tides during each cycle. Although diurnal and semidiurnal tides occur regularly, the mixed tide occurs most frequently and was therefore chosen for model application. A mixed tide similar to that measured during the second verification period (fig. 11) was used as the repeating tide (fig. 22). To simplify analysis of results, the tidal period was adjusted to 24 hours (an even multiple of the time step) and small irregularities in the second verification tide were eliminated by assuring smooth first and second differences in tidal stage (table 9).

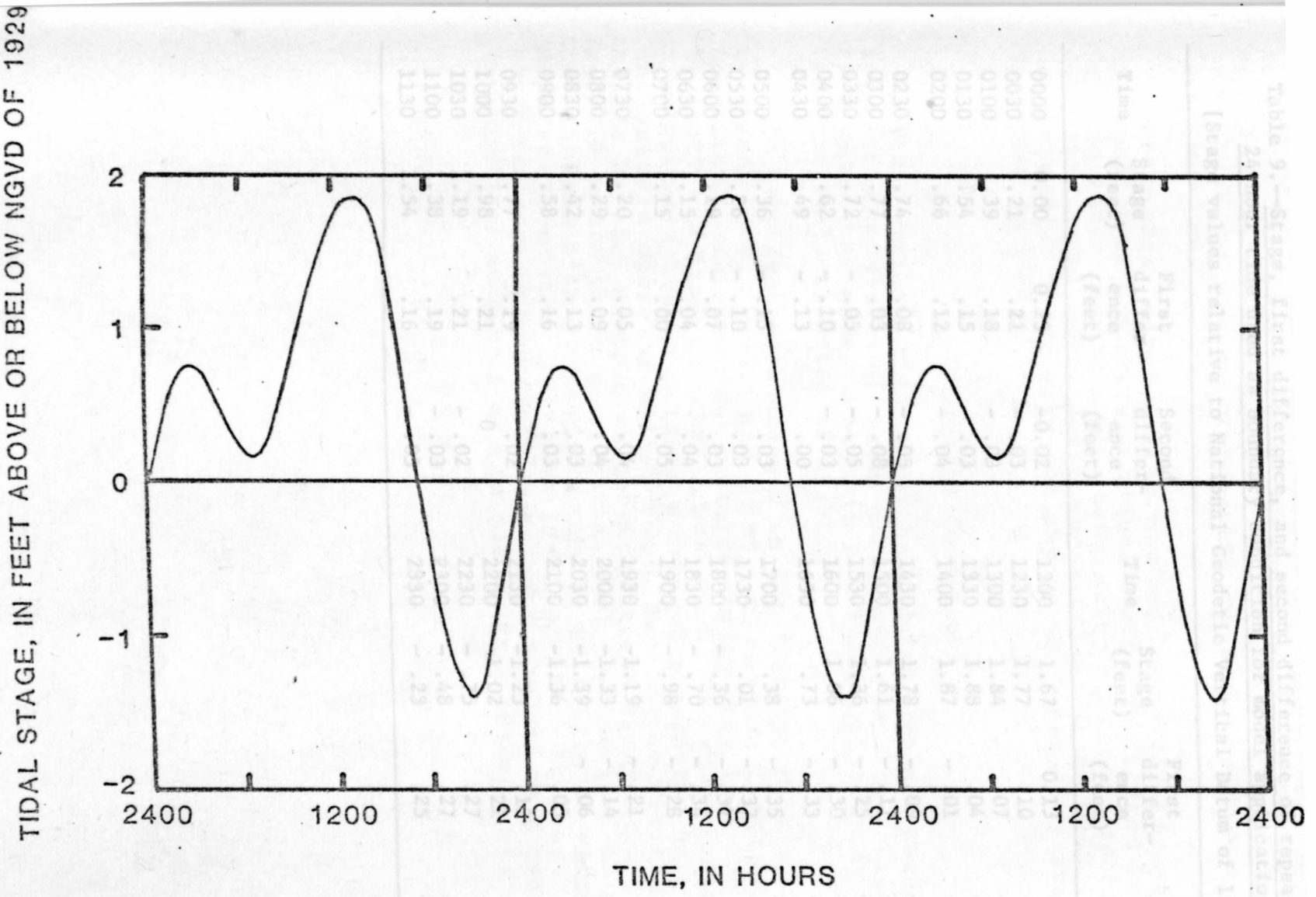

Figure 22.--Repeating, 24-hour tide used as boundary condition for model application.

Table 9.--Stage, first difference, and second difference of repeating, 24-hour tide used as boundary condition for model application

[Stage values relative to National Geodetic Vertical Datum of 1929]

Time	Stage (feet)	First difference (feet)	Second difference (feet)	Time	Stage (feet)	First difference (feet)	Second difference (feet)
0000	0.00	0.23	-0.02	1200	1.67	0.13	-0.03
0030	.21	.21	- .03	1230	1.77	.10	- .03
0100	.39	.18	- .03	1300	1.84	.07	- .03
0130	.54	.15	- .03	1330	1.88	.04	- .05
0200	.66	.12	- .04	1400	1.87	- .01	- .08
0230	.74	.08	- .05	1430	1.78	- .09	- .08
0300	.77	.03	- .08	1500	1.61	- .17	- .08
0330	.72	- .05	- .05	1530	1.36	- .25	- .05
0400	.62	- .10	- .03	1600	1.06	- .30	- .03
0430	.49	- .13	.00	1630	.73	- .33	- .02
0500	.36	- .13	.03	1700	.38	- .35	- .02
0530	.26	- .10	.03	1730	.01	- .37	.00
0600	.19	- .07	.03	1800	- .36	- .37	.03
0630	.15	- .04	.04	1830	- .70	- .34	.06
0700	.15	.00	.05	1900	- .98	- .28	.07
0730	.20	.05	.04	1930	-1.19	- .21	.07
0800	.29	.09	.04	2000	-1.33	- .14	.08
0830	.42	.13	.03	2030	-1.39	- .06	.09
0900	.58	.16	.03	2100	-1.36	.03	.10
0930	.77	.19	.02	2130	-1.23	.13	.08
1000	.98	.21	0	2200	-1.02	.21	.06
1030	1.19	.21	- .02	2230	- .75	.27	.00
1100	1.38	.19	- .03	2300	- .48	.27	- .02
1130	1.54	.16	- .03	2330	- .23	.25	- .02

An assumed zero wind condition was considered least likely to mask tidal flow, circulation, and flushing changes, so it was used for all model applications. Changes in flow, circulation, and flushing due to wind were beyond the scope of this investigation.

Freshwater river inflow was held constant for each model application at the average annual discharges listed in table 3. Cooling water used by power generating stations was treated as described under model development for 1972 and 1985 levels of development. There were not any power generating stations on Tampa Bay in 1880.

Initial Conditions

Tidal currents throughout the modeled area are assumed to be zero at the start of each model application. Tidal stage throughout the modeled area is initially constant at National Geodetic Vertical Datum of 1929.

To help determine changes in the flushing rate of Tampa Bay between 1880, 1972, and 1985, a single, representative constituent distribution, measured during July 1975 and reported by Goetz and Goodwin (1980), was used. The distribution (fig. 23) indicates that a primary source of phosphorus existed along the eastern shore of Hillsborough Bay in the vicinity of the Alafia River. Phosphorus concentrations throughout Tampa Bay were 10 to 100 times greater than that hypothesized to be needed to maintain primary productivity in this area of Florida (U.S. Department of the Interior, 1969, p. 24). At these elevated concentrations, phosphorus can be considered to be a conservative (nonreactive) substance and is useful as a tracer.

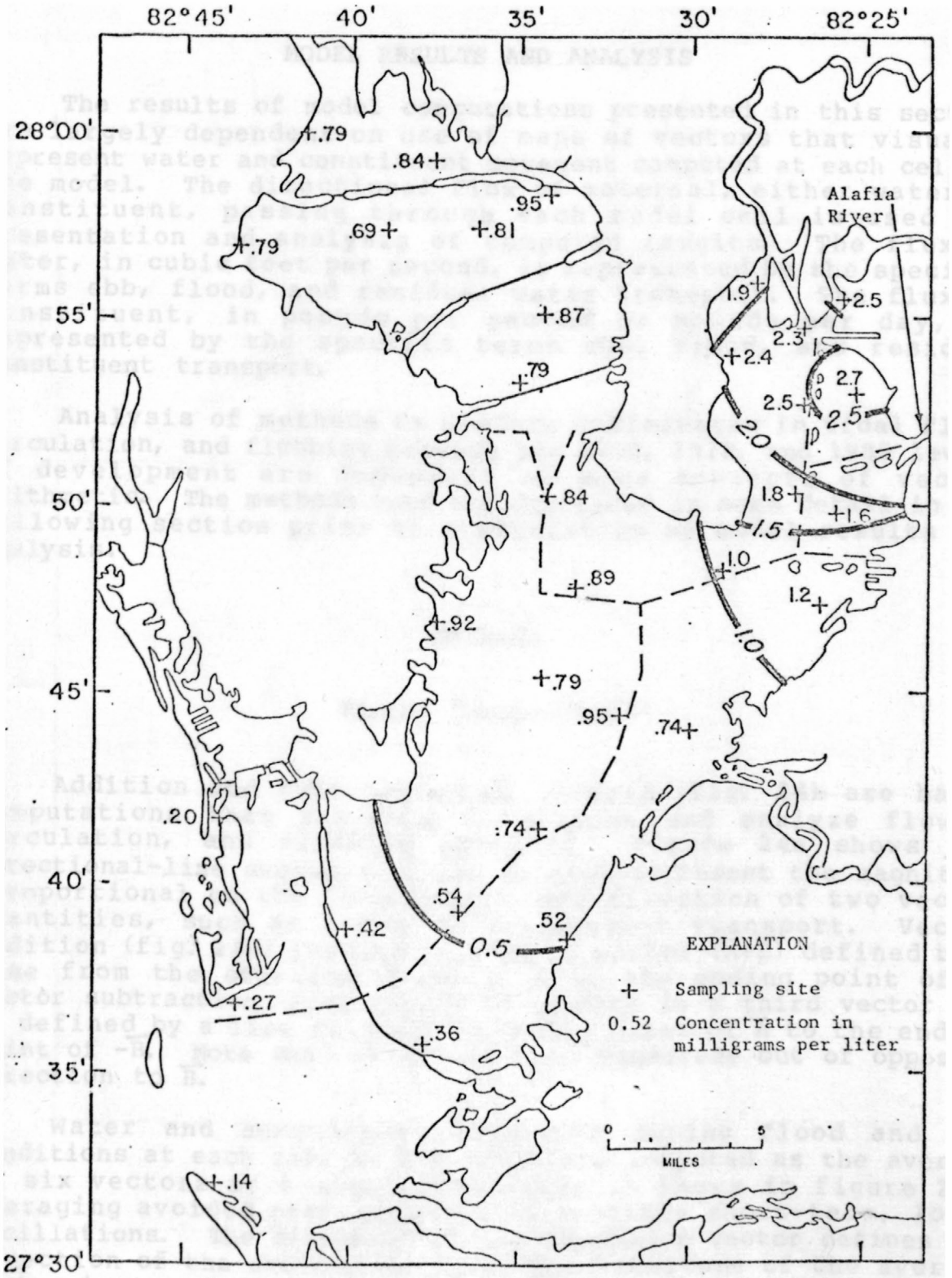

Figure 23.--Phosphorus distribution in Tampa Bay, July 1975 (from Goetz and Goodwin, 1980).

MODEL RESULTS AND ANALYSIS

The results of model computations presented in this section are largely dependent on use of maps of vectors that visually represent water and constituent movement computed at each cell of the model. The directional flux of material, either water or constituent, passing through each model cell is used for presentation and analysis of computed results. The flux of water, in cubic feet per second, is represented by the specific terms ebb, flood, and residual water transport. The flux of constituent, in pounds per second or pounds per day, is represented by the specific terms ebb, flood, and residual constituent transport.

Analysis of methods to discern differences in tidal flow, circulation, and flushing between the 1880, 1972, and 1985 levels of development are dependent on some concepts of vector arithmetic. The methods used are described in some detail in the following section prior to presentation of model results and analysis.

Methods

Vector Computations

Addition and subtraction of vectors (fig. 24) are basic computations that are used to present and analyze flow, circulation, and flushing patterns. Figure 24a shows two directional-line segments, $\overline{A}$ and $\overline{B}$, that represent the magnitude (proportional to the line length) and direction of two vector quantities, such as water or constituent transport. Vector addition (fig. 24b) results in a third vector $(\overline{A}+\overline{B})$ defined by a line from the starting point of $\overline{A}$ to the ending point of $\overline{B}$. Vector subtraction (fig. 24c) also results in a third vector $(\overline{A}-\overline{B})$ defined by a line from the starting point of $\overline{A}$ to the ending point of $-\overline{B}$. Note that $-\overline{B}$ is the same magnitude but of opposite direction to $\overline{B}$.

Water and constituent transport during flood and ebb conditions at each cell in the model are computed as the average of six vectors at 5-minute intervals as shown in figure 25a. Averaging avoided over-emphasis of possible short-term, local oscillations. The direction of the summation vector defines the direction of the average vector. The magnitude of the average vector is one-sixth the summation vector.

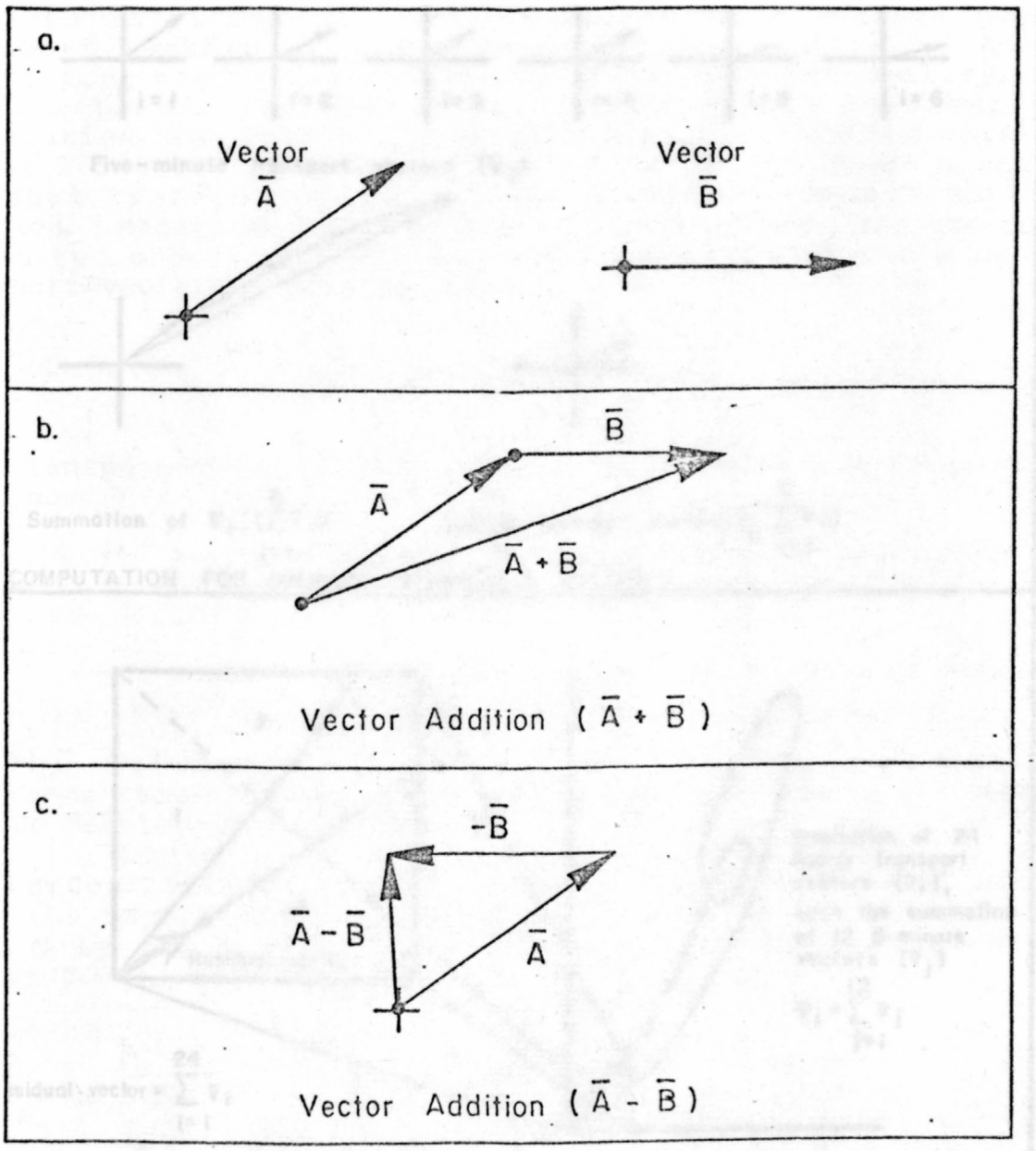

Figure 24.--Computations for vector addition and subtraction.

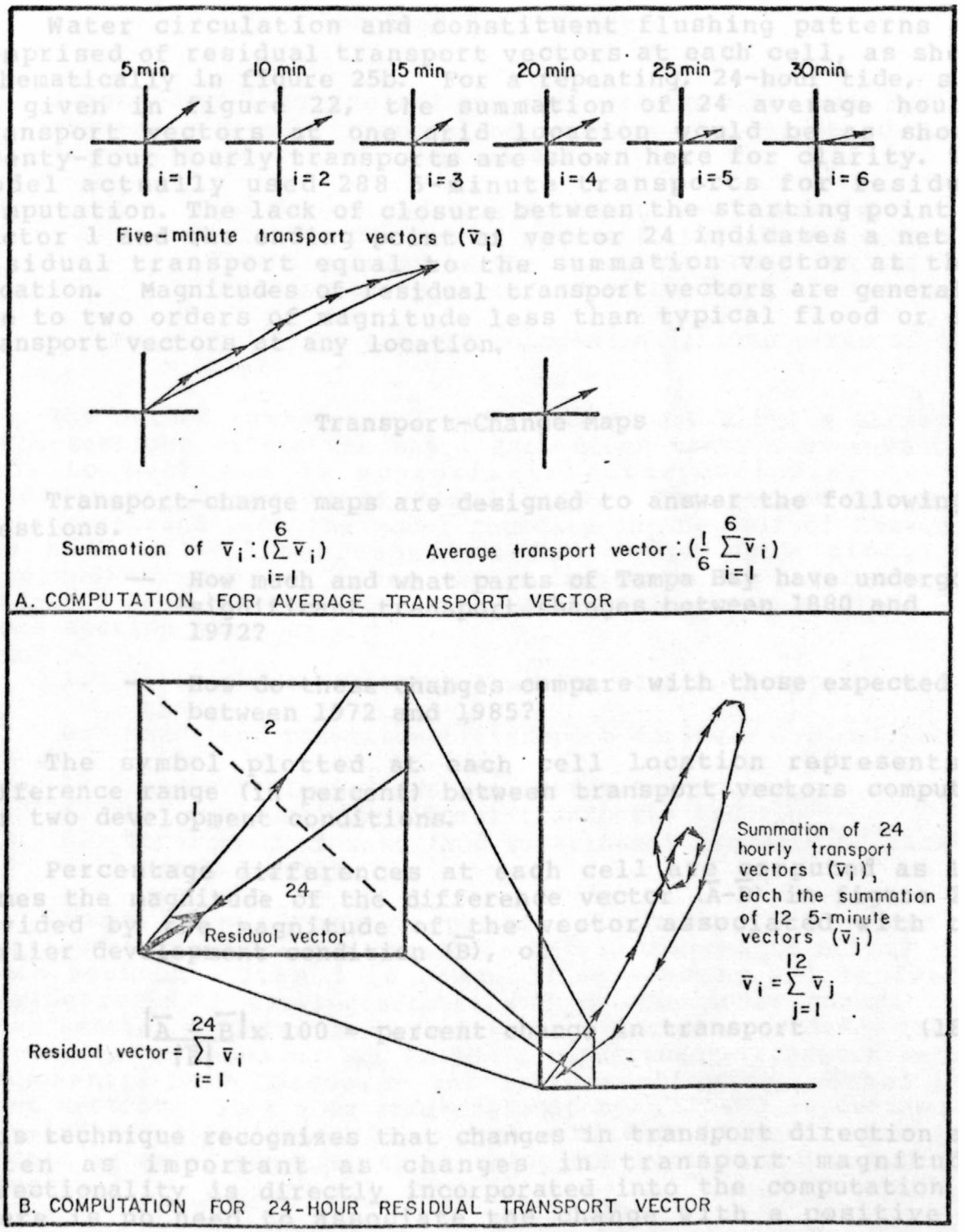

Figure 25.--Computations for flood, ebb, and residual transport vectors.

Water circulation and constituent flushing patterns are comprised of residual transport vectors at each cell, as shown schematically in figure 25b. For a repeating, 24-hour tide, such as given in figure 22, the summation of 24 average hourly transport vectors at one grid location would be as shown. Twenty-four hourly transports are shown here for clarity. The model actually used 288 5-minute transports for residual computation. The lack of closure between the starting point of vector 1 and the ending point of vector 24 indicates a net or residual transport equal to the summation vector at that location. Magnitudes of residual transport vectors are generally one to two orders of magnitude less than typical flood or ebb transport vectors at any location.

Transport-Change Maps

Transport-change maps are designed to answer the following questions.

-- How much and what parts of Tampa Bay have undergone significant transport changes between 1880 and 1972?

-- How do these changes compare with those expected between 1972 and 1985?

The symbol plotted at each cell location represents a difference range (in percent) between transport vectors computed for two development conditions.

Percentage differences at each cell are computed as 100 times the magnitude of the difference vector ($\bar{A}-\bar{B}$) in figure 24c divided by the magnitude of the vector associated with the earlier development condition ($\bar{B}$), or

$$\frac{|\bar{A} - \bar{B}|}{|\bar{B}|} \times 100 = \text{percent change in transport} \qquad (18)$$

This technique recognizes that changes in transport direction are often as important as changes in transport magnitude. Directionality is directly incorporated into the computation so there is no need to associate the change with a positive or negative concept of directionality.

Longitudinal Summary

A method of longitudinal summary was developed to further evaluate the effect of changes indicated by the transport-change maps to answer the following questions.

-- Has dredge and fill construction (channels, islands, causeways, and so forth) caused significant changes to the overall circulation and flushing characteristics of the bay?

-- How large are the changes in various parts of the bay?

The method summarizes computed transport along a series of cross sections within the bay. Each cross section extends from bank to bank and is approximately perpendicular to the predominant direction of tidal flow. The series of cross sections extend from the model boundary in the Gulf of Mexico to the head of Hillsborough and Old Tampa Bays along the longitudinal summary lines shown in figure 26. Information extracted from the model for each level of development along each cross section include:

1. Water and constituent transport during a typical flood tide;
2. Water and constituent transport during a typical ebb tide;
3. Landward-flowing residual water transport;
4. Net residual constituent transport; and
5. Total mass of water and constituent landward of each cross section.

Items 1 and 2 are computed by summing all water or constituent, flood or ebb transport-vector components normal to a cross section. Item 3 is computed by summing all landward-flowing residual water-transport vector components normal to a cross section. Gulfward-flowing vectors are disregarded. Item 4 is computed by summing all residual constituent-transport vector components, both landward- and Gulfward-flowing, normal to a cross section. Item 5 is self-explanatory. Item 3 is defined as tide-induced circulation for purposes of this report. Item 4 is defined as total constituent flushing due to tide and streamflow effects.

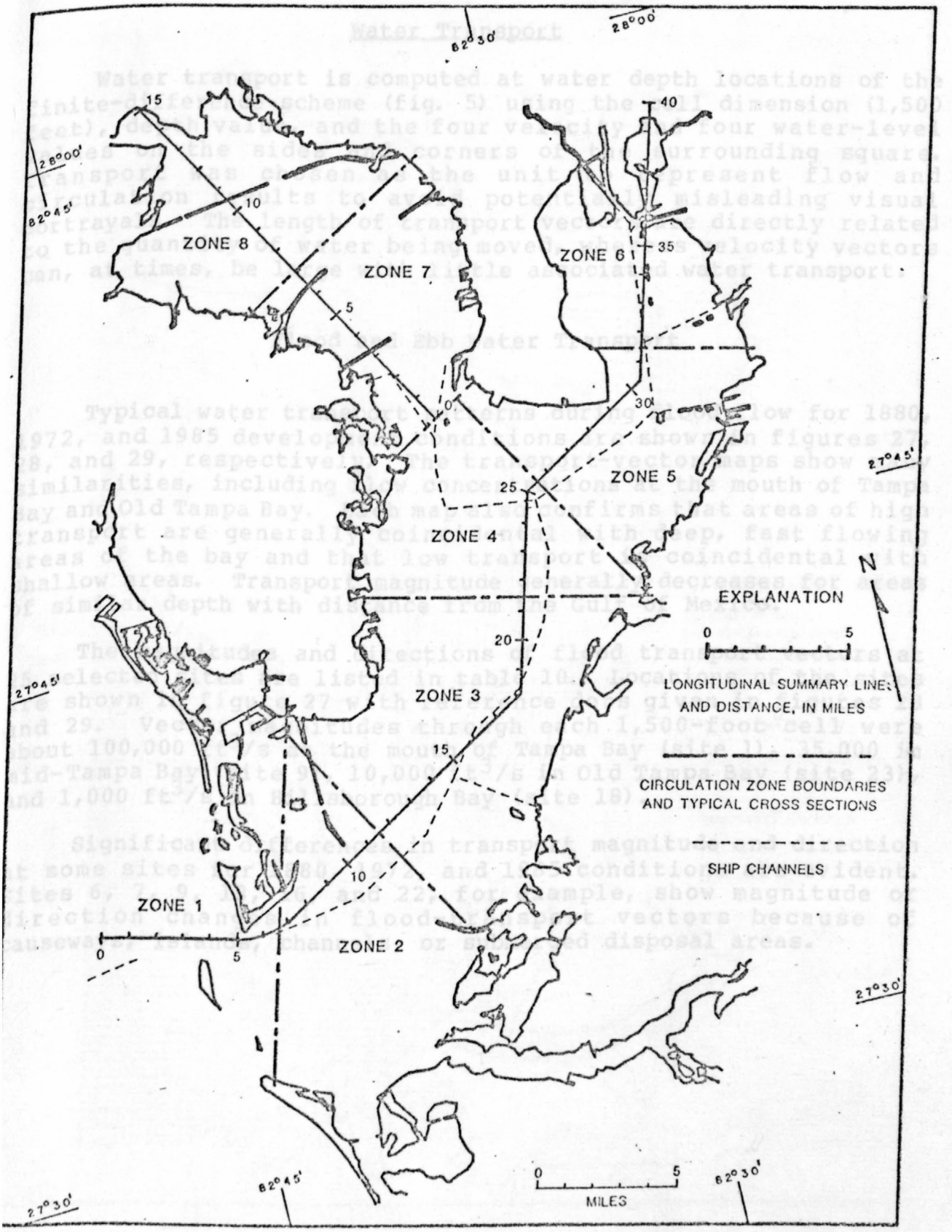

Figure 26.--Longitudinal summary lines and circulation zones.

Water Transport

Water transport is computed at water depth locations of the finite-difference scheme (fig. 5) using the cell dimension (1,500 feet), depth value, and the four velocity and four water-level values on the sides and corners of the surrounding square. Transport was chosen as the unit to represent flow and circulation results to avoid potentially misleading visual portrayals. The length of transport vectors are directly related to the quantity of water being moved, whereas velocity vectors can, at times, be large with little associated water transport.

Flood and Ebb Water Transport

Typical water transport patterns during flood flow for 1880, 1972, and 1985 development conditions are shown in figures 27, 28, and 29, respectively. The transport-vector maps show many similarities, including flow concentrations at the mouth of Tampa Bay and Old Tampa Bay. Each map also confirms that areas of high transport are generally coincidental with deep, fast flowing areas of the bay and that low transport is coincidental with shallow areas. Transport magnitude generally decreases for areas of similar depth with distance from the Gulf of Mexico.

The magnitudes and directions of flood transport vectors at 25 selected sites are listed in table 10. Locations of the sites are shown in figure 27 with reference dots given in figures 28 and 29. Vector magnitudes through each 1,500-foot cell were about 100,000 ft^3/s at the mouth of Tampa Bay (site 1), 35,000 in mid-Tampa Bay (site 9), 10,000 ft^3/s in Old Tampa Bay (site 23), and 1,000 ft^3/s in Hillsborough Bay (site 18).

Significant differences in transport magnitude and direction at some sites for 1880, 1972, and 1985 conditions are evident. Sites 6, 7, 9, 13, 16, and 22, for example, show magnitude or direction changes in flood-transport vectors because of causeways, islands, channels, or submerged disposal areas.

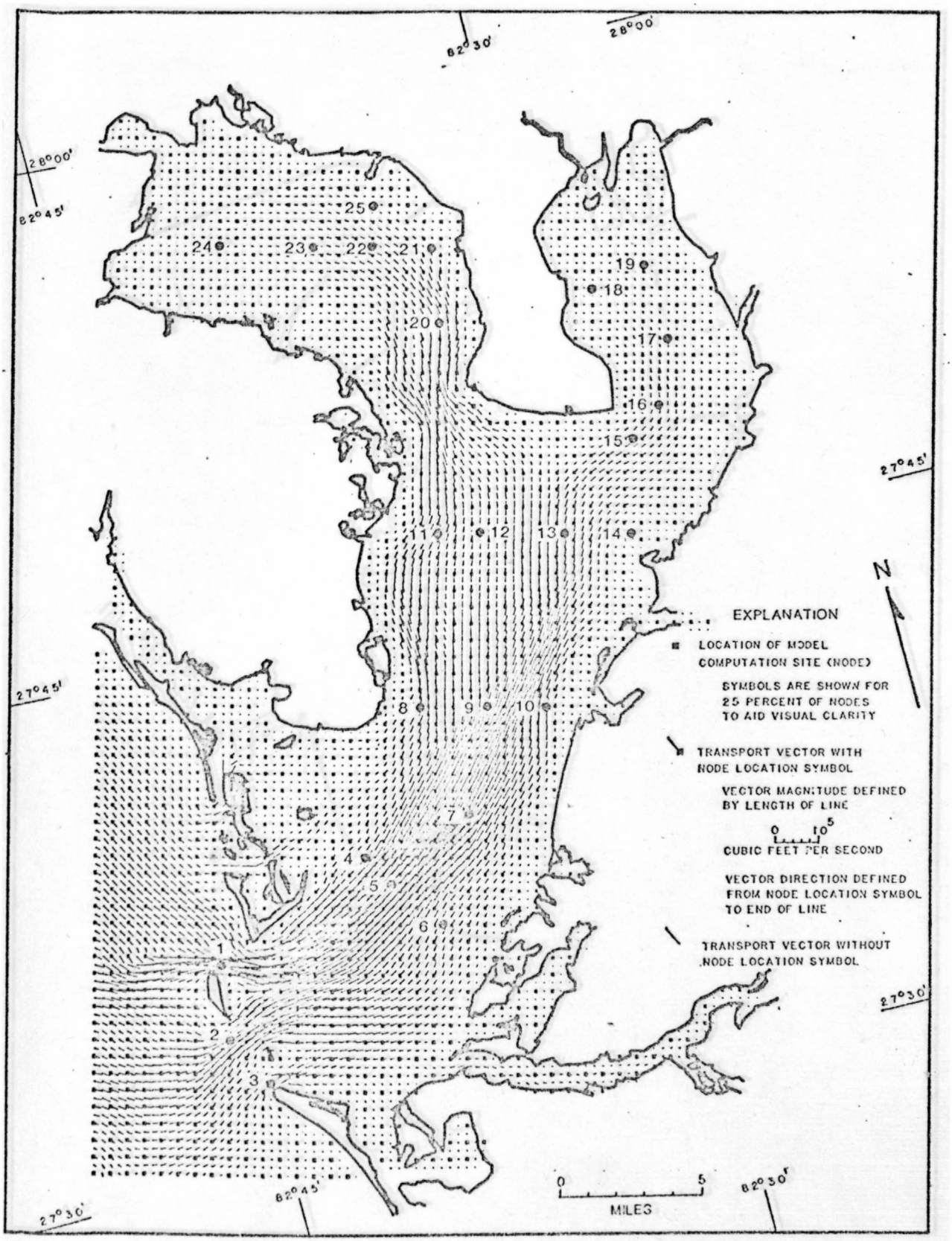

Figure 27.--Water-transport pattern during typical flood tide for 1880 level of development. (Numbers refer to sites listed in tables 10, 11, 13, 15, 16, and 18.)

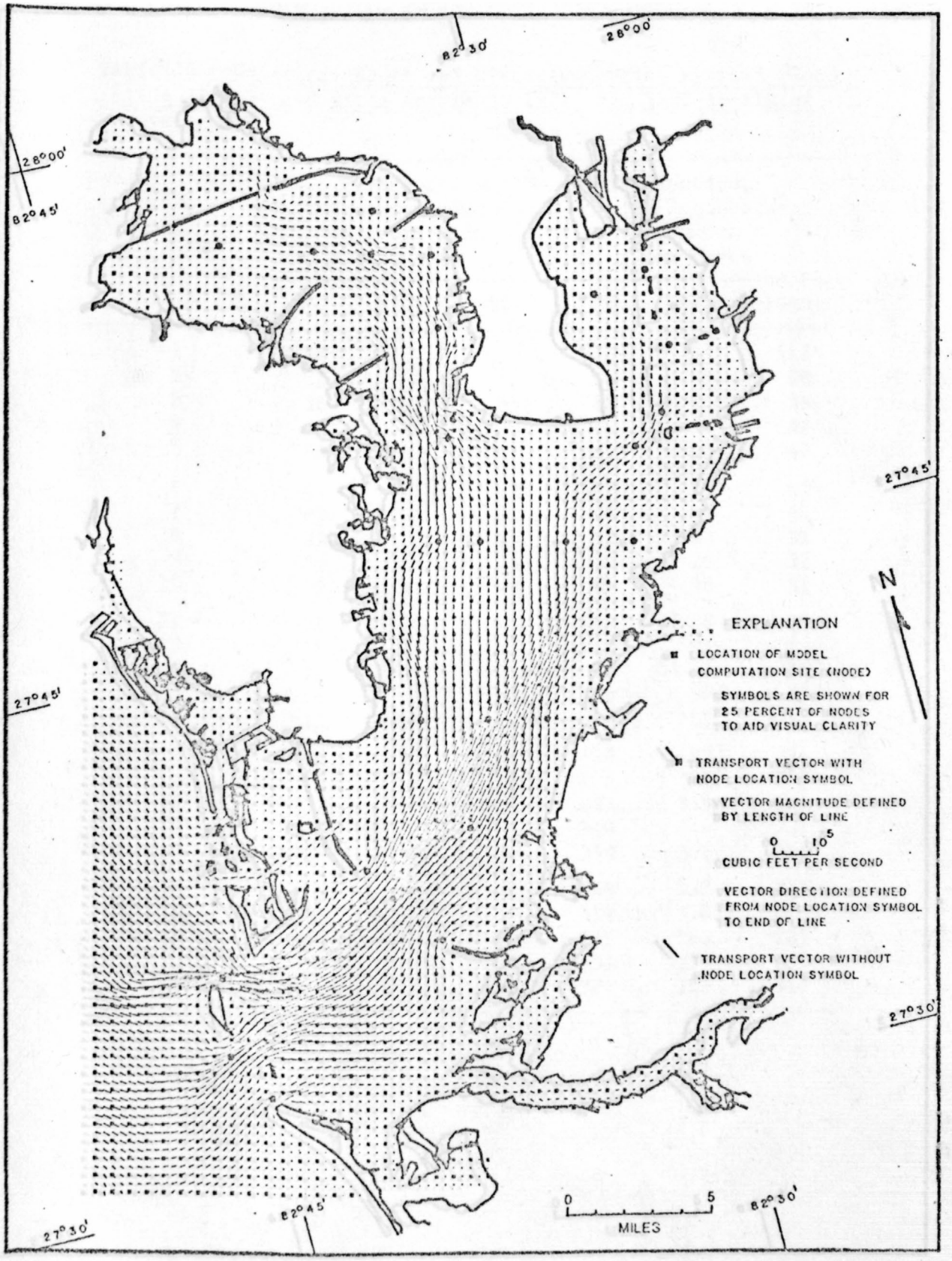

Figure 28.--Water-transport pattern during typical flood tide for 1972 level of development.

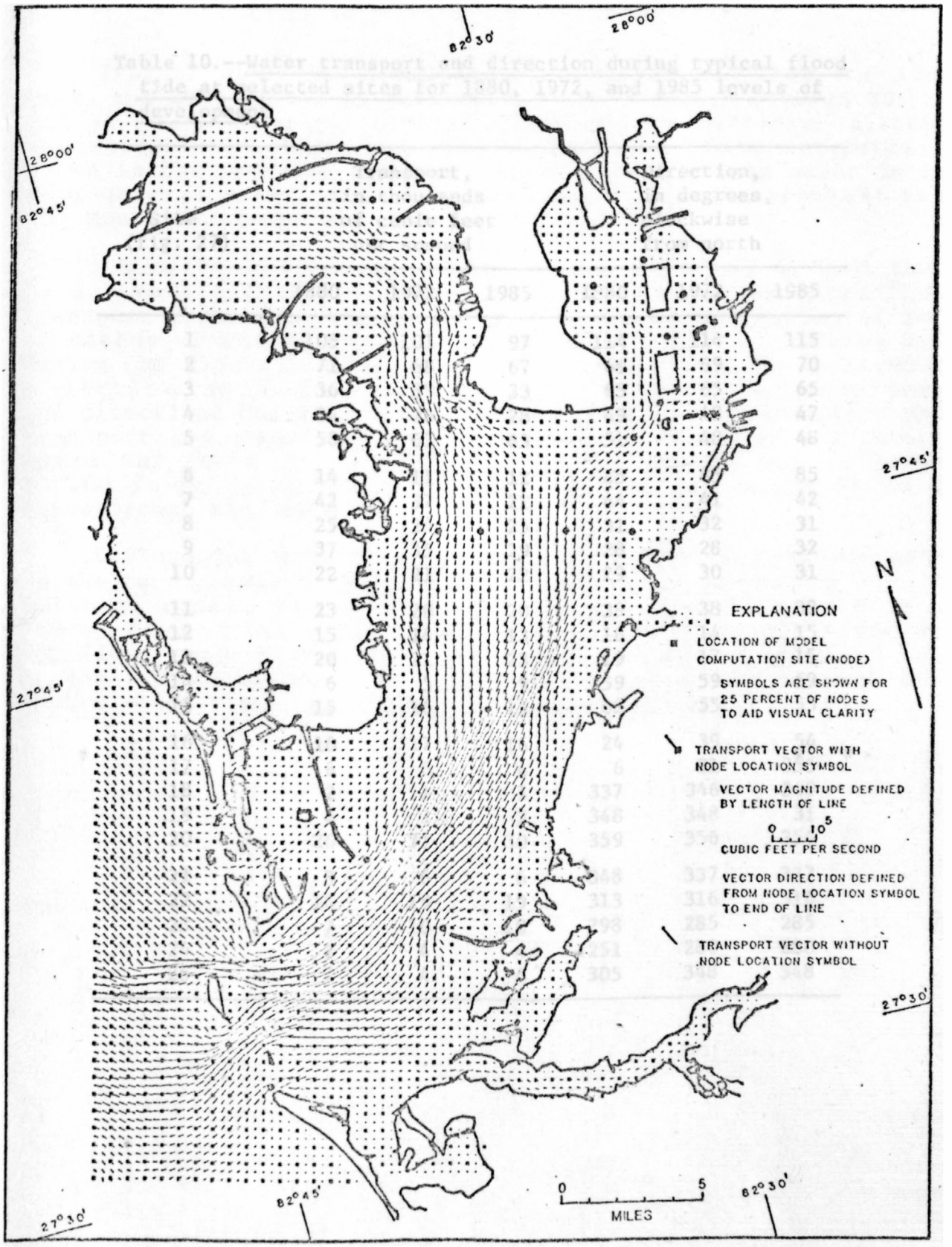

Figure 29.--Water-transport pattern during typical flood tide for 1985 level of development.

Table 10.--Water transport and direction during typical flood tide at selected sites for 1880, 1972, and 1985 levels of development

Site (fig. 27)	Transport, in thousands of cubic feet per second			Direction, in degrees, clockwise from north		
	1880	1972	1985	1880	1972	1985
1	105	101	97	114	114	115
2	71	68	67	69	69	70
3	36	33	33	65	65	65
4	24	28	28	49	48	47
5	58	63	65	51	48	48
6	14	11	12	45	85	85
7	42	37	22	44	41	42
8	25	24	25	31	32	31
9	37	35	29	28	28	32
10	22	21	22	29	30	31
11	23	20	20	39	38	38
12	15	14	13	16	14	15
13	20	21	23	19	17	15
14	6	5	5	59	59	59
15	15	16	15	62	55	55
16	10	17	16	24	39	54
17	6	6	4	6	31	355
18	2	1	1	337	346	349
19	4	1	2	348	348	31
20	26	31	30	359	356	356
21	8	6	6	348	337	337
22	14	19	19	313	316	316
23	7	10	10	298	285	285
24	2	4	4	251	280	280
25	7	4	4	305	348	348

Typical water-transport patterns during ebb flow for 1880, 1972, and 1985 levels of development are shown in figures 30, 31, and 32, respectively. Overall ebb-transport patterns, although opposite in direction, are similar to flood-transport patterns shown in the previous section. Flow concentrations occur in the same general areas, and transport magnitudes are greatest near the mouth and least near the head of the bay.

One difference between flood and ebb transport is that there is substantially greater magnitude of maximum ebb than flood transport throughout the bay. This is caused by the faster rate of change of water level for falling tide than for rising tide during the simulation (fig. 22). The faster rate is balanced by a shorter time of ebb-flow duration. Ebb-transport magnitudes and directions for 25 selected sites are given in table 11. Ebb-transport magnitudes were about 230,000 ft^3/s at the entrance to Tampa Bay (site 1), 50,000 ft^3/s in mid-Tampa Bay (site 9), 13,000 ft^3/s in Old Tampa Bay (site 23), and 3,000 ft^3/s in Hillsborough Bay (site 18).

Differences between flood and ebb transport patterns occur in sheltered areas protected from the current on the lee side of islands, causeways, or points of land. A good example is at Egmont Key, at the mouth of Tampa Bay (fig. 1), where flood and ebb flows produce low transport magnitudes to the east and west of the island, respectively. The sheltering effect is much more subtle where there are natural or manmade shoals.

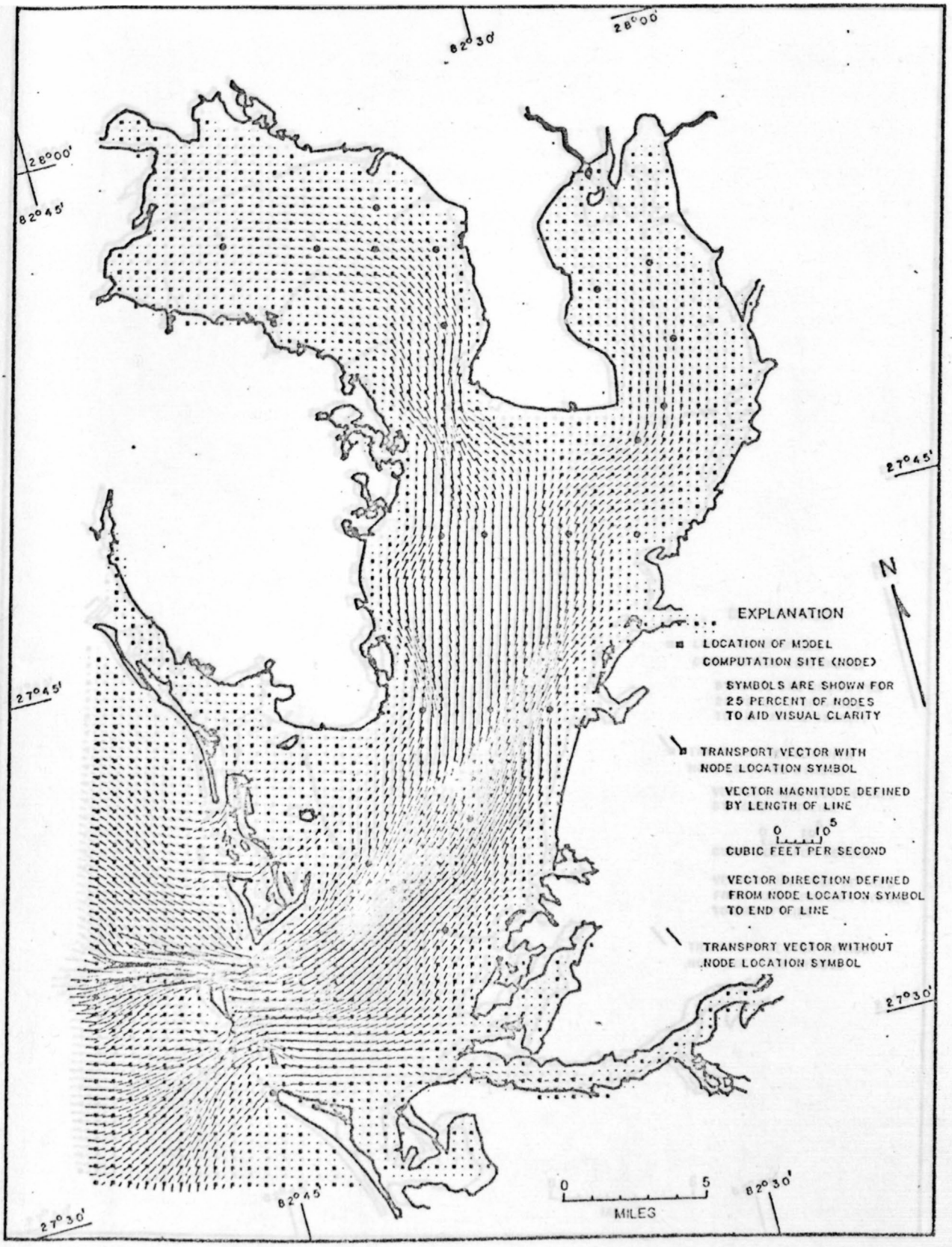

Figure 30.--Water-transport pattern during typical ebb tide for 1880 level of development.

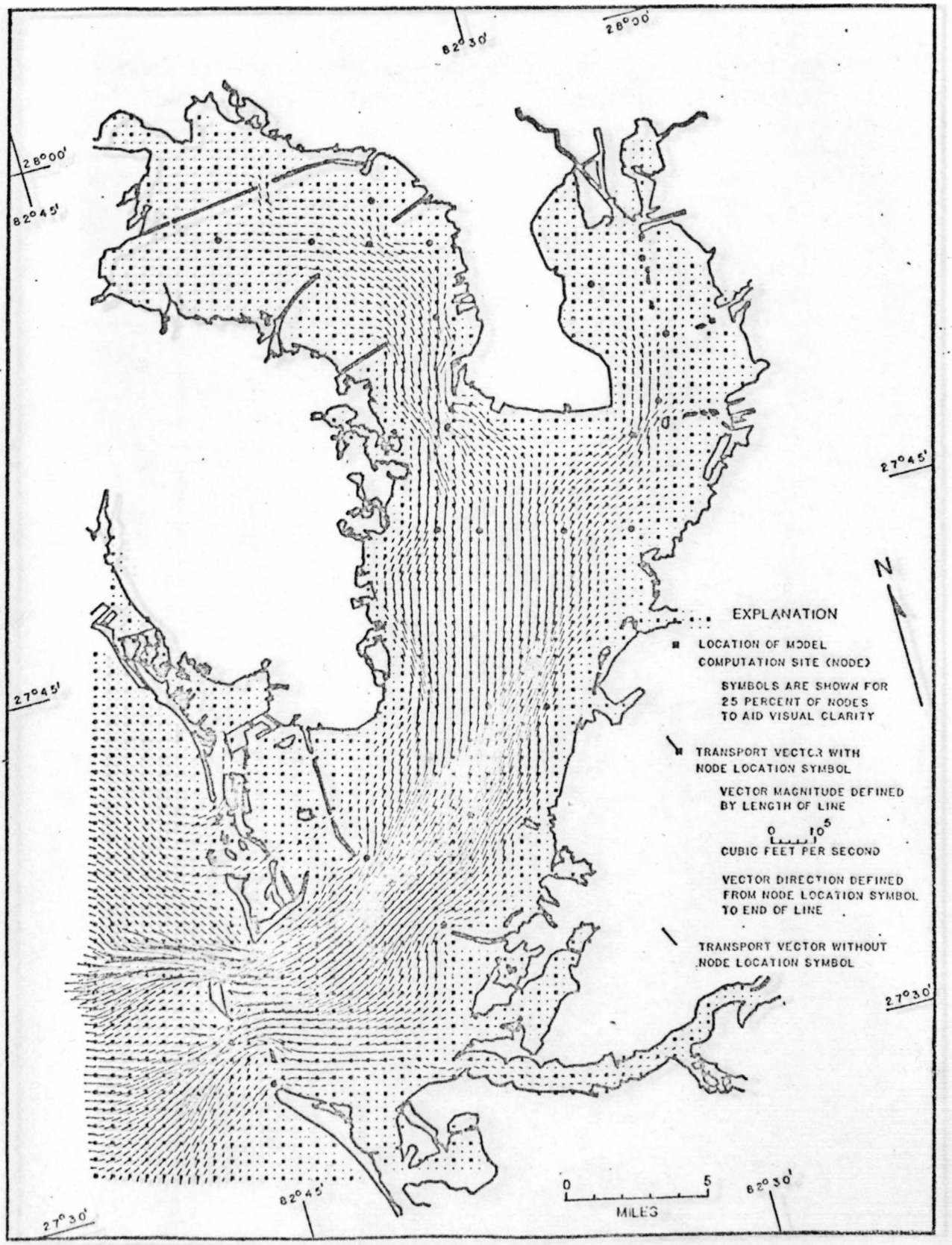

Figure 31.--Water-transport pattern during typical ebb tide for 1972 level of development.

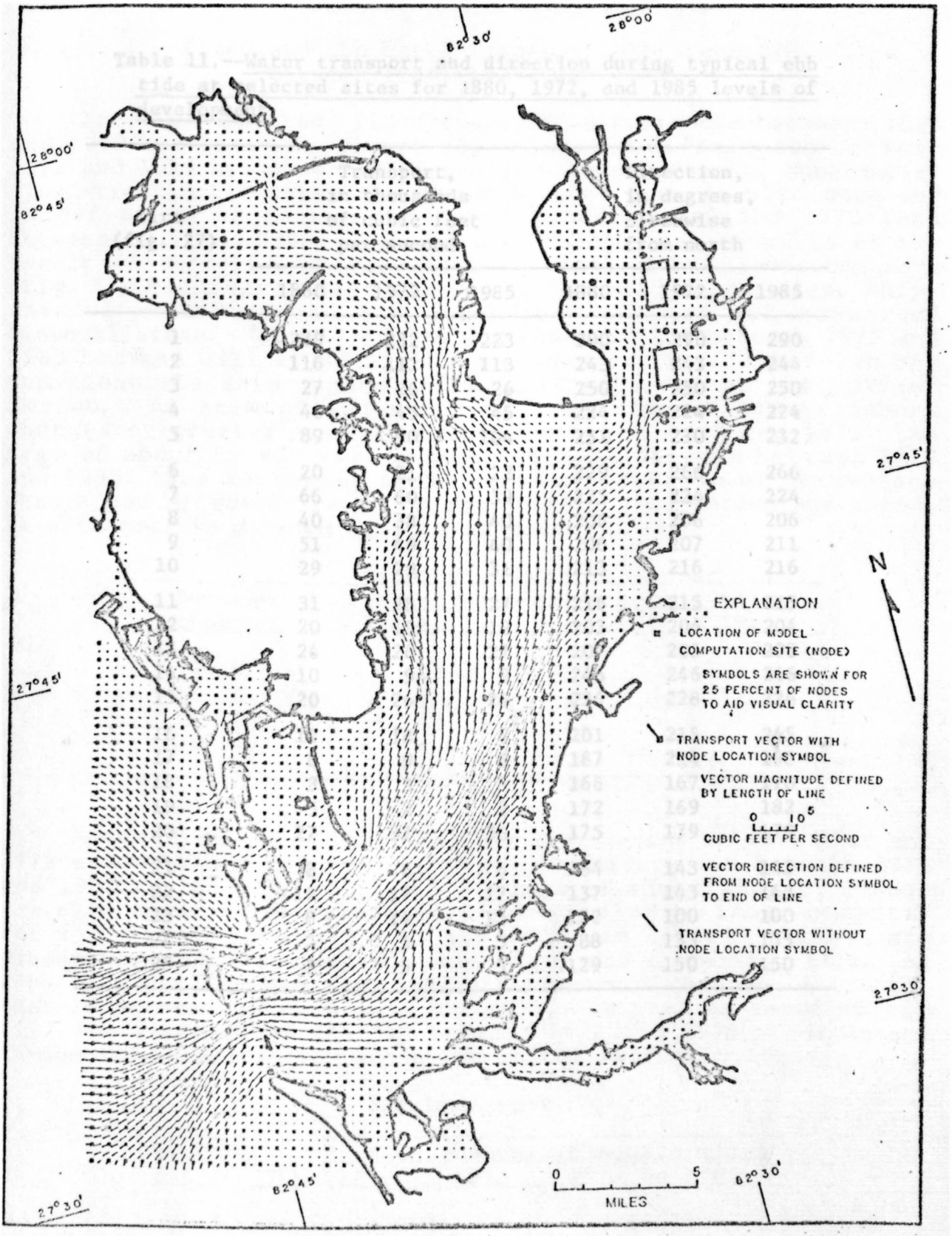

Figure 32.--Water-transport pattern during typical ebb tide for 1985 level of development.

Table 11.--Water transport and direction during typical ebb tide at selected sites for 1880, 1972, and 1985 levels of development

Site (fig. 27)	Transport, in thousands of cubic feet per second			Direction, in degrees, clockwise from north		
	1880	1972	1985	1880	1972	1985
1	239	232	223	290	290	290
2	116	112	113	243	243	244
3	27	26	26	250	250	250
4	40	45	45	224	224	224
5	89	90	104	231	230	232
6	20	21	22	229	266	266
7	66	60	39	225	224	224
8	40	38	40	206	206	206
9	51	49	40	206	207	211
10	29	29	31	213	216	216
11	31	28	27	216	215	215
12	20	19	18	203	204	204
13	24	26	27	207	205	203
14	10	9	9	246	246	246
15	20	26	24	234	228	226
16	14	18	6	201	215	245
17	8	9	6	187	214	198
18	3	3	3	166	167	170
19	5	2	2	172	169	182
20	27	37	36	175	179	179
21	8	6	6	164	143	143
22	12	17	17	137	143	143
23	8	14	13	122	100	100
24	2	5	5	88	135	135
25	7	5	5	129	150	150

Flood and Ebb Water-Transport Differences Between 1880, 1972, and 1985

Areas of computed flood-transport differences between 1880 and 1972 are shown in figure 33. Computed differences between 1972 and 1985 are shown in figure 34. Large areas of substantial flood-transport changes are shown in both figures with more and larger areas of change indicated between 1880 and 1972 than between 1972 and 1985. The greatest changes are shown to be the result of shoreline changes in Boca Ciega and Hillsborough Bays (fig. 1), causeways associated with four major roadways, ship-channel construction, and associated islands and submerged disposal areas. Channel and island construction between 1972 and 1985 has and will cause additional changes in Hillsborough Bay and along the ship channel from mid-Tampa Bay to the Gulf of Mexico. An area of about 218 mi^2 sustained flood-transport changes of greater than 10 percent between 1880 and 1972. An area of about 52 mi^2 will sustain similar changes between 1972 and 1985. The following table gives a breakdown of percentage change and affected areas. The computation of percentage change at each cell is defined earlier as equation 18.

Flood transport

Percent change	Area of change, in square miles 1880 to 1972	1972 to 1985
0-10	244	393
11-50	160	44
51-100	51	8
101-200	6	1
>200	1	0

Areas of computed ebb-transport differences between 1880 and 1972 are shown in figure 35. Computed differences between 1972 and 1985 are shown in figure 36. Areas of ebb-transport change are also shown to be substantial and similar to those computed for flood transport (figs. 33 and 34). The largest changes are closest to channels, islands, causeways, and shoreline fills. An area of about 188 mi^2 sustained ebb-transport changes of greater than 10 percent between 1880 and 1972. An area of about 45 mi^2 will sustain similar changes between 1972 and 1985. Percentage change and area involved are given in the following table.

Ebb transport

Percent change	Area of change, in square miles 1880 to 1972	1972 to 1985
0-10	274	400
11-50	130	38
51-100	53	7
101-200	5	1
>200	0	0

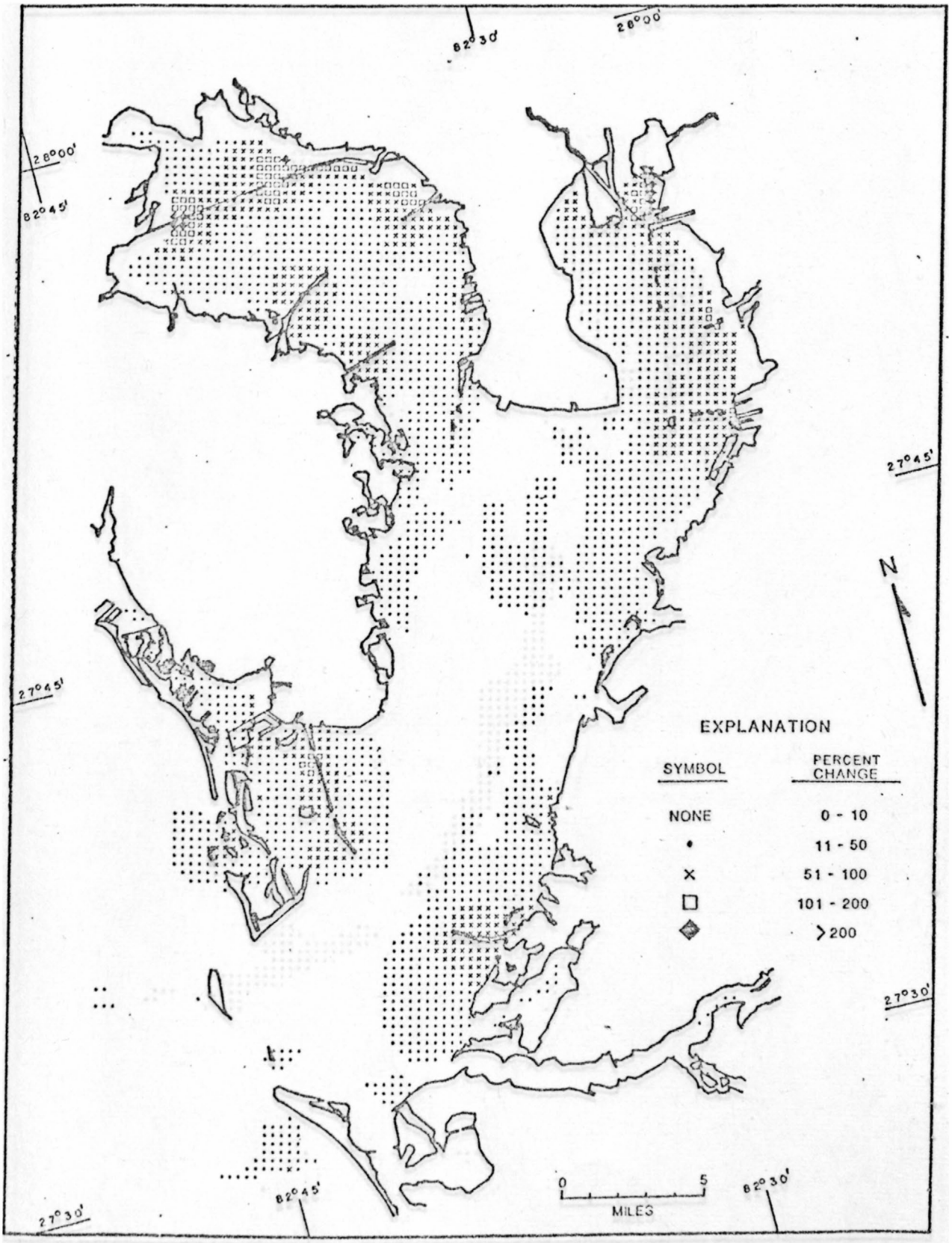

Figure 33.--Change in water transport for typical flood tide between 1880 and 1972 levels of development.

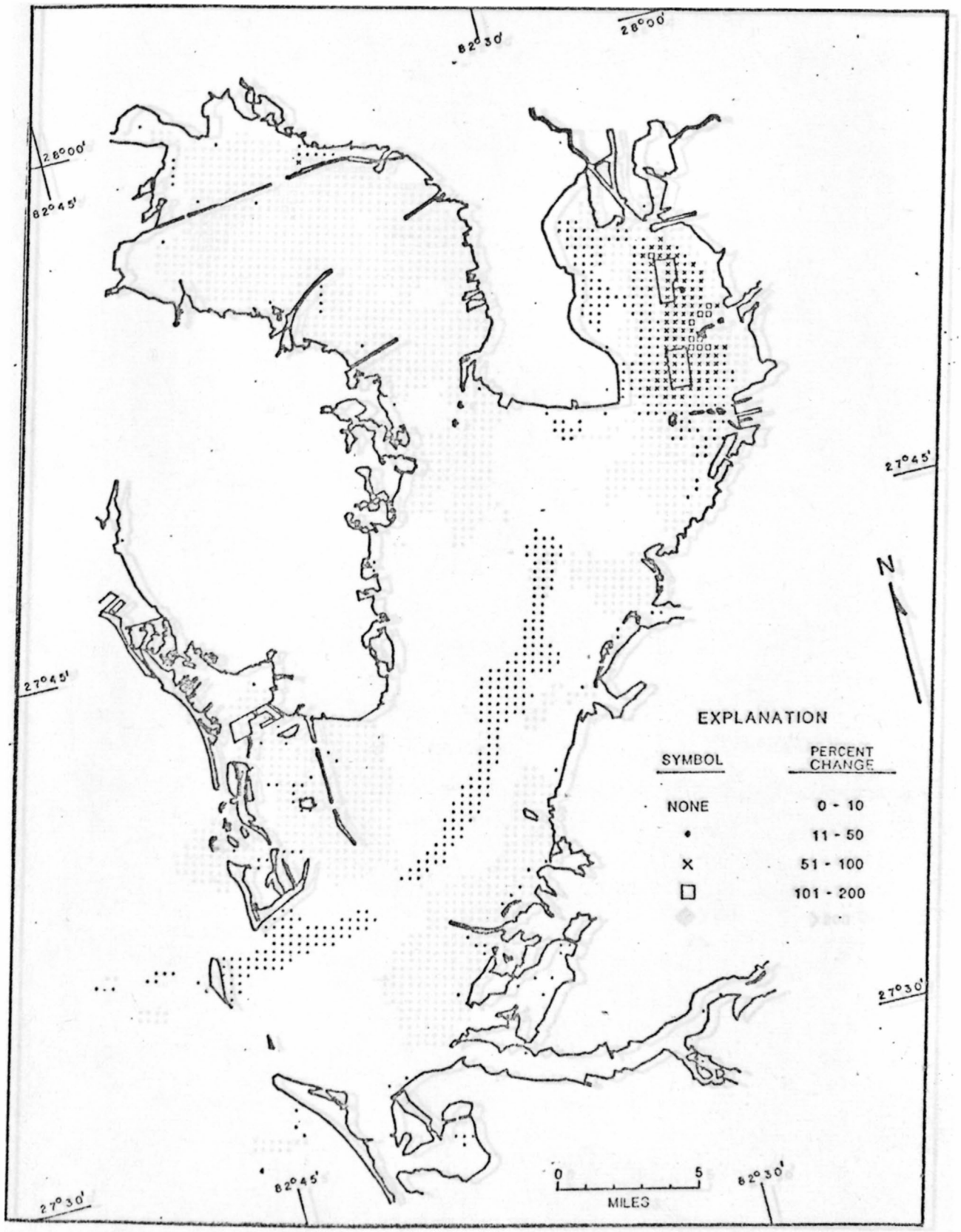

Figure 34.--Change in water transport for typical flood tide between 1972 and 1985 levels of development.

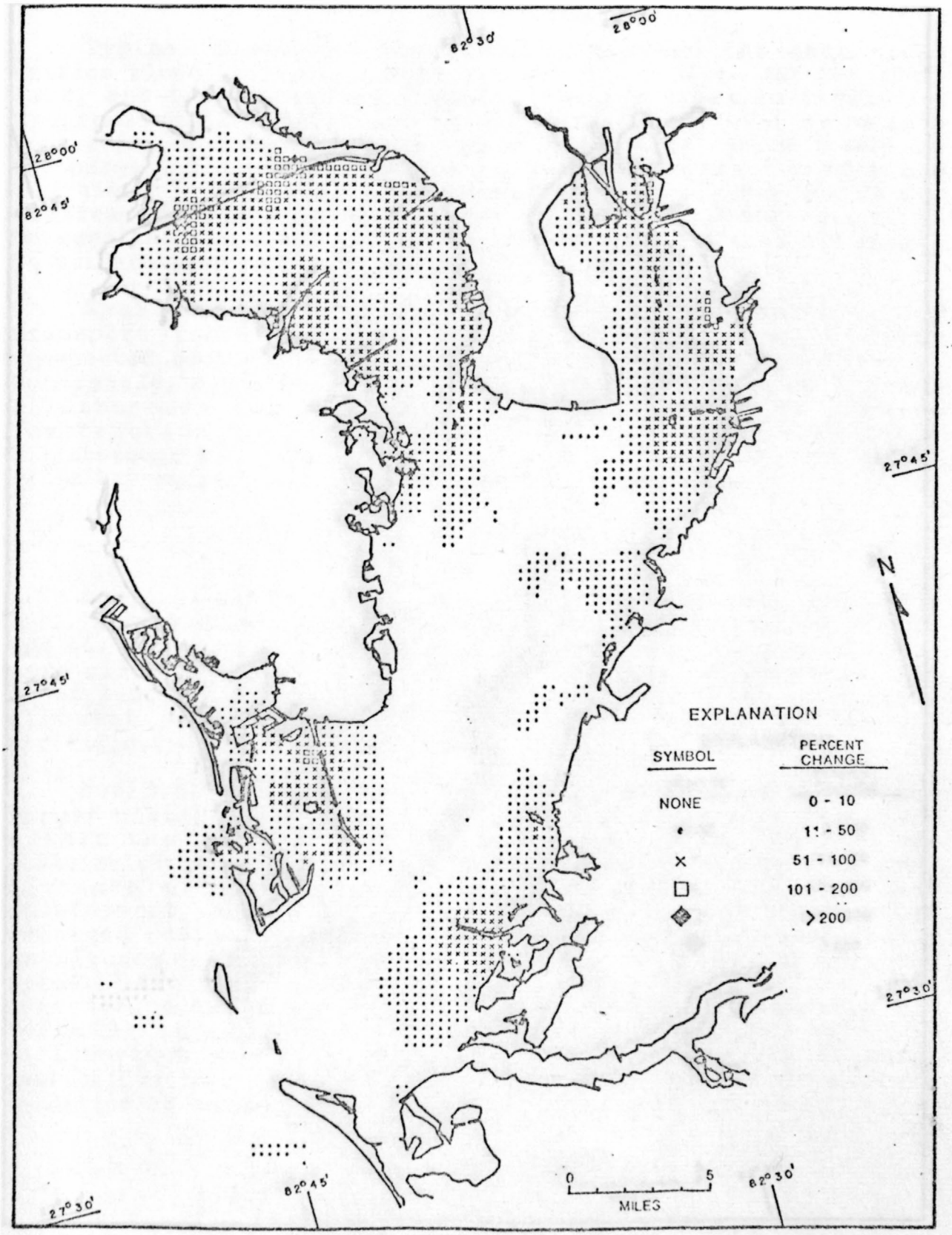

Figure 35.--Change in water transport for typical ebb tide between 1880 and 1972 levels of development.

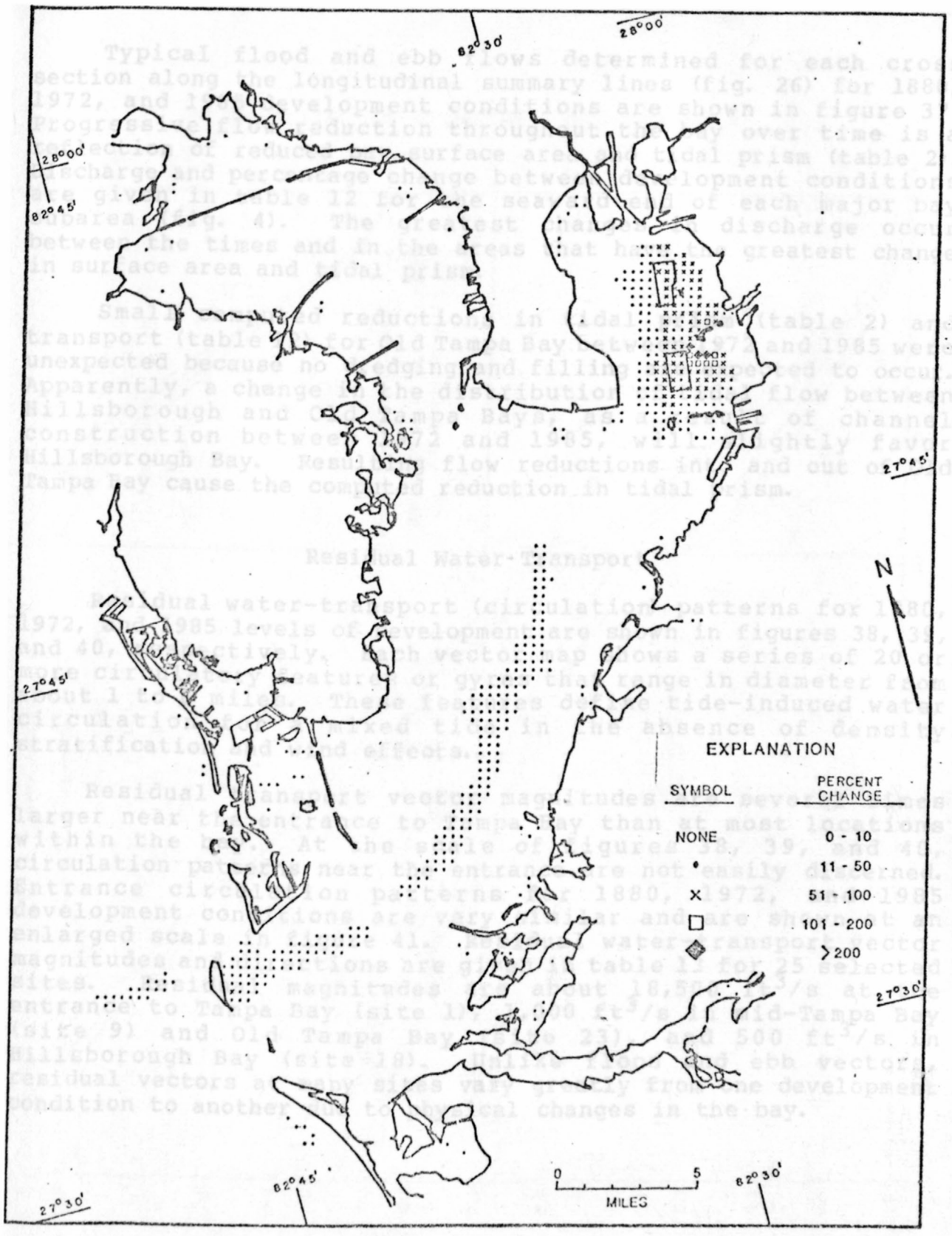

Figure 36.--Change in water transport for typical ebb tide between 1972 and 1985 levels of development.

Typical flood and ebb flows determined for each cross section along the longitudinal summary lines (fig. 26) for 1880, 1972, and 1985 development conditions are shown in figure 37. Progressive flow reduction throughout the bay over time is a reflection of reduced bay surface area and tidal prism (table 2). Discharge and percentage change between development conditions are given in table 12 for the seaward end of each major bay subarea (fig. 4). The greatest changes in discharge occur between the times and in the areas that have the greatest change in surface area and tidal prism.

Small computed reductions in tidal prism (table 2) and transport (table 12) for Old Tampa Bay between 1972 and 1985 were unexpected because no dredging and filling are expected to occur. Apparently, a change in the distribution of tidal flow between Hillsborough and Old Tampa Bays, as a result of channel construction between 1972 and 1985, will slightly favor Hillsborough Bay. Resulting flow reductions into and out of Old Tampa Bay cause the computed reduction in tidal prism.

Residual Water Transport

Residual water-transport (circulation) patterns for 1880, 1972, and 1985 levels of development are shown in figures 38, 39, and 40, respectively. Each vector map shows a series of 20 or more circulatory features or gyres that range in diameter from about 1 to 6 miles. These features define tide-induced water circulation for a mixed tide in the absence of density stratification and wind effects.

Residual transport vector magnitudes are several times larger near the entrance to Tampa Bay than at most locations within the bay. At the scale of figures 38, 39, and 40, circulation patterns near the entrance are not easily discerned. Entrance circulation patterns for 1880, 1972, and 1985 development conditions are very similar and are shown at an enlarged scale in figure 41. Residual water-transport vector magnitudes and directions are given in table 13 for 25 selected sites. Residual magnitudes are about 18,500 ft^3/s at the entrance to Tampa Bay (site 1), 1,000 ft^3/s in mid-Tampa Bay (site 9) and Old Tampa Bay (site 23), and 500 ft^3/s in Hillsborough Bay (site 18). Unlike flood and ebb vectors, residual vectors at many sites vary greatly from one development condition to another due to physical changes in the bay.

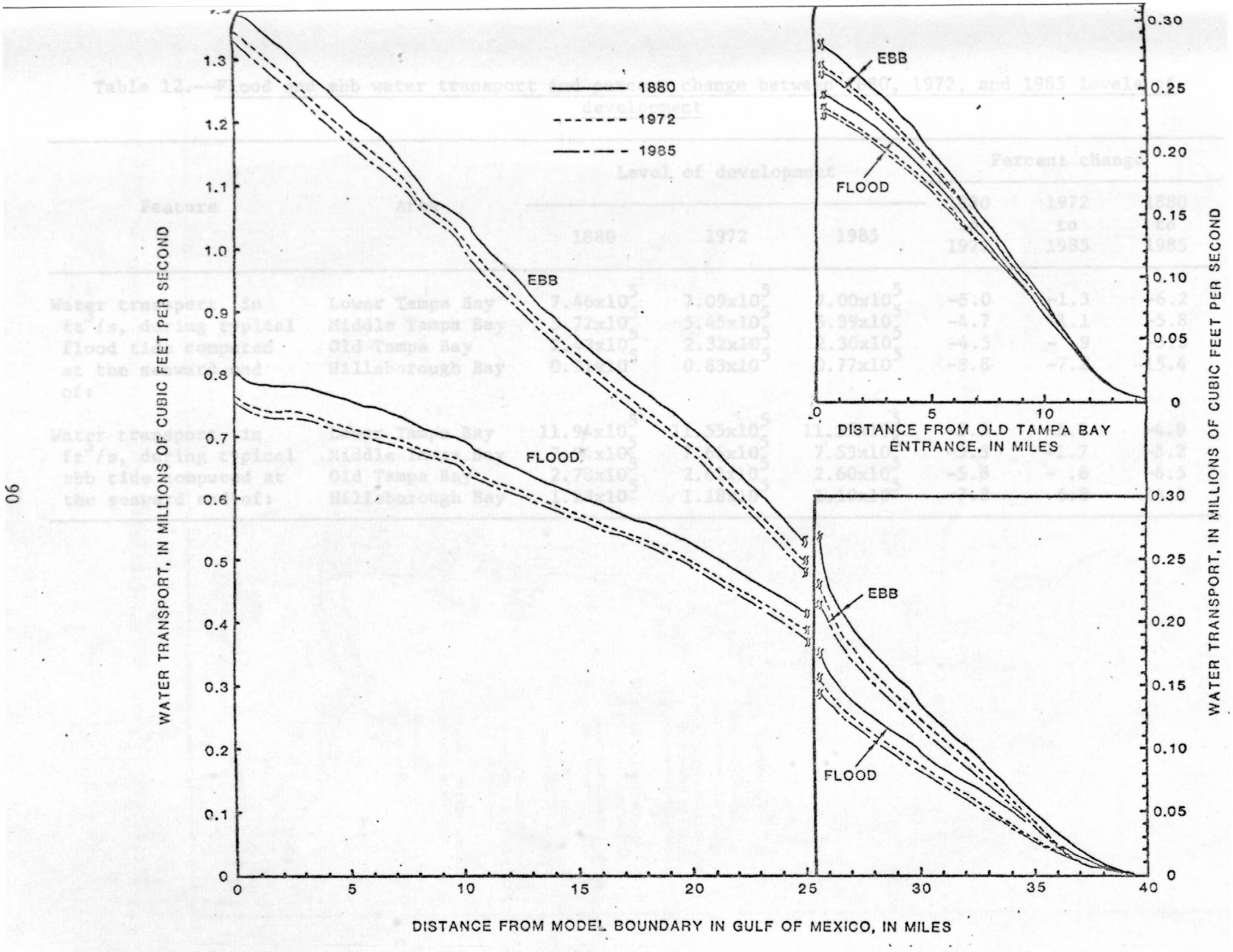

Figure 37.--Water transport along longitudinal summary limes (fig. 26) during typical flood and ebb tides for 1800, 1972, and 1985 levels of development.

Table 12.--Flood and ebb water transport and percent change between 1880, 1972, and 1985 levels of development

Feature	Area	Level of development			Percent change		
		1880	1972	1985	1880 to 1972	1972 to 1985	1880 to 1985
Water transport, in ft^3/s, during typical flood tide computed at the seaward end of:	Lower Tampa Bay	7.46×10^5	7.09×10^5	7.00×10^5	-5.0	-1.3	-6.2
	Middle Tampa Bay	5.72×10^5	5.45×10^5	5.39×10^5	-4.7	-1.1	-5.8
	Old Tampa Bay	2.43×10^5	2.32×10^5	2.30×10^5	-4.5	- .9	-5.3
	Hillsborough Bay	0.91×10^5	0.83×10^5	0.77×10^5	-8.8	-7.2	-15.4
Water transport, in ft^3/s, during typical ebb tide computed at the seaward end of:	Lower Tampa Bay	11.94×10^5	11.55×10^5	11.35×10^5	-3.3	-1.7	-4.9
	Middle Tampa Bay	7.94×10^5	7.66×10^5	7.53×10^5	-3.5	-1.7	-5.2
	Old Tampa Bay	2.78×10^5	2.62×10^5	2.60×10^5	-5.8	- .8	-6.5
	Hillsborough Bay	1.28×10^5	1.18×10^5	1.10×10^5	-7.8	-6.8	-14.1

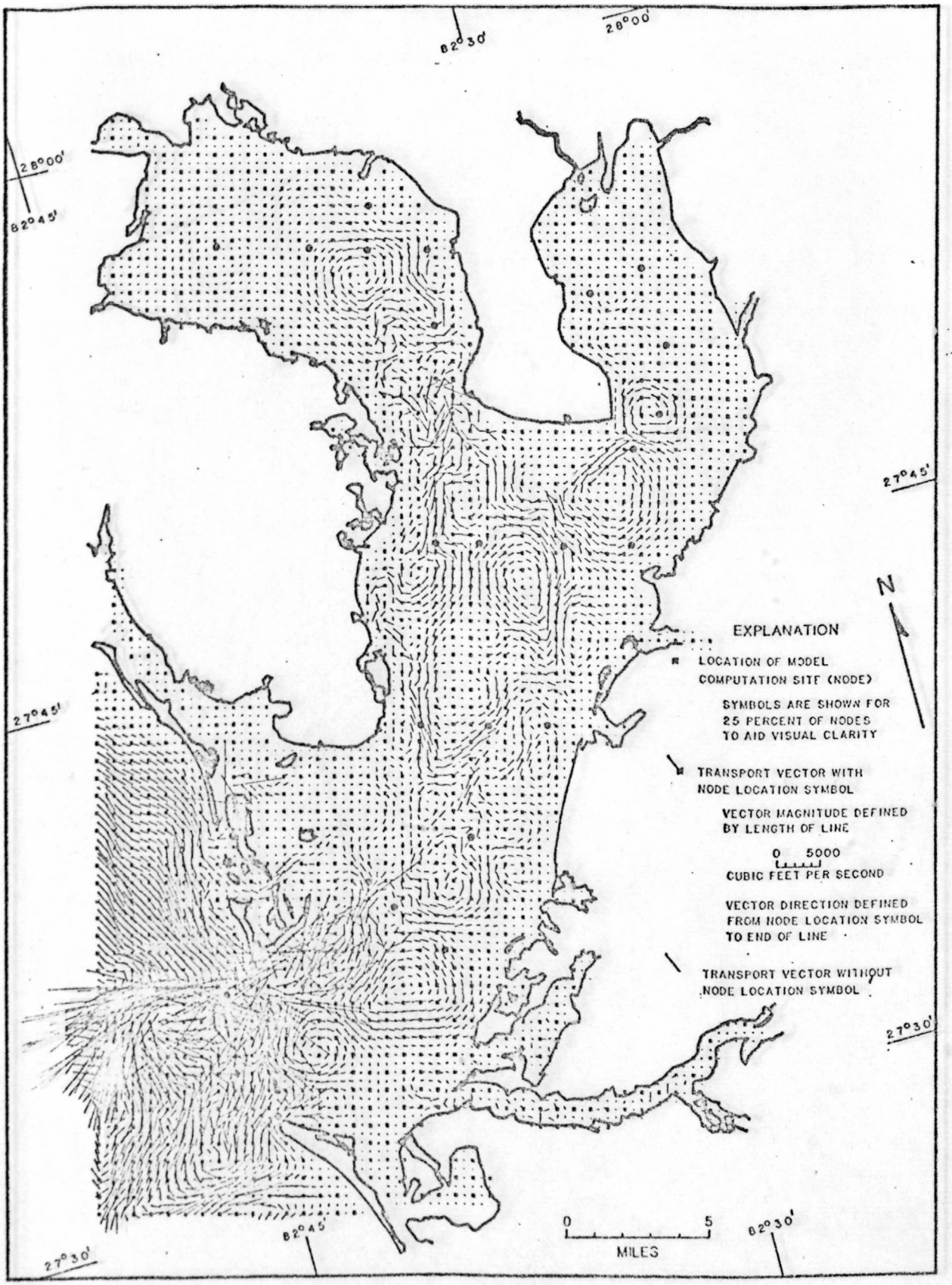

Figure 38.--Residual water-transport pattern for 1880 level of development.

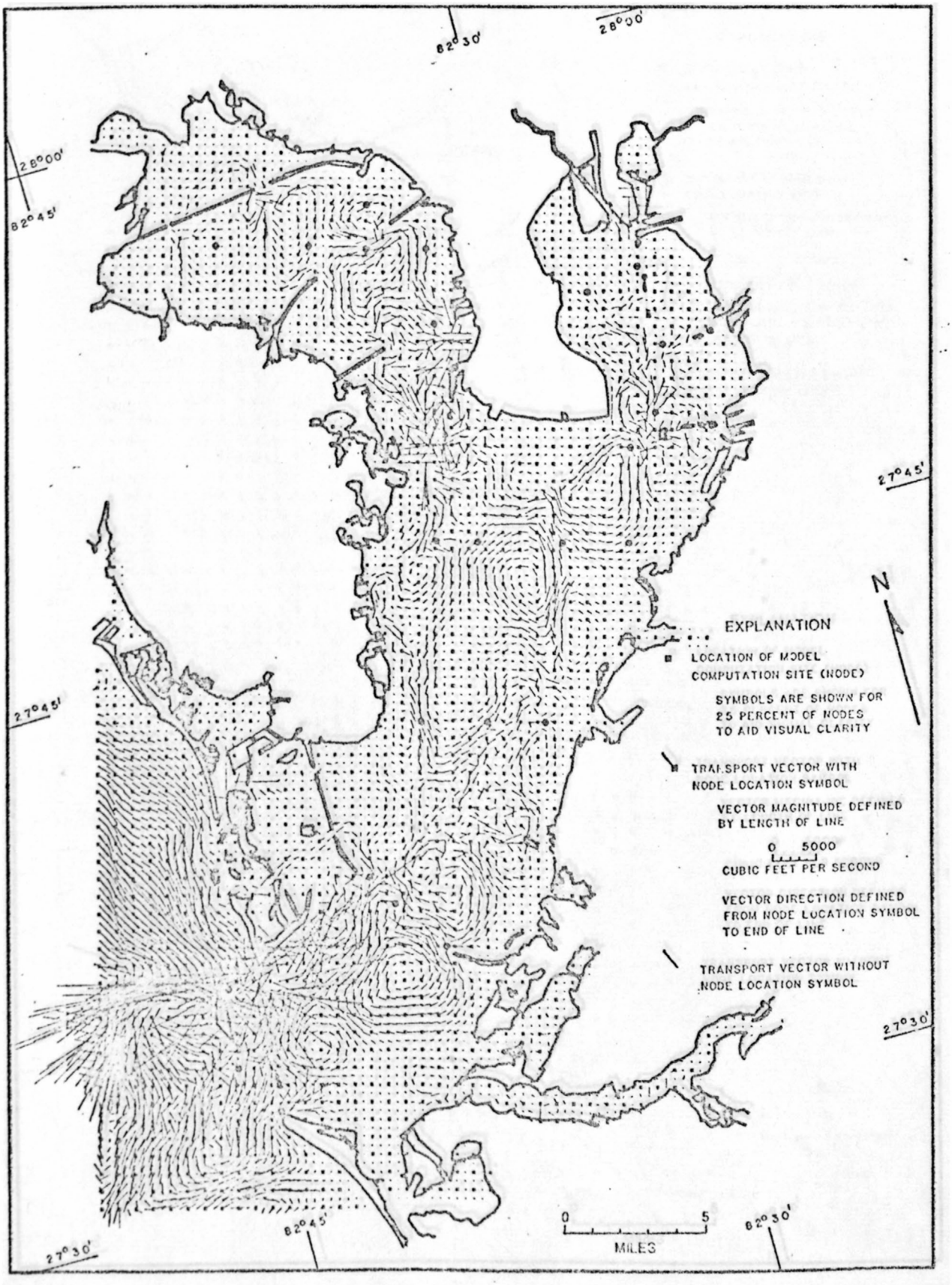

Figure 39.--Residual water-transport pattern for 1972 level of development.

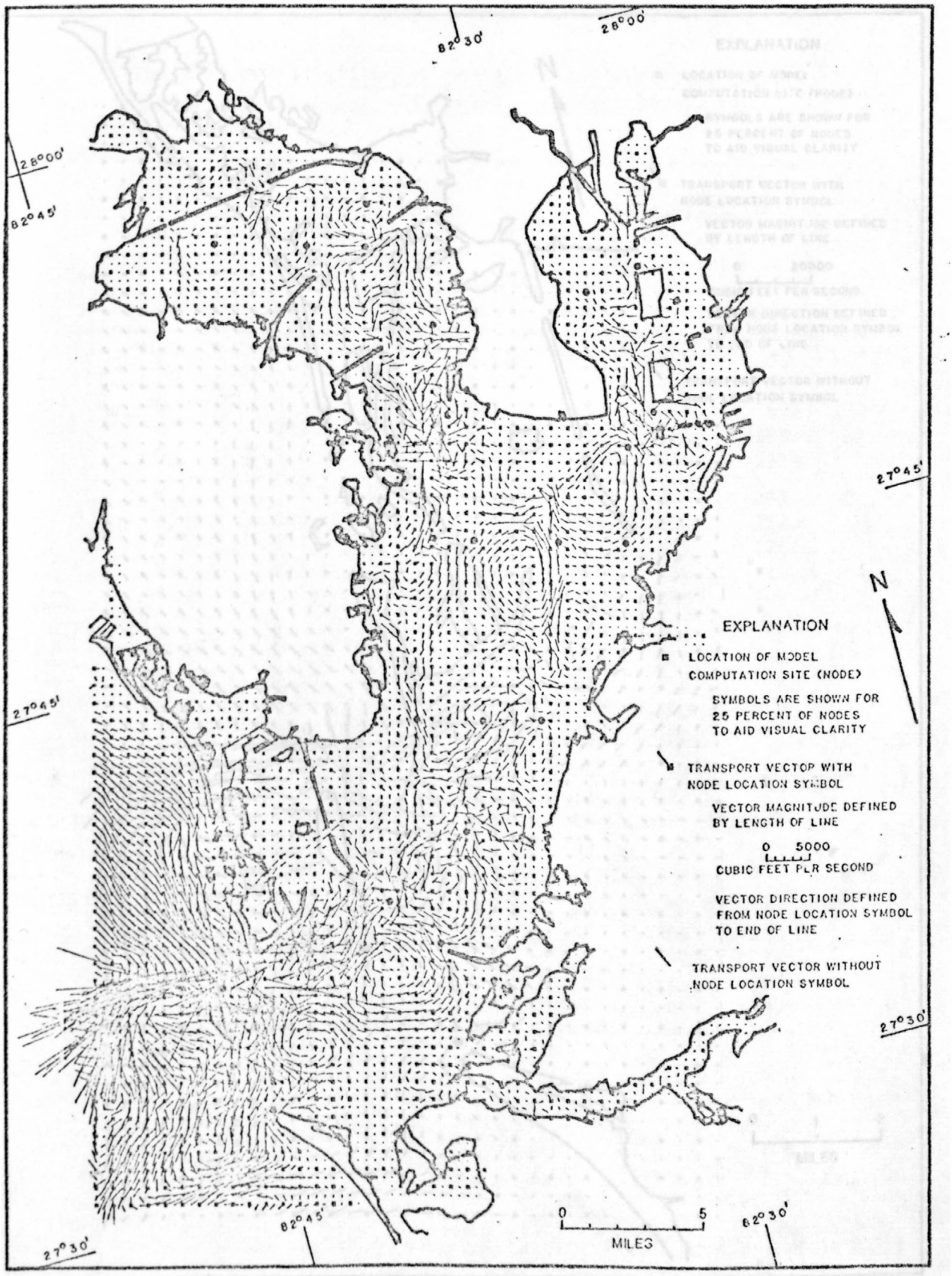

Figure 40.--Residual water-transport pattern for 1985 level of development.

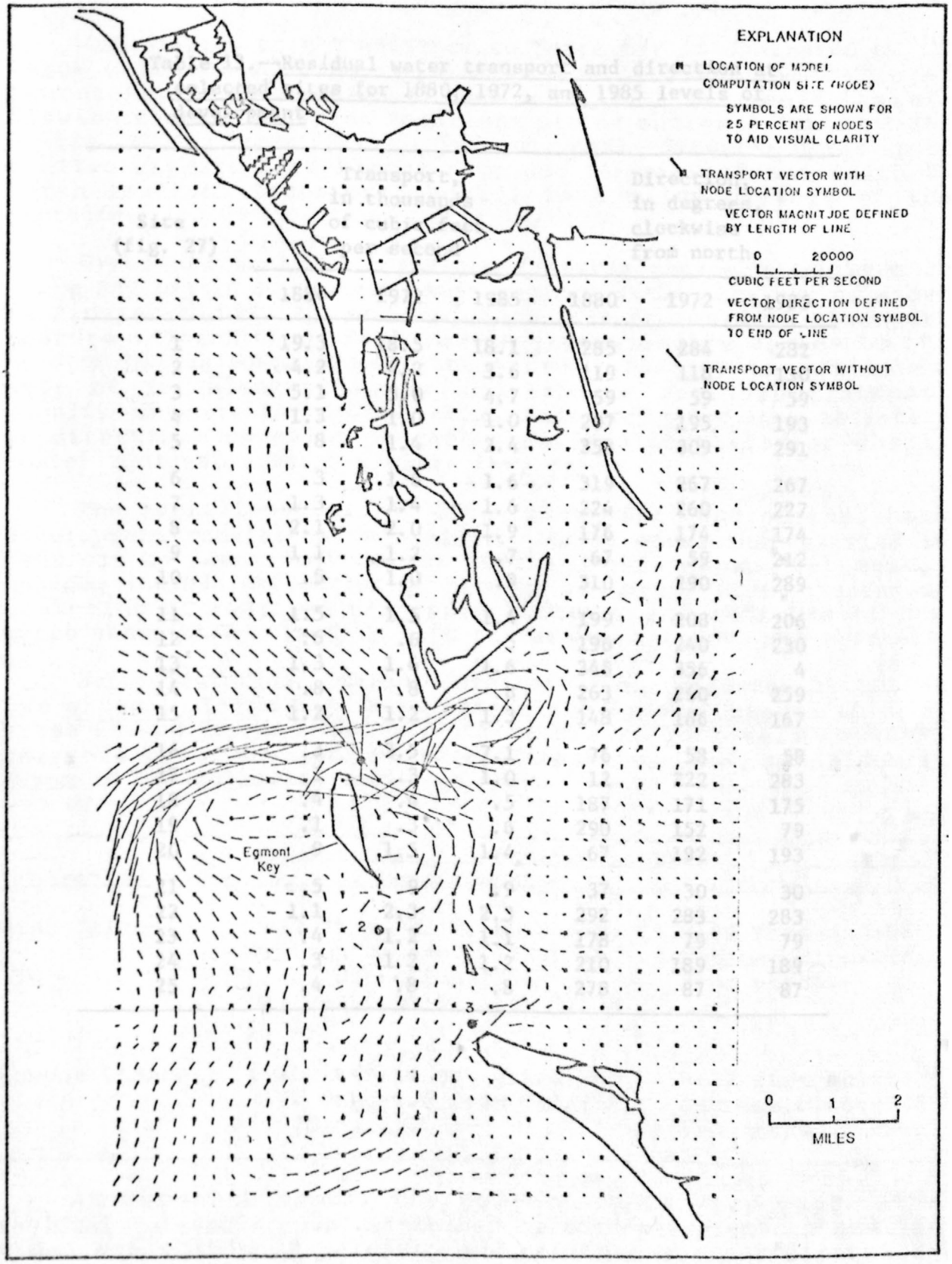

Figure 41.--Representative residual water-transport pattern at the entrance to Tampa Bay, 1972 level of development. (Numbers refer to sites listed in table 13.)

Table 13.--Residual water transport and direction at selected sites for 1880, 1972, and 1985 levels of development

Site (fig. 27)	Transport, in thousands of cubic feet per second			Direction, in degrees, clockwise from north		
	1880	1972	1985	1880	1972	1985
1	19.3	18.5	18.1	285	284	282
2	4.2	4.2	3.6	119	118	130
3	5.1	5.0	4.7	59	59	59
4	1.3	1.0	1.0	207	195	193
5	.8	1.4	2.4	353	309	291
6	.3	1.6	1.6	319	267	267
7	1.3	1.4	1.6	224	260	227
8	2.1	2.0	1.9	176	174	174
9	1.1	1.2	.7	67	59	212
10	.5	1.0	.9	310	290	289
11	1.5	1.5	1.4	199	208	206
12	.6	.6	.5	196	240	230
13	1.3	1.6	1.6	345	356	4
14	.8	.8	.8	263	260	259
15	1.2	1.2	1.3	148	166	167
16	.3	3.5	7.1	76	58	58
17	.1	.3	1.0	12	222	283
18	.4	.4	.5	187	171	175
19	.1	.3	.6	290	152	79
20	.9	1.5	1.4	67	192	193
21	.5	.9	.9	37	30	30
22	1.1	2.3	2.3	292	283	283
23	.4	1.2	1.1	178	79	79
24	.3	1.2	1.2	210	189	189
25	.4	.8	.8	278	87	87

Circulation at the entrance to Tampa Bay is dominated by (1) large Gulfward-flowing vectors in the deep channel north of Egmont Key (site 1, fig. 41 and table 13); (2) small bayward flowing vectors at other locations at the entrance (sites 2 and 3, fig. 41 and table 13); (3) intense, small-diameter gyres up to 4 miles bayward from Egmont Key; and (4) significant south to north residual transport about 1 to 2 miles bayward of the entrance.

Gyres and residual transport features near the entrance to Tampa Bay adjoin other less intense gyres within the bay as shown in figures 38, 39, 40, and 41. Each gyre or residual transport feature adjoins other features in a progressive series to the head of Hillsborough and Old Tampa Bays. Some gyres mesh like a pair of interlocking gears and enhance residual transport magnitudes where they join. Other pairs of gyres seem to rotate in directions opposite to each other and partially or wholly cancel residual transport where they join.

The overall pattern of circulation for each of the three development conditions is similar. Major gyres that existed in 1880 can be identified in the 1972 and 1985 maps. Detectable changes include deflection or skewing of gyres, strengthening or weakening of residual transport vectors, and addition of new gyres associated primarily with causeways, islands, and channels.

Sufficient tidal current data have been collected by NOS at two sites in Tampa Bay, Ross Island and Egmont Channel (fig. 8, sites 25 and 26, and table 7), to determine long-term residual currents for comparison with model results. The comparison is given in the following table.

Location	Residual current	
	Measurements	Model
Ross Island	0.12 ft/s (C. R. Muirhead, written commun., 1983) in flood direction (358 degrees from Dinardi (1978, p. 34)	0.09 ft/s at 306 degrees clockwise from north.
Egmont Channel	0.29 ft/s in ebb direction (289 degrees) from Dinardi, (1978, p. 30)	0.27 ft/s at 284 degrees clockwise from north.

At Egmont Channel, the comparison is very good. The residual current speeds determined by both measurements and the model are within 10 percent, and residual current directions coincide within 5 degrees. At the Ross Island site, the comparison is not as good as at Egmont Channel, but sufficient to indicate a fair level of agreement between measurements and model values, particularly in a region of very complex, computed residual transport (fig. 39).

Comparison of residual currents at these two sites is not sufficient to judge the model's ability to accurately simulate residual currents throughout the modeled area. Results of the comparisons, although encouraging, may be spurious for several reasons.

1. The accuracy of residual currents computed from measurements is not known.
2. Residual currents computed throughout the bay are on the same order as reported standard errors between observed and computed tidal currents (table 8), indicating the probability of high percentage errors associated with residual currents at the Egmont Channel and Ross Island sites.
3. Two sites do not adequately represent the range of conditions within the modeled area.

Although these shortcomings are recognized, the use of residual computations is considered useful and instructive, particularly for assessing relative changes caused by physical modification to Tampa Bay. It is likely that computed changes in residual water and constituent transports are more reliable than the residual values computed for each level of development.

Residual Water-Transport Differences Between 1880, 1972, and 1985

Areas of residual water-transport differences between 1880 and 1972 are shown in figure 42. Differences between 1972 and 1985 are shown in figure 43. Computed changes from 1880 to 1972 are extensive, occur throughout the bay, and extend into the nearshore region of the Gulf of Mexico. The largest changes are associated with causeway construction in Old Tampa Bay; ship channel and port-facility construction at the mouth of Old Tampa Bay; residential, commercial, port-facility, and ship-channel construction in and at the mouth of Hillsborough Bay; and causeway, port-facility, and ship-channel construction in lower Tampa Bay.

All residual-transport changes from 1972 to 1985 are due to ship-channel construction and associated submergent and emergent dredged material disposal sites. Areas of major change occur in Hillsborough Bay and near the boundary between middle and lower Tampa Bay. Some change also occurs offshore of the Tampa Bay entrance.

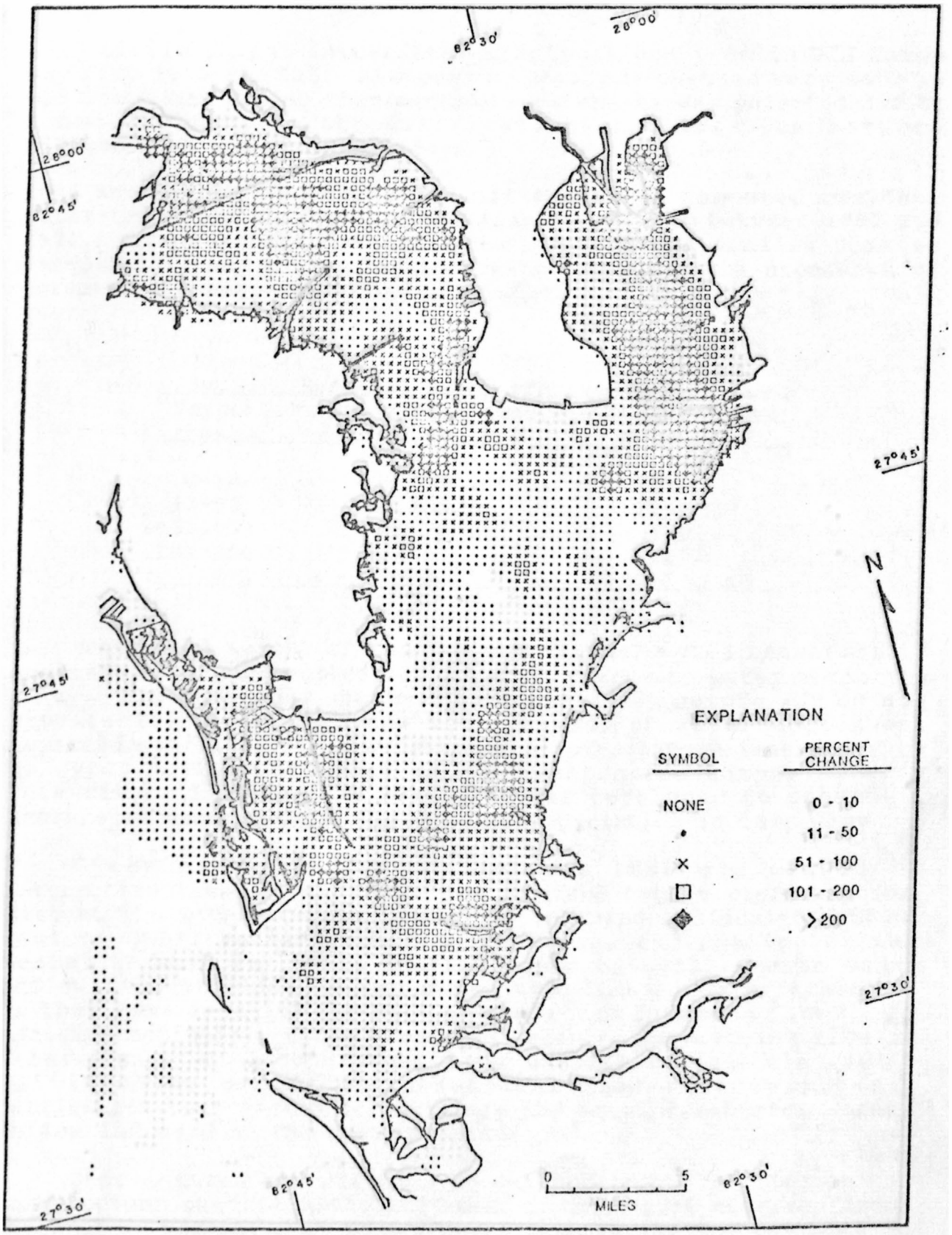

Figure 42.--Change in residual water transport between 1880 and 1972 levels of development.

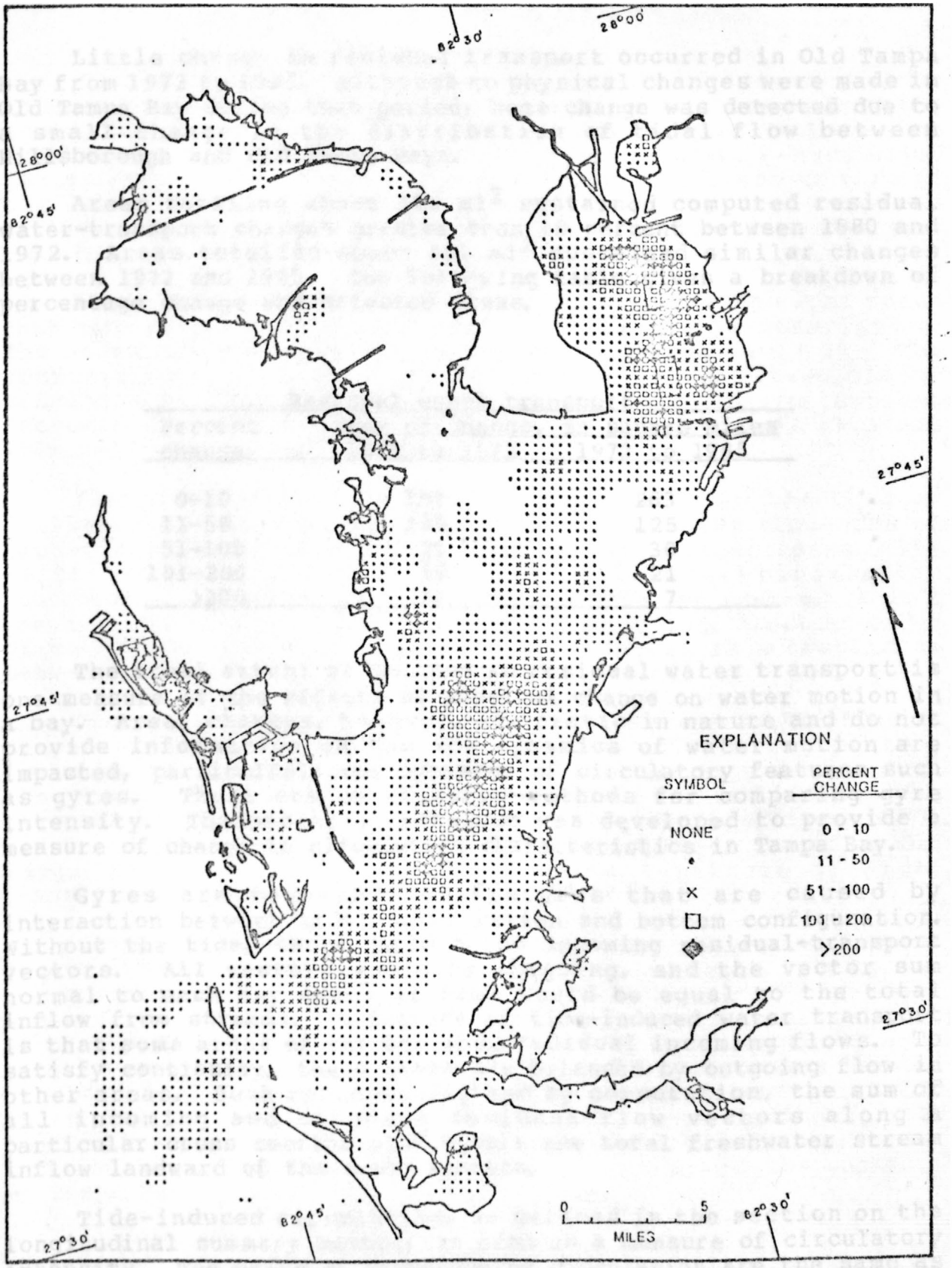

Figure 43.--Change in residual water transport between 1972 and 1985 levels of development.

Little change in residual transport occurred in Old Tampa Bay from 1972 to 1985. Although no physical changes were made in Old Tampa Bay during that period, some change was detected due to a small change in the distribution of tidal flow between Hillsborough and Old Tampa Bays.

Areas totaling about 306 mi^2 sustained computed residual water-transport changes greater than 10 percent between 1880 and 1972. Areas totaling about 182 mi^2 sustained similar changes between 1972 and 1985. The following table gives a breakdown of percentage change and affected areas.

Residual water transport		
Percent change	Area of change, in square miles	
	1880 to 1972	1972 to 1985
0-10	157	263
11-50	139	125
51-100	71	30
101-200	59	21
>200	37	7

The areal extent of changes in residual water transport is one measure of the effects of physical change on water motion in a bay. Areal changes, however, are static in nature and do not provide information on how the dynamics of water motion are impacted, particularly the dynamics of circulatory features such as gyres. There are no standard methods for comparing gyre intensity. Therefore, a technique was developed to provide a measure of change in circulation characteristics in Tampa Bay.

Gyres are tide-induced features that are caused by interaction between tidal water motion and bottom configuration. Without the tide, there could be no incoming residual-transport vectors. All vectors would be outgoing, and the vector sum normal to each bay cross section would be equal to the total inflow from streams. A feature of tide-induced water transport is that some areas of the bay show residual incoming flows. To satisfy continuity, these areas are balanced by outgoing flow in other areas. Both conceptually and by computation, the sum of all incoming and outgoing residual-flow vectors along a particular cross section also equals the total freshwater stream inflow landward of the cross section.

Tide-induced circulation, as defined in the section on the longitudinal summary method, is used as a measure of circulatory intensity. The units of tide-induced circulation are the same as for streamflow, so direct comparisons can be made between tide- and streamflow-induced residual flows.

Figure 44 shows circulation, as the sum of incoming tide-induced residual transport, plotted against distance along the longitudinal summary lines (fig. 26) for each level of development. Tributary streamflow is also shown. Circulation ranges from about 60,000 ft^3/s in the Gulf of Mexico to zero at the head of Hillsborough and Old Tampa Bays. Except in Hillsborough Bay, tide-induced circulation is many times greater than the average inflow from streams.

Based on figure 44, Tampa Bay was divided into eight zones that have significantly different circulation characteristics. The zones are shown in figure 26 and listed in table 14. The computed average circulation in each zone for each development condition is also given in table 14 along with the percentage increase or decrease between 1880 and 1972, between 1972 and 1985, and between 1880 and 1985.

The progression from the Gulf of Mexico to the head of Hillsborough and Old Tampa Bays consists of three sequences of high-circulation, transition, and low-circulation zones. The first sequence (zones 1, 2, and 3) defines circulation characteristics within the lower half of the bay system. Zone 1 has high circulation. Zone 3 has low circulation, about an order of magnitude less than zone 1. Zone 2 serves as a transition between zones 1 and 3.

The second sequence (zones 4, 5, and 6) depicts circulation characteristics in the northeastern part of the bay system, including Hillsborough Bay. Again, zone 4 has high circulation, zone 6 has low circulation, and zone 5 is a transition between them. Although not as obvious, the third sequence (zones 4, 7, and 8) in the northwestern part of the bay system, including Old Tampa Bay, also shows the same general pattern of high, transitional, and low circulation.

Computed tide-induced circulation in zone 1 averaged about 45,500 ft^3/s for 1880 development conditions (table 14), by far the greatest of any area in the bay. About 3.93×10^9 ft^3 of water was tidally interchanged in this zone every day, about 11 percent of the total water volume in the zone. Circulation throughout zone 1 was greatest for 1880 conditions. Circulation was reduced by about 1,600 ft^3/s for 1972 conditions and by another 2,800 ft^3/s for 1985 conditions. These reductions indicate that cumulative physical changes have reduced circulation or tidal interchange of water between the Gulf of Mexico and the entrance of Tampa Bay by about 10 percent.

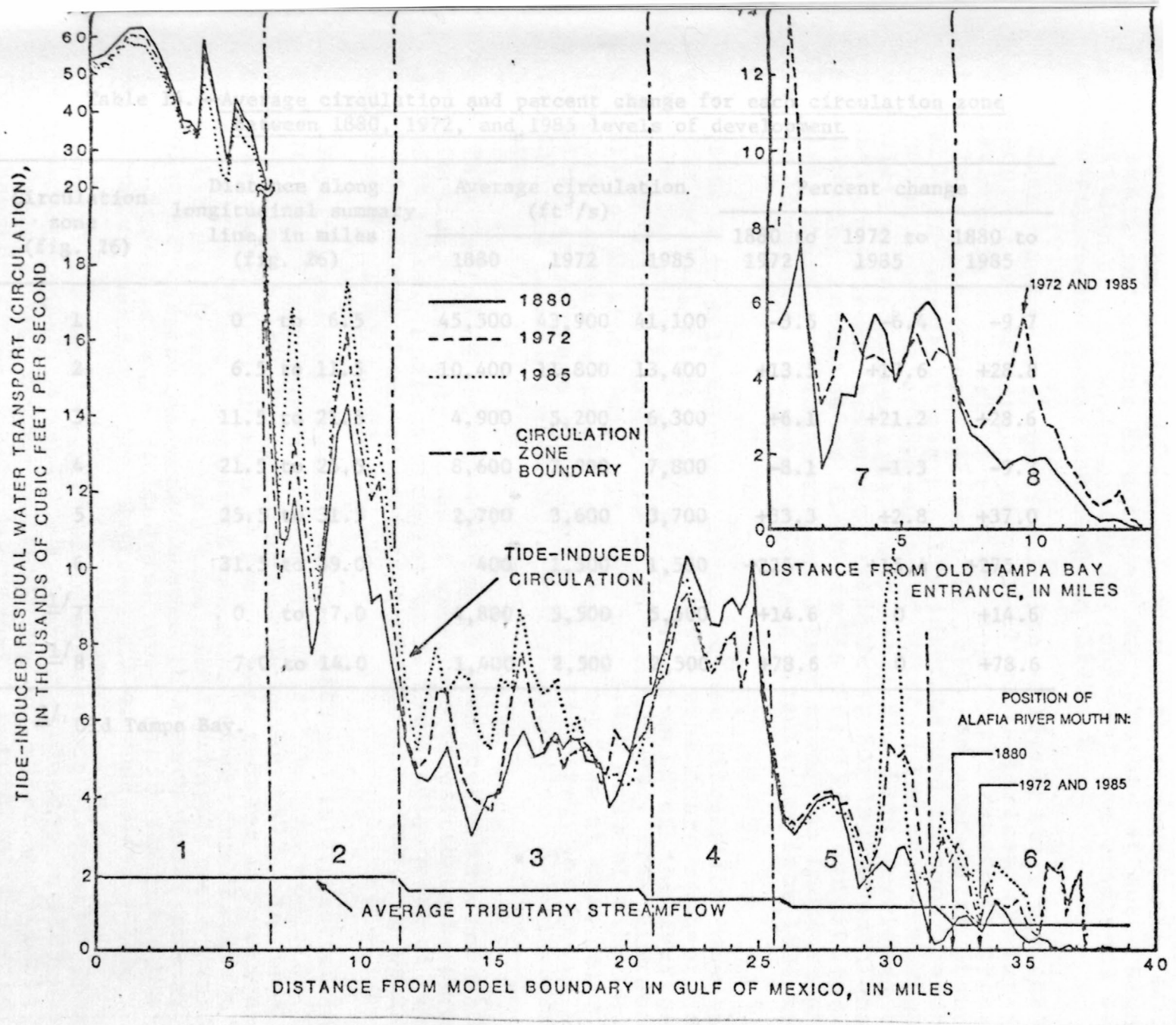

Figure 44.--Average tributary streamflow and tide-induced circulation along longitudinal summary lines for 1880, 1972, and 1985 levels of development.

Table 14.--Average circulation and percent change for each circulation zone between 1880, 1972, and 1985 levels of development

Circulation zone (fig. 26)	Distance along longitudinal summary line, in miles (fig. 26)	Average circulation (ft^3/s)			Percent change		
		1880	1972	1985	1880 to 1972	1972 to 1985	1880 to 1985
1	0 to 6.5	45,500	43,900	41,100	-3.5	-6.4	-9.7
2	6.5 to 11.5	10,400	11,800	13,400	+13.5	+13.6	+28.8
3	11.5 to 21.5	4,900	5,200	6,300	+6.1	+21.2	+28.6
4	21.5 to 25.5	8,600	7,900	7,800	-8.1	-1.3	-9.3
5	25.5 to 31.5	2,700	3,600	3,700	+33.3	+2.8	+37.0
6	31.5 to 39.0	400	1,300	1,500	+225	+15.4	+275
7 [1/]	0 to 7.0	4,800	5,500	5,500	+14.6	0	+14.6
8 [1/]	7.0 to 14.0	1,400	2,500	2,500	+78.6	0	+78.6

[1/] Old Tampa Bay.

Circulation reduction in zone 1 is not considered a significant factor influencing overall flushing and constituent interchange rates of Tampa Bay. Circulation magnitudes are so high at the bay mouth, in comparison with other areas (fig. 44), that small reductions do not have any limiting effect. High circulation at the mouth causes the observed low gradients of most constituents (Goetz and Goodwin, 1980).

Zone 2 had an average circulation of 10,400 ft^3/s for 1880 development conditions. Zone 2 is characterized by large variations in circulation that are apparently caused by gyres that have little interaction. In 1880, an average of about 0.90×10^9 ft^3 of water was tidally interchanged in zone 2 each day, about 5 percent of the volume of water in the zone. Average circulation throughout zone 2 was least for 1880 development conditions with an increase of 1,400 ft^3/s for 1972 conditions and another increase of 1,600 ft^3/s for 1985 conditions. Physical changes in and near zone 2 have caused an increase of nearly 30 percent in computed average circulation from 1880 to 1985.

Zone 3 is a 10-mile-long region of low circulation between regions of high circulation. In 1880, zone 3 had an average circulation of about 4,900 ft^3/s, about half of the average circulation in adjacent zones 2 and 4 (table 14). The minimum circulation in zone 3 was very low, only 3,000 ft^3/s at mile 14.2 (fig. 44), about double the tributary streamflow at that point. In 1880, an average of 0.42×10^9 ft^3 of water was tidally interchanged in zone 3 each day, about 1 percent of the volume of the zone.

This region of low circulation is interpreted as a natural constriction to the interchange of water and constituents between adjacent zones. Limited circulation is the likely cause of the steep specific-conductance gradients reported in zone 3 by Goetz and Goodwin (1980, p. 23).

Physical changes in zone 3 between 1880 and 1972 resulted in an average circulation increase of 300 ft^3/s. An additional increase of 1,100 ft^3/s occurred between 1972 and 1985. Cumulative physical changes in zone 3 have reduced its natural constrictive effect by about 30 percent. Long-term results of increased circulation in this area could mean (1) more rapid flushing of waterborne constituents that have their primary source north of zone 3, and (2) more rapid intrusion of constituents that have their source south of zone 3.

Zone 4 is a 4-mile region of larger average circulation than in adjacent zones 3, 5, and 7. Average circulation in 1880 was about 8,600 ft^3/s. About 0.74×10^9 ft^3 of water was tidally interchanged in zone 4 each day, about 5 percent of the water volume in the zone. Zone 4 functions for Hillsborough and Old Tampa Bays in the same way that zone 1 functions at the entrance to Tampa Bay. Rather than constrict water and constituent interchange, as in zone 3, zones 1 and 4 provide rapid, large-

scale mixing that contributes to rapid removal of constituents that have their source to the north and rapid intrusion of constituents that have their source in the south.

Physical changes in zone 4 between 1880 and 1972 caused a reduction in average circulation of 700 ft^3/s (table 14). An additional reduction of 100 ft^3/s occurred between 1972 and 1985. The cumulative circulation reduction of 9 percent in zone 4, accompanied by a 30-percent cumulative circulation increase in zone 3, largely erased the contrast between these zones from 1880 to 1985.

Zone 5, leading into Hillsborough Bay, was characterized in 1880 by a gradually reducing circulation that provided a transition to the very low circulation levels in zone 6. The increase in circulation at mile 30 (fig. 44) in 1972 and 1985 is caused by the combination of powerplant cooling-water flow, dredged channels, and spoil islands at the mouth of Hillsborough Bay.

Average circulation in 1880 was computed to be 2,700 ft^3/s. About 0.23×10^9 ft^3 of water was tidally interchanged each day, about 1 percent of the total water volume in zone 5. Largely as a result of the powerplant cooling-water discharge and channel construction, the average circulation in the zone rose to 3,600 ft^3/s in 1972 and 3,700 ft^3/s in 1985, a cumulative circulation increase of 37 percent.

Zone 6 at the head of Hillsborough Bay has the least circulation of any zone in Tampa Bay. Circulation in 1880 averaged 400 ft^3/s, less than the average discharge of the Hillsborough River, 636 ft^3/s. Tidal water interchange each day was about 0.035×10^9 ft^3 or only 0.4 percent of the water volume in zone 6. A powerplant cooling-water discharge at mile 36 and extensive dredging and filling throughout the zone caused an increase in average circulation of 900 ft^3/s by 1972 and another 200 ft^3/s increase by 1985. This is a cumulative circulation increase of 275 percent, the largest of any zone in the bay. Even with this large increase, however, zone 6 has and will continue to have the poorest circulation of any zone in Tampa Bay.

Zone 7, the lower half of Old Tampa Bay, is also a transition zone between higher and lower average circulation in zones 4 and 8, respectively. Because physical changes are not expected in Old Tampa Bay between 1972 and 1985, only one line is shown in figure 44 representing both conditions. Circulation increases at miles 3 and 13 are attributed to cooling-water discharge from powerplants. The increase in circulation in zone 8 at mile 9.5 is due to effects of the Courtney Campbell Causeway (fig. 1).

In 1880, circulation in zone 7 was 4,800 ft^3/s. About 0.42×10^9 ft^3, or nearly 4 percent of the water volume, was tidally interchanged each day. Physical changes between 1880 and 1972 caused an average circulation increase of 700 ft^3/s, or about 15 percent. In 1880, circulation in zone 8 was 1,400 ft^3/s. About 0.21×10^9 ft^3, less than 1 percent of the water volume, was tidally interchanged each day. Physical changes in zone 8 between 1880 and 1972 caused an average circulation increase of 1,100 ft^3/s, or about 79 percent. Changes in circulation in zones 7 and 8 between 1972 and 1985 are very minor due to no expected physical changes.

Constituent Transport

The patterns of flood, ebb, and residual constituent transport are developed and presented in a manner analogous to that used for water transport. A hypothetical constituent is used having an initial concentration distribution closely matching that measured for phosphorus in July 1975 (fig. 23). Constituent transport and flushing results that are given in this report are applicable for this distribution only. Comparison of results for 1880, 1972, and 1985 levels of development, however, provides a means for assessing constituent-transport changes due to physical changes in Tampa Bay.

Flood and Ebb Constituent Transport

Constituent transport patterns during flood flow for 1880, 1972, and 1985 are shown in figures 45, 46, and 47, respectively. The maps show many similarities, including low constituent transport near the bay mouth where concentrations are low and high constituent transport in the upper parts of the bay where concentrations are high. The magnitudes and directions of constituent transport vectors at 25 selected sites during flood tide are listed in table 15. The sites are the same as those chosen for water transport (fig. 27). Vector magnitudes through each 1,500-foot cell were about 0.6 lb/s at the entrance to Tampa Bay (site 1), 0.9 lb/s at mid-Tampa Bay (site 9), 0.6 lb/s in Old Tampa Bay (site 23), and 0.2 lb/s in Hillsborough Bay (site 18).

Significant differences in constituent-transport magnitude and direction at some sites for 1880, 1972, and 1985 conditions are evident. Sites 6, 13, 16, 19, 24, and 25, for example, show changes due to construction of causeways, islands, channels, or submerged disposal areas.

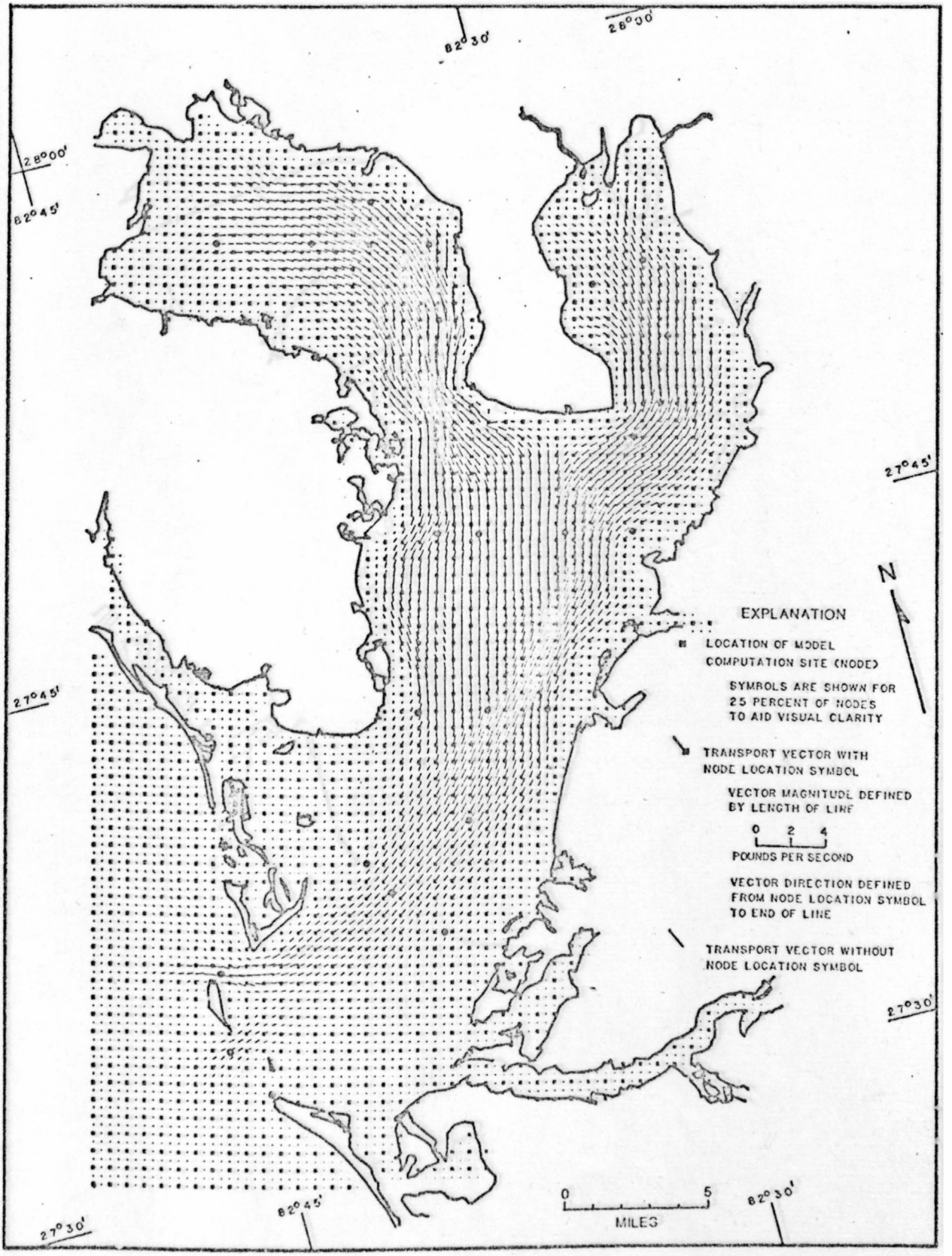

Figure 45.--Constituent-transport pattern during typical flood tide for 1880 level of development.

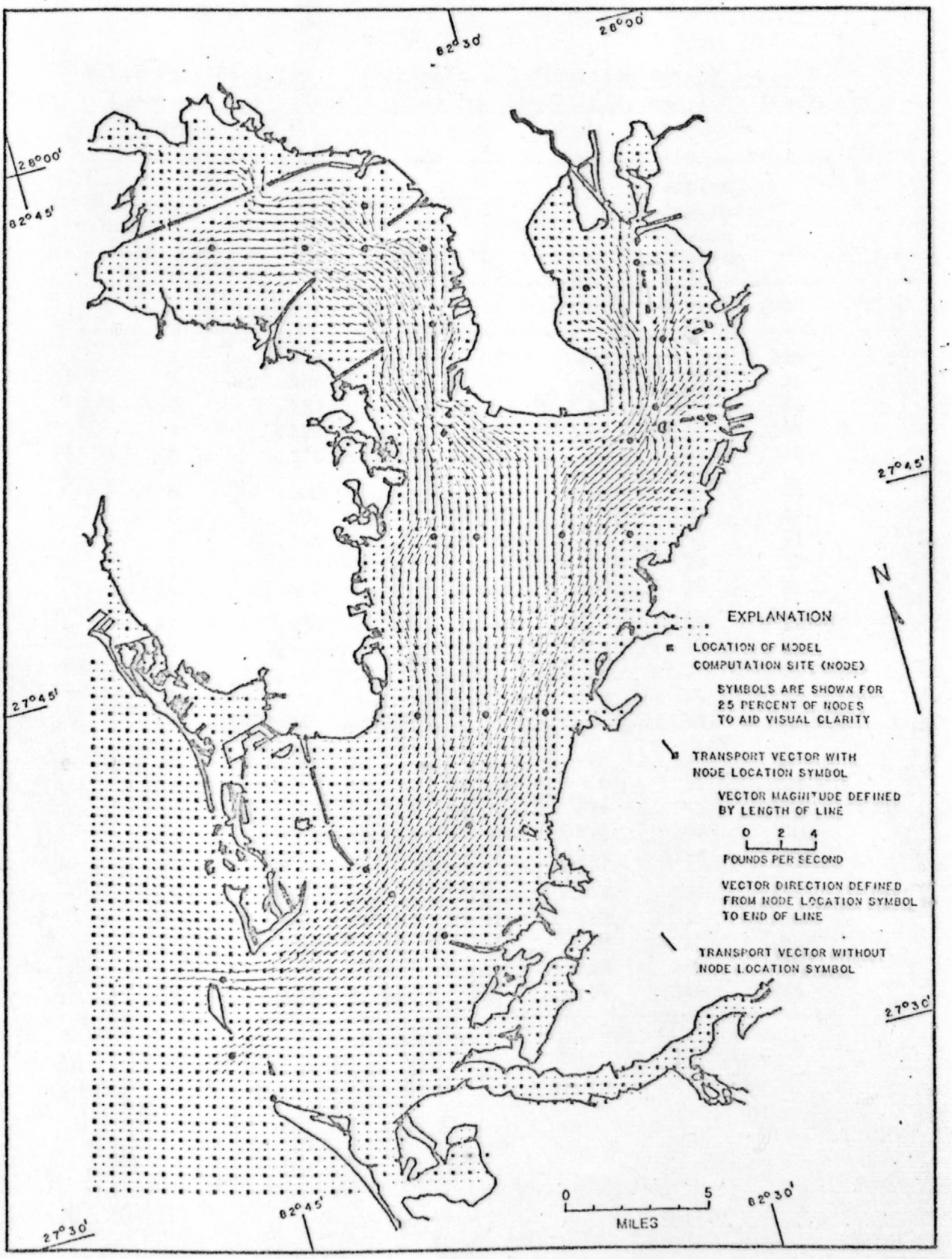

Figure 46.--Constituent-transport pattern during typical flood tide for 1972 level of development.

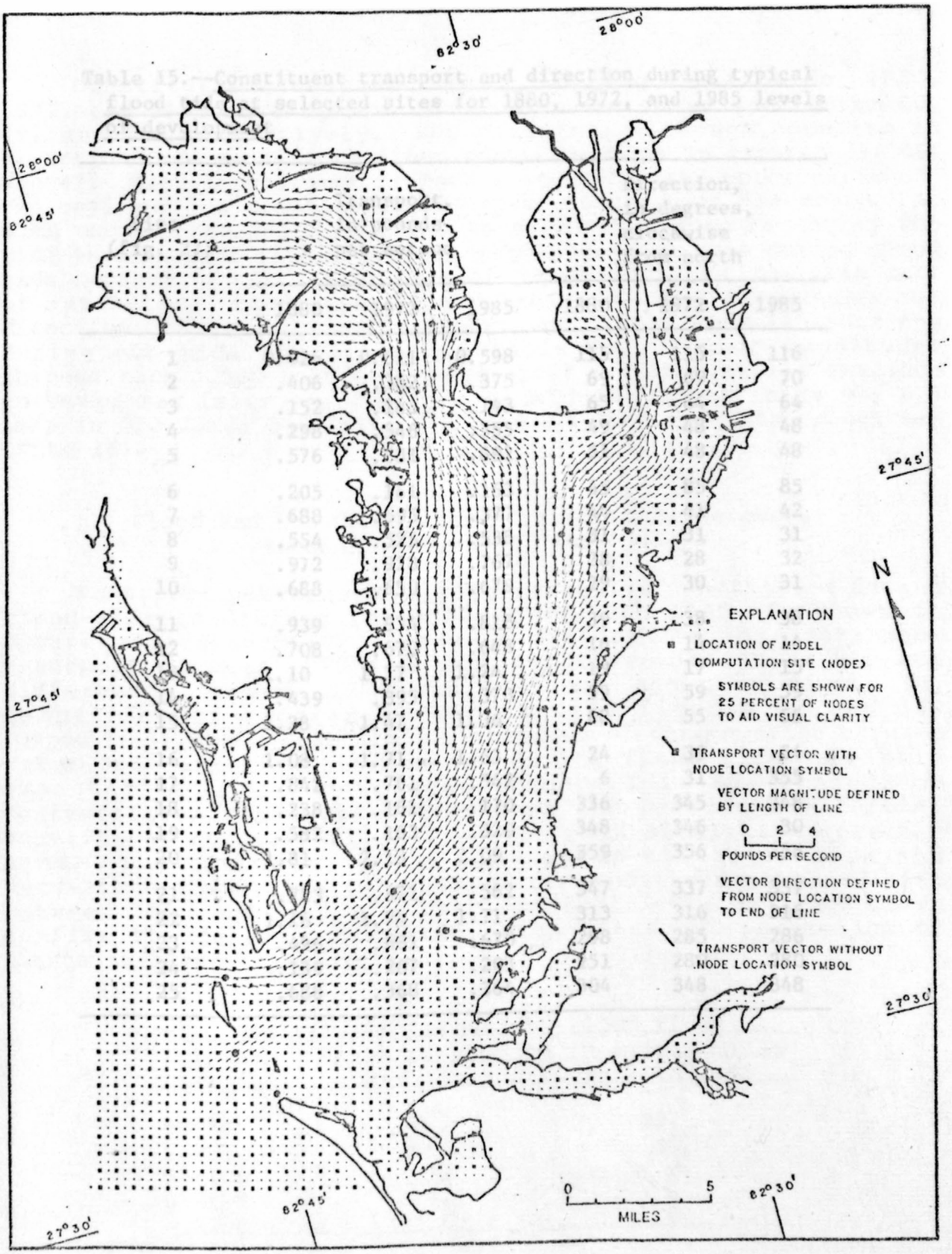

Figure 47.--Constituent-transport pattern during typical flood tide for 1985 level of development.

Table 15.--Constituent transport and direction during typical flood tide at selected sites for 1880, 1972, and 1985 levels of development

Site (fig. 27)	Transport, in pounds per second			Direction, in degrees, clockwise from north		
	1880	1972	1985	1880	1972	1985
1	0.626	0.611	0.598	115	115	116
2	.406	.382	.375	69	69	70
3	.152	.143	.143	65	64	64
4	.298	.346	.355	49	48	48
5	.576	.631	.692	51	48	48
6	.205	.161	.163	45	85	85
7	.688	.595	.377	44	41	42
8	.554	.525	.538	31	31	31
9	.972	.928	.767	28	28	32
10	.688	.650	.679	29	30	31
11	.939	.834	.818	39	38	38
12	.708	.670	.648	16	14	14
13	1.10	1.17	1.24	19	17	15
14	.439	.395	.373	59	59	59
15	1.28	1.47	1.36	62	55	55
16	1.08	1.71	1.63	24	39	54
17	.842	.761	.542	6	31	355
18	.238	.161	.170	336	345	348
19	.582	.163	.320	348	346	30
20	1.81	2.13	2.09	359	356	356
21	.723	.571	.562	347	337	337
22	1.16	1.74	1.71	313	316	316
23	.496	.681	.670	298	285	286
24	.139	.207	.203	251	280	280
25	.688	.368	.364	304	348	348

Constituent-transport patterns during ebb flow for 1880, 1972, and 1985 development conditions are shown in figures 48, 49, and 50, respectively. Ebb patterns, although opposite in direction, are similar to flood patterns shown in figures 45, 46, and 47. High constituent transport occurs in the upper parts of the bay, and low constituent transport occurs near the mouth. As with water transport, maximum constituent transport during ebb tide is of substantially greater magnitude than that during flood tide because of the faster rate of water-level decline than rate of water-level rise (fig. 22 and table 9). The magnitudes and directions of constituent-transport vectors at 25 selected sites during ebb tide are listed in table 16. Vector magnitudes through each 1,500-foot cell were about 1.8 lb/s at the entrance to Tampa Bay (site 1), 1.5 lb/s in mid-Tampa Bay (site 9), 0.8 lb/s in Old Tampa Bay (site 23), and 0.4 lb/s in Hillsborough Bay (site 18).

Flood and Ebb Constituent-Transport Differences Between 1880, 1972, and 1985

Transport patterns of a representative constituent during flood-tide conditions for 1880, 1972, and 1985 are shown in figures 45 through 47. Areas of differences in constituent transport between 1880 and 1972 are shown in figure 51, and differences between 1972 and 1985 are shown in figure 52. Comparison of figures 51 and 52 with figures 33 and 34, respectively, show that similar patterns of change exist between water and constituent transport during flood tide. This is expected because constituent transport is the product of concentration times water transport and because the initial constituent concentrations used for each simulation were the same. The following table summarizes the total area and percentage change for constituent transport during flood tide between 1880 and 1972 and 1972 and 1985. The figures shown confirm the general similarity with areas and percentage of change in flood transport.

Constituent transport--flood tide		
Percent change	Area of change, in square miles	
	1880 to 1972	1972 to 1985
0-10	260	397
11-50	144	41
51-100	52	8
101-200	7	1
>200	1	0

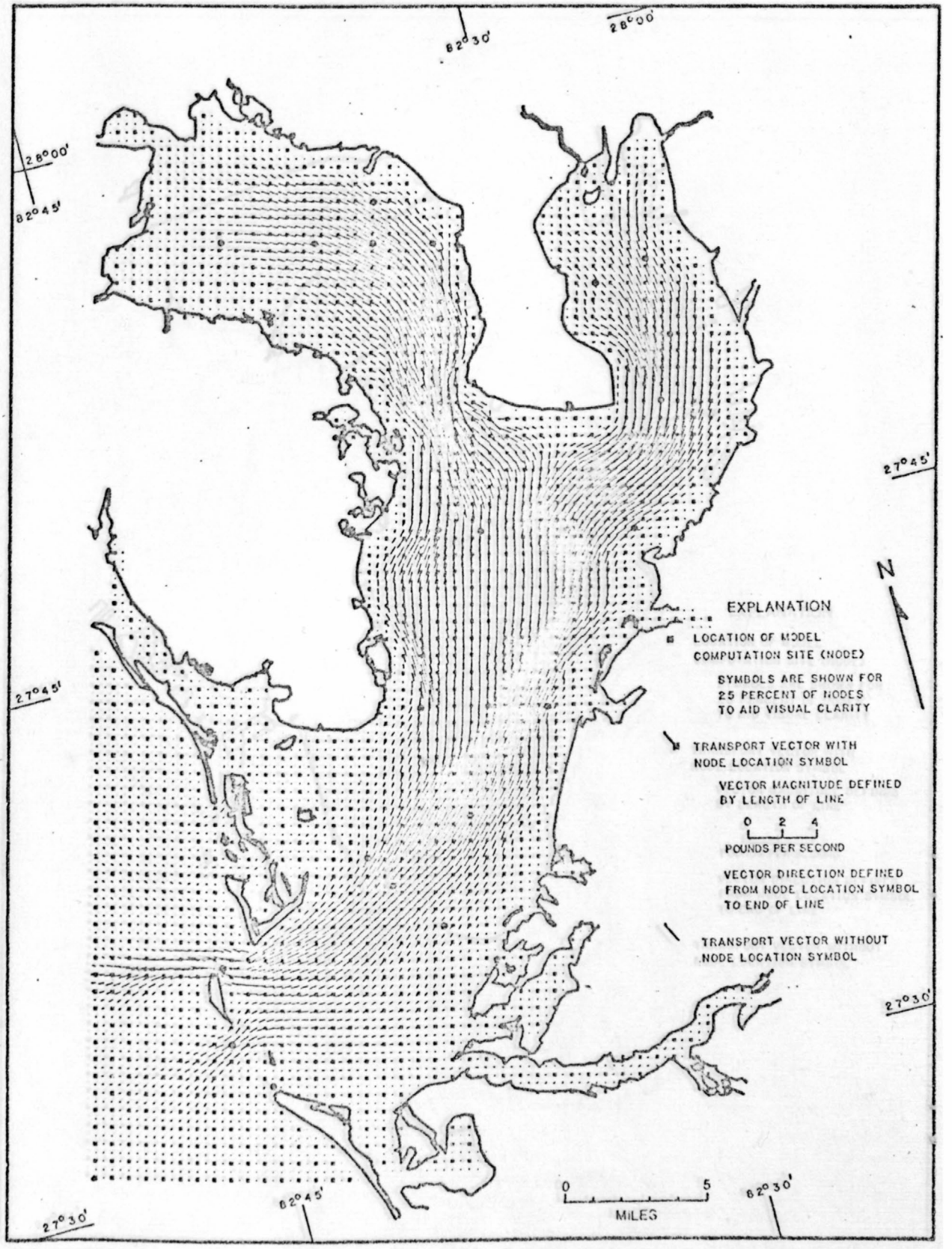

Figure 48.--Constituent-transport pattern during typical ebb tide for 1880 level of development.

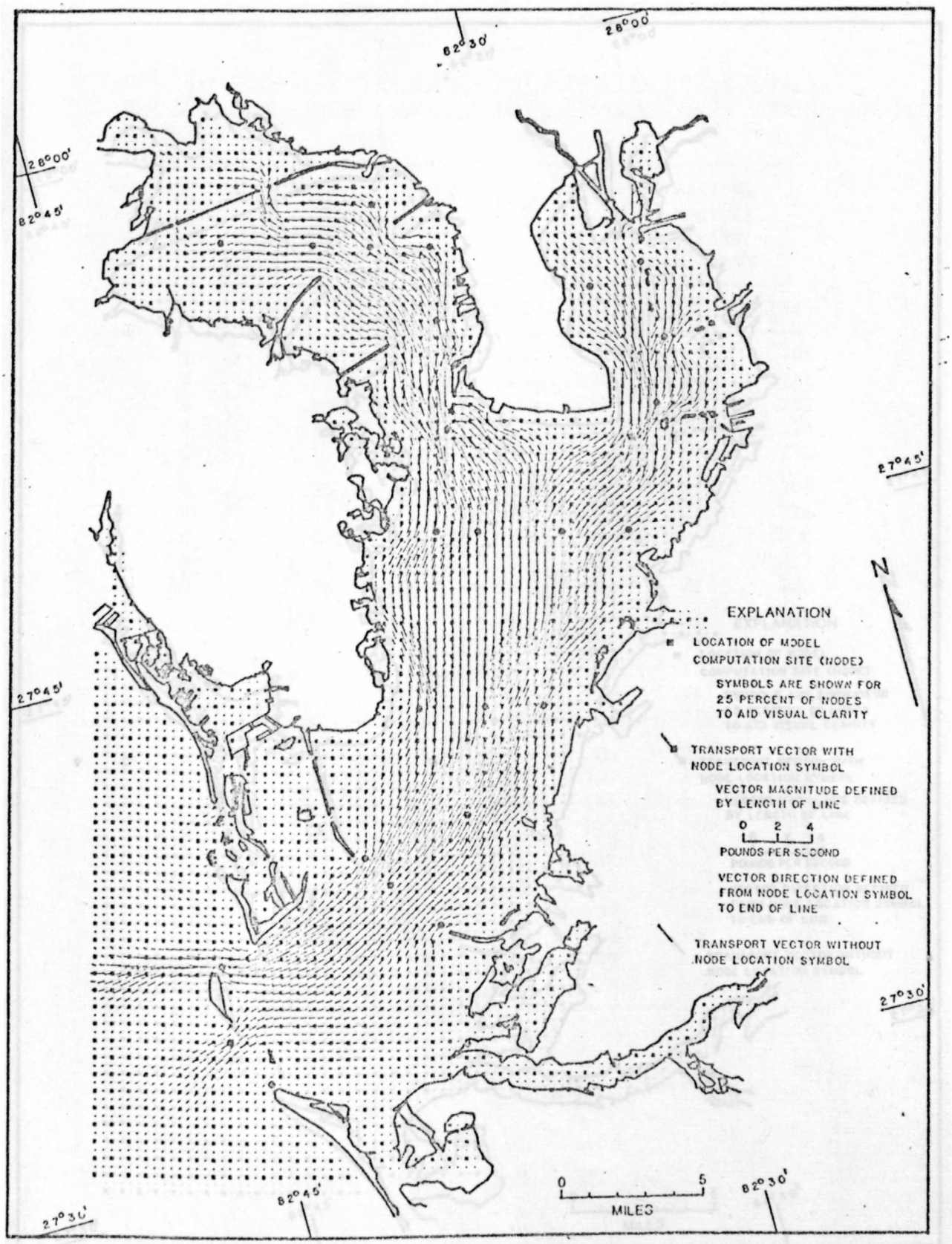

Figure 49.--Constituent-transport pattern during typical ebb tide for 1972 level of development.

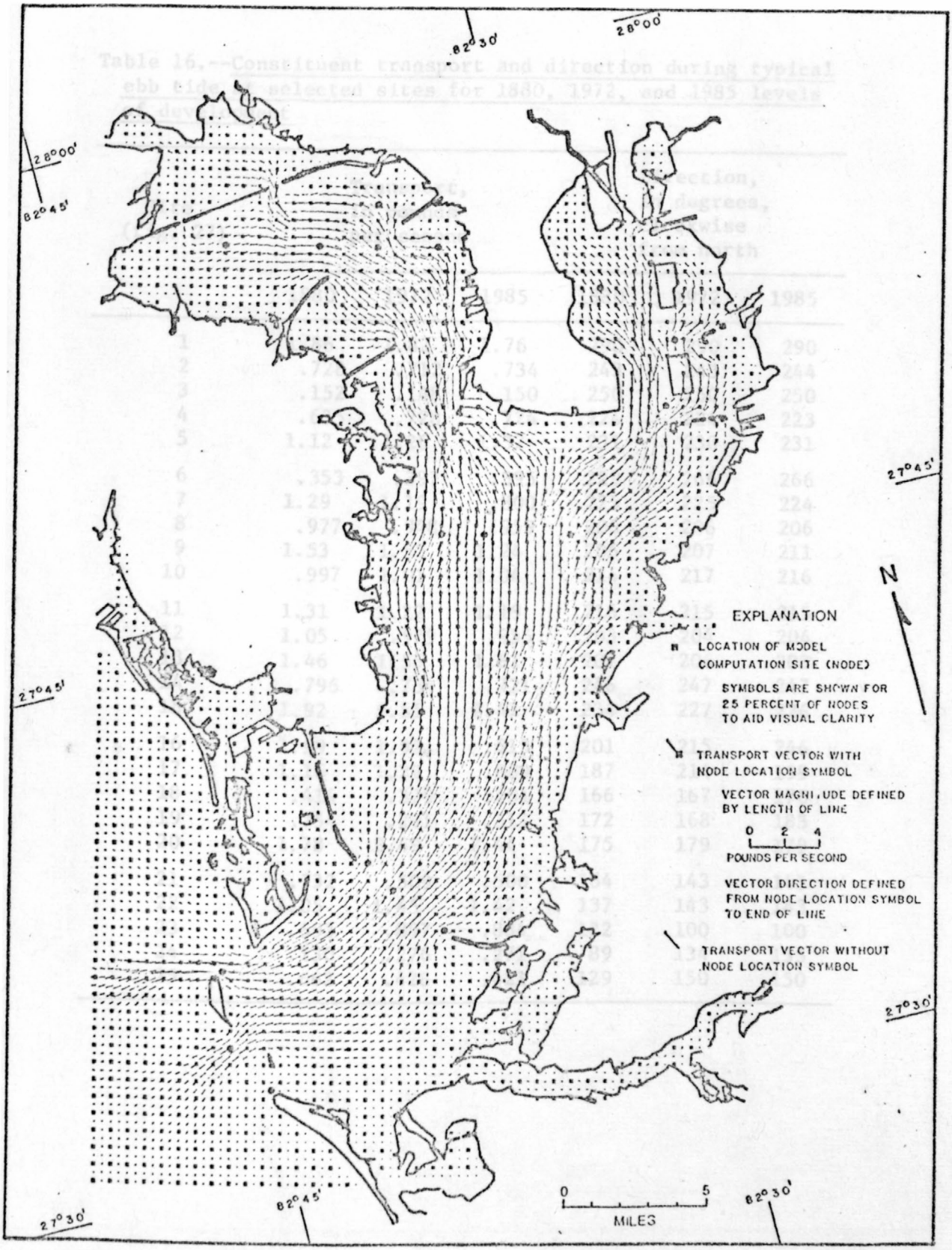

Figure 50.--Constituent-transport pattern during typical ebb tide for 1985 level of development.

Table 16.--Constituent transport and direction during typical ebb tide at selected sites for 1880, 1972, and 1985 levels of development

Site (fig. 27)	Transport, in pounds per second			Direction, in degrees, clockwise from north		
	1880	1972	1985	1880	1972	1985
1	1.86	1.82	1.76	290	290	290
2	.728	.712	.734	243	243	244
3	.152	.148	.150	250	250	250
4	.635	.728	.724	224	224	223
5	1.12	1.26	1.32	231	230	231
6	.353	.397	.395	229	266	266
7	1.29	1.19	.800	225	225	224
8	.977	.948	.959	206	206	206
9	1.53	1.52	1.24	206	207	211
10	.997	1.01	1.04	214	217	216
11	1.31	1.22	1.19	216	215	215
12	1.05	.979	.955	203	204	204
13	1.46	1.55	1.61	207	206	203
14	.796	.754	.721	246	247	247
15	1.92	2.55	2.42	234	227	226
16	1.59	1.92	.613	201	215	246
17	1.16	1.29	.809	187	214	199
18	.414	.379	.401	166	167	170
19	.754	.291	.311	172	168	183
20	1.78	2.49	2.44	175	179	179
21	.732	.509	.500	164	143	143
22	1.05	1.45	1.42	137	143	143
23	.593	.897	.884	122	100	100
24	.130	.276	.271	89	134	135
25	.662	.428	.421	129	150	150

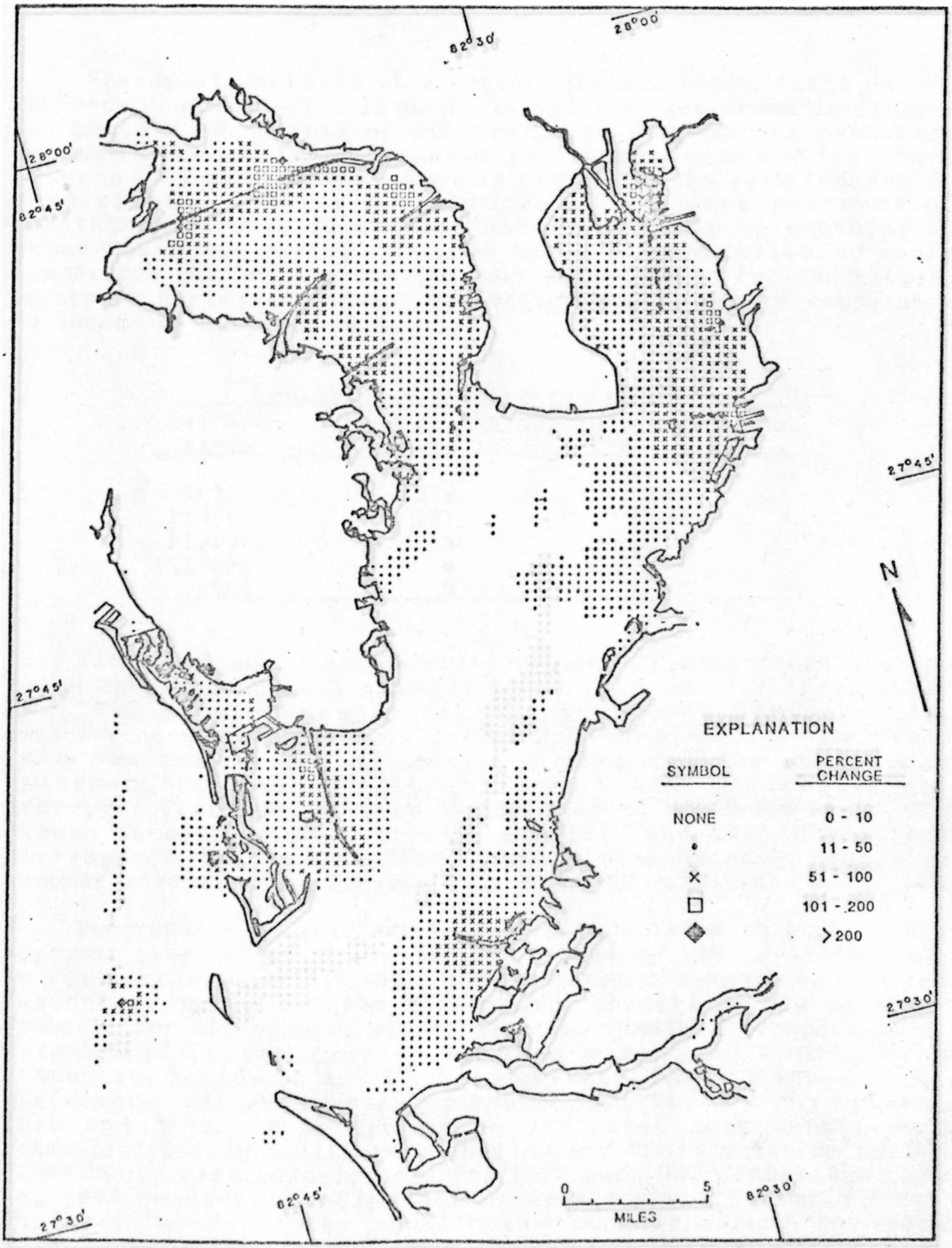

Figure 51.--Change in constituent transport for typical flood tide between 1880 and 1972 levels of development.

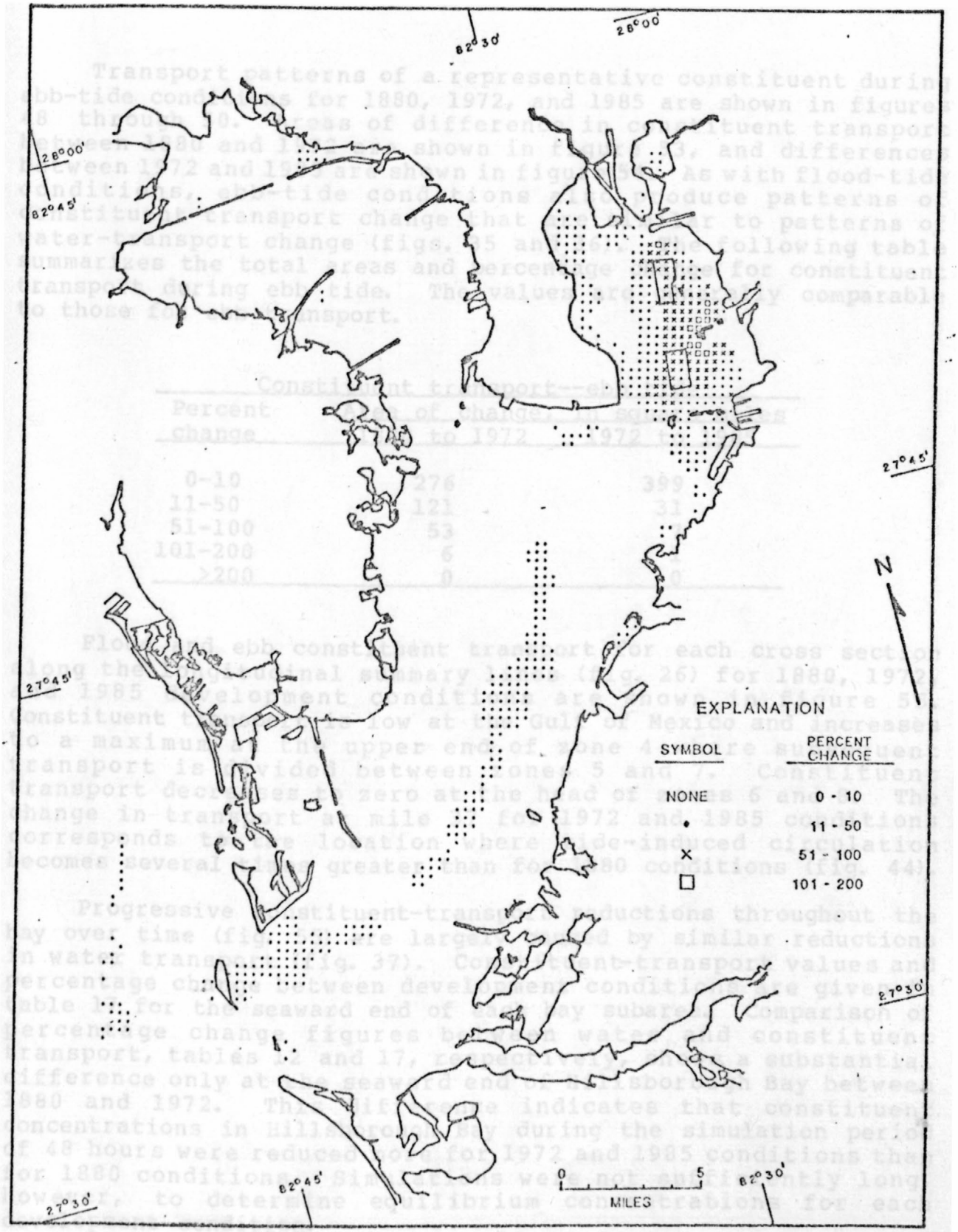

Figure 52.--Change in constituent transport for typical flood tide between 1972 and 1985 levels of development.

Transport patterns of a representative constituent during ebb-tide conditions for 1880, 1972, and 1985 are shown in figures 48 through 50. Areas of difference in constituent transport between 1880 and 1972 are shown in figure 53, and differences between 1972 and 1985 are shown in figure 54. As with flood-tide conditions, ebb-tide conditions also produce patterns of constituent-transport change that are similar to patterns of water-transport change (figs. 35 and 36). The following table summarizes the total areas and percentage change for constituent transport during ebb tide. The values are generally comparable to those for ebb transport.

Constituent transport--ebb tide

Percent change	Area of change, in square miles	
	1880 to 1972	1972 to 1985
0-10	276	399
11-50	121	31
51-100	53	7
101-200	6	1
>200	0	0

Flood and ebb constituent transport for each cross section along the longitudinal summary lines (fig. 26) for 1880, 1972, and 1985 development conditions are shown in figure 55. Constituent transport is low at the Gulf of Mexico and increases to a maximum at the upper end of zone 4 where subsequent transport is divided between zones 5 and 7. Constituent transport decreases to zero at the head of zones 6 and 8. The change in transport at mile 37 for 1972 and 1985 conditions corresponds to the location where tide-induced circulation becomes several times greater than for 1880 conditions (fig. 44).

Progressive constituent-transport reductions throughout the bay over time (fig. 55) are largely caused by similar reductions in water transport (fig. 37). Constituent-transport values and percentage change between development conditions are given in table 17 for the seaward end of each bay subarea. Comparison of percentage change figures between water and constituent transport, tables 12 and 17, respectively, shows a substantial difference only at the seaward end of Hillsborough Bay between 1880 and 1972. This difference indicates that constituent concentrations in Hillsborough Bay during the simulation period of 48 hours were reduced more for 1972 and 1985 conditions than for 1880 conditions. Simulations were not sufficiently long, however, to determine equilibrium concentrations for each development condition.

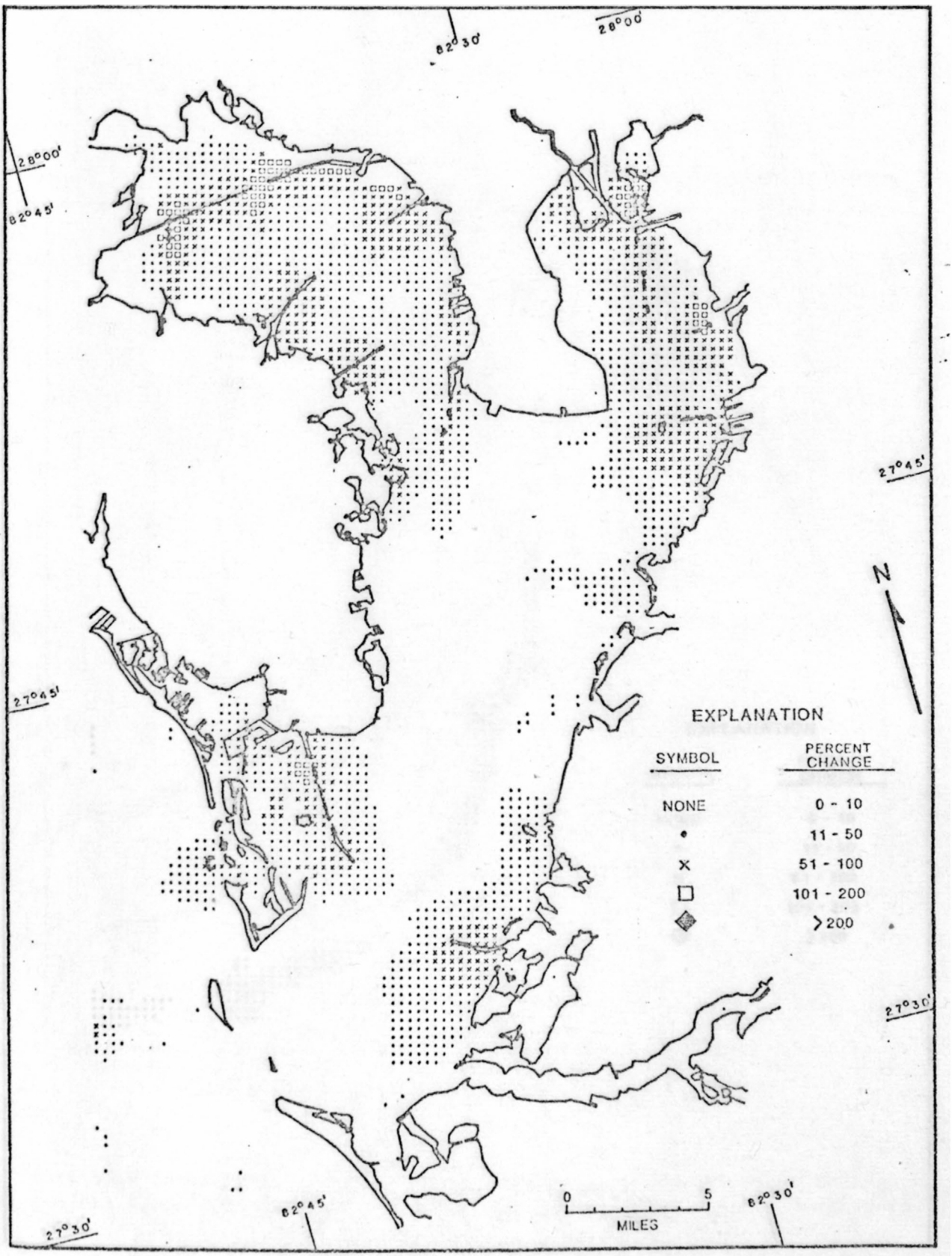

Figure 53.--Change in constituent transport for typical ebb tide between 1880 and 1972 levels of development.

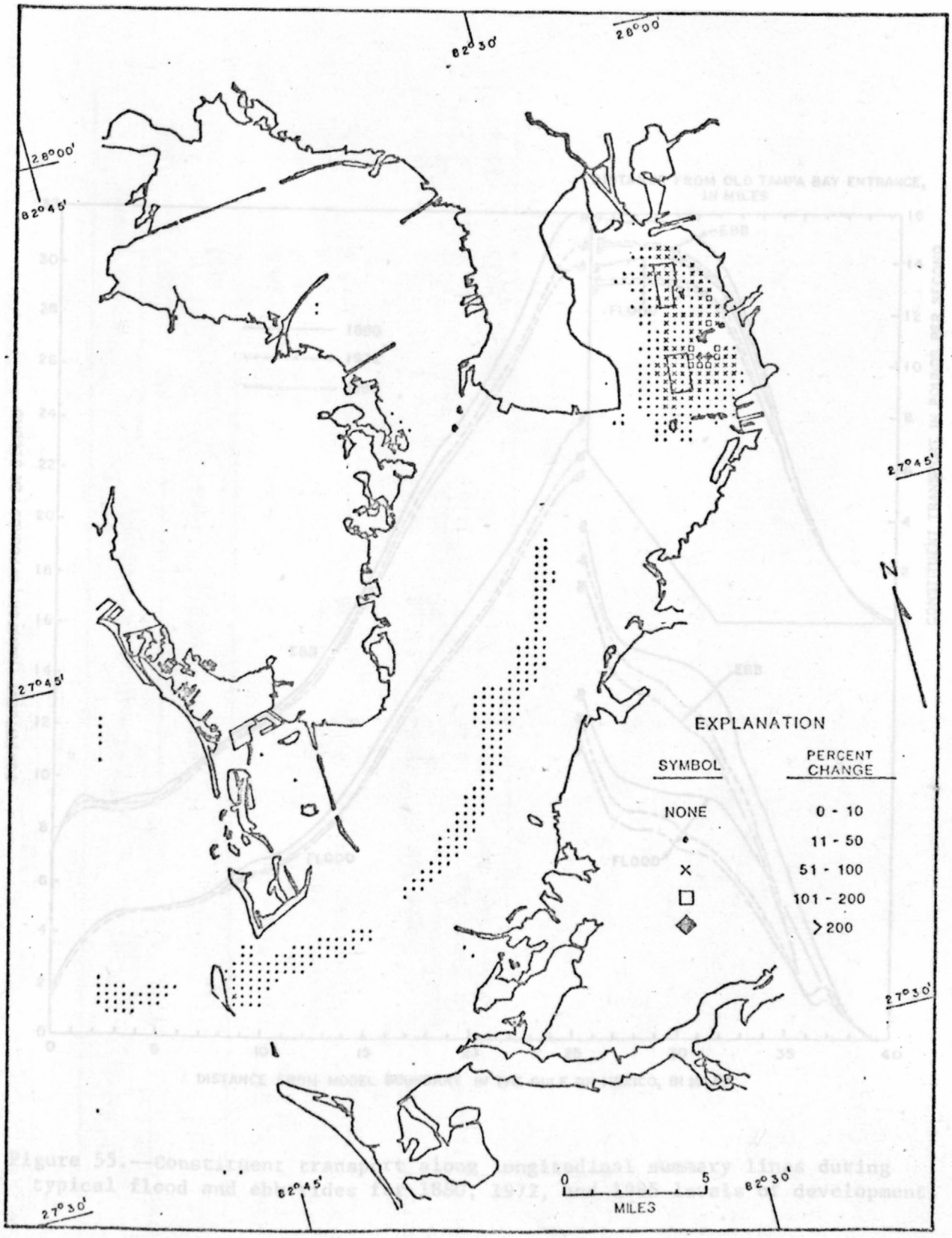

Figure 54.--Change in constituent transport for typical ebb tide between 1972 and 1985 levels of development.

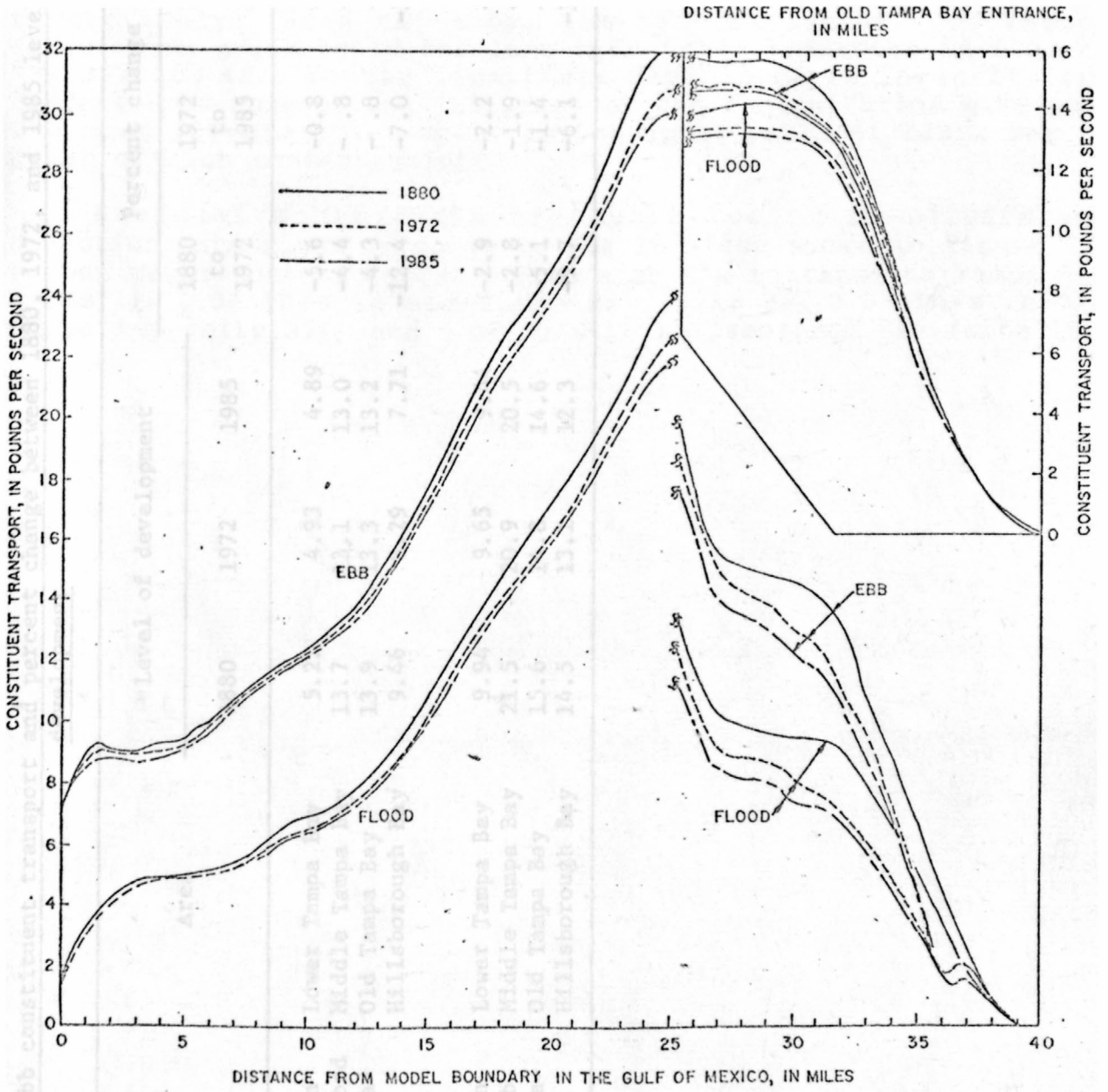

Figure 55.--Constituent transport along longitudinal summary lines during typical flood and ebb tides for 1880, 1972, and 1985 levels of development.

Table 17.--Flood and ebb constituent transport and percent change between 1880, 1972, and 1985 levels of development

Characteristic	Area	Level of development			Percent change		
		1880	1972	1985	1880 to 1972	1972 to 1985	1880 to 1985
Constituent transport, in lb/s, during typical flood tide computed at the seaward end of:	Lower Tampa Bay	5.22	4.93	4.89	-5.6	-0.8	-6.3
	Middle Tampa Bay	13.7	13.1	13.0	-4.4	- .8	-5.1
	Old Tampa Bay	13.9	13.3	13.2	-4.3	- .8	-5.0
	Hillsborough Bay	9.46	8.29	7.71	-12.4	-7.0	-18.5
Constituent transport, in lb/s, during typical ebb tide computed at the seaward end of:	Lower Tampa Bay	9.94	9.65	9.44	-2.9	-2.2	-5.0
	Middle Tampa Bay	21.5	20.9	20.5	-2.8	-1.9	-4.7
	Old Tampa Bay	15.6	14.8	14.6	-5.1	-1.4	-6.4
	Hillsborough Bay	14.5	13.1	12.3	-9.7	-6.1	-15.2

Residual Constituent Transport

Residual constituent-transport patterns for 1880, 1972, and 1985 levels of development are shown in figures 56, 57, and 58, respectively. Each map shows the same series of circulatory features or gyres found for long-term water transport in figures 38, 39, and 40. Vector magnitudes devining gyre intensity are different because of the influence of the concentration gradient. The most intense gyres occur in the upper parts of Tampa Bay in areas of high concentrations.

Residual constituent-transport vector magnitudes and directions are given in table 18 for 25 sites shown in figure 27. Vector magnitudes are about 0.2 lb/s at the entrance to Tampa Bay (site 1), 0.04 lb/s in mid-Tampa Bay (site 9), 0.07 lb/s in Old Tampa Bay (site 22), and 0.06 lb/s in Hillsborough Bay (site 18).

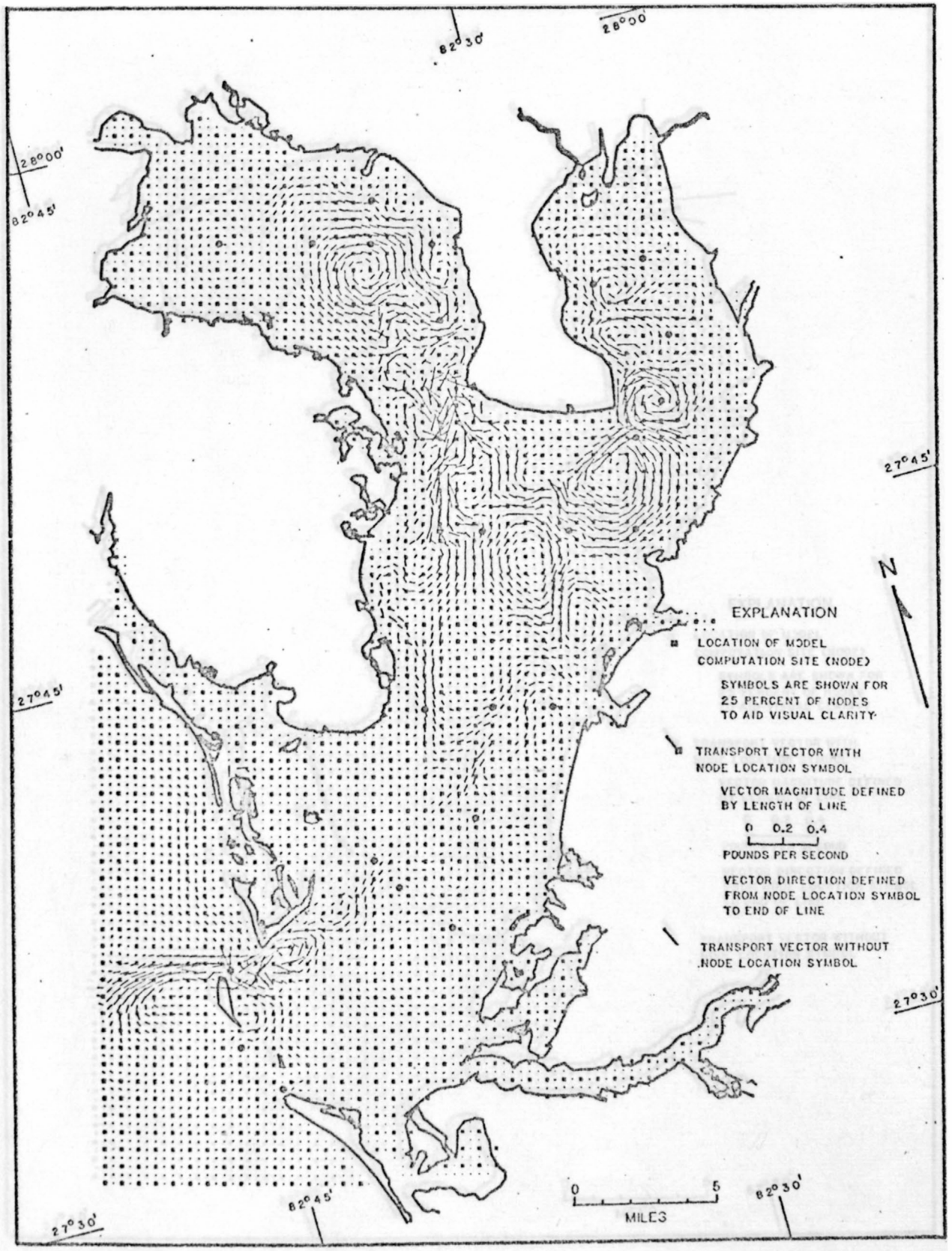

Figure 56.--Residual constituent-transport pattern for 1880 level of development.

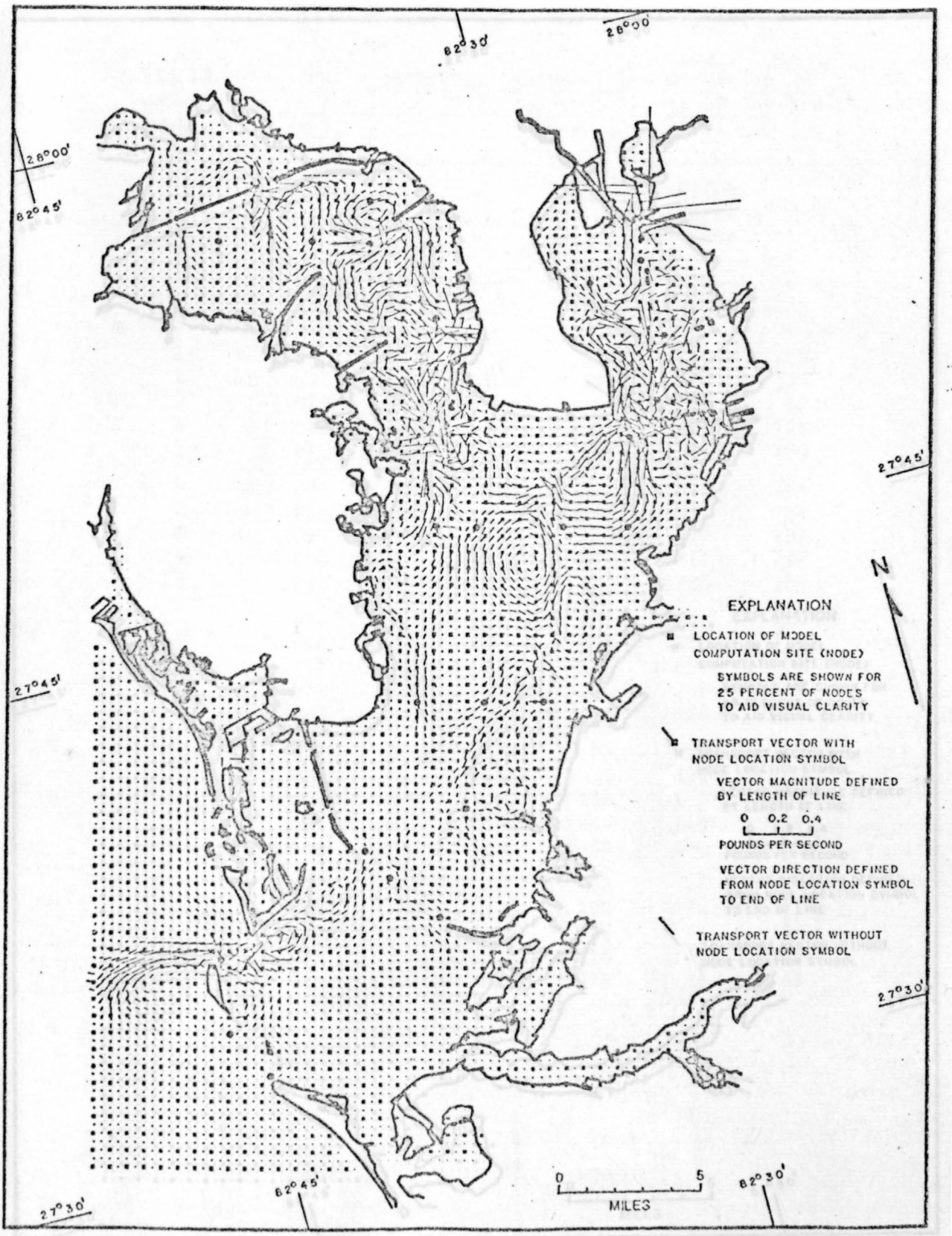

Figure 57.--Residual constituent-transport pattern for 1972 level of development.

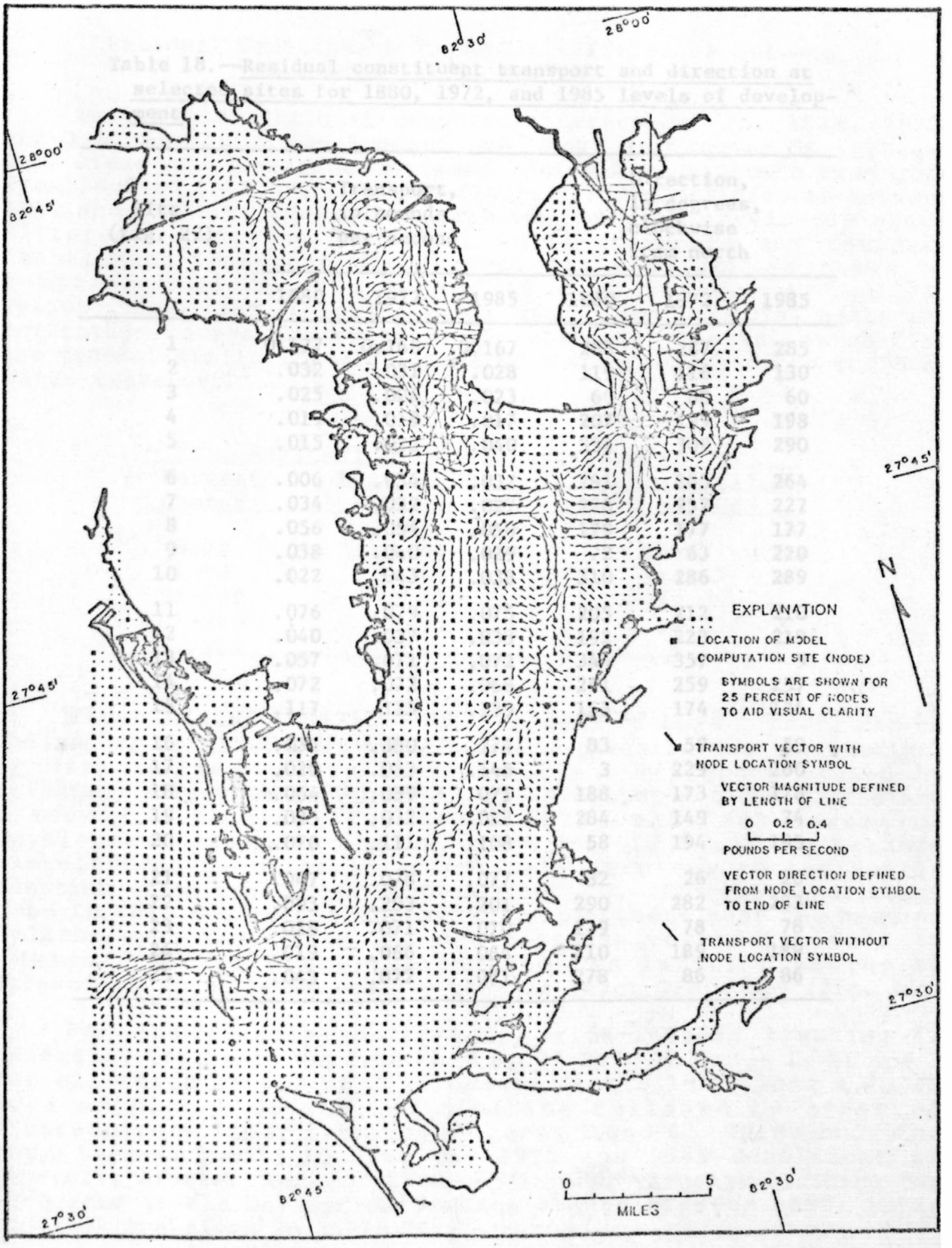

Figure 58.--Residual constituent-transport pattern for 1985 level of development.

Table 18.--Residual constituent transport and direction at selected sites for 1880, 1972, and 1985 levels of development

Site (fig. 27)	Transport, in pounds per second			Direction, in degrees, clockwise from north		
	1880	1972	1985	1880	1972	1985
1	0.177	0.168	0.167	288	287	285
2	.032	.031	.028	119	118	130
3	.025	.024	.023	60	60	60
4	.019	.018	.017	207	199	198
5	.015	.023	.040	334	309	290
6	.006	.034	.032	291	265	264
7	.034	.032	.027	226	257	227
8	.056	.054	.050	179	177	177
9	.038	.040	.029	72	63	220
10	.022	.043	.038	310	286	289
11	.076	.079	.075	205	212	210
12	.040	.037	.033	192	228	219
13	.057	.071	.072	344	357	9
14	.072	.072	.068	261	259	257
15	.117	.125	.139	153	174	176
16	.032	.380	.774	83	59	59
17	.020	.043	.145	3	229	280
18	.064	.059	.071	188	173	176
19	.025	.032	.088	284	149	74
20	.070	.111	.108	58	194	195
21	.047	.078	.077	32	26	26
22	.093	.203	.201	290	282	283
23	.028	.071	.070	179	78	78
24	.019	.066	.064	210	189	189
25	.043	.072	.071	278	86	86

Residual Constituent-Transport Differences Between 1880, 1972, and 1985

Patterns of residual constituent transport for 1880, 1972, and 1985 levels of development are shown in figures 56 through 58. Areas of differences between residual constituent transport from 1800 to 1972 are shown in figure 59, and differences between 1972 and 1985 are shown in figure 60. As with previously shown difference patterns, residual water-transport and residual constituent-transport differences are similar, as shown by comparison of figures 59 and 60 with figures 42 and 43, respectively. The following table summarizes the total areas and percentage change in constituent transport. The values confirm the general similarity with areas of change computed for residual water transport.

Residual constituent transport		
Percent change	Area of change, in square miles	
	1880 to 1972	1972 to 1985
0-10	98	241
11-50	166	144
51-100	83	32
101-200	72	24
>200	45	6

Tide-induced flushing, for purposes of this report, can be defined as total constituent flushing, given in the longitudinal summary section, minus the constituent transport caused by tributary streamflow. Figure 61 shows computed tide-induced and streamflow flushing for 1880, 1972, and 1985 levels of development. Results are not given for Old Tampa Bay because tide-induced flushing is effectively zero due to the nearly constant constituent distribution (fig. 23). For the constituent used in this study, concentrations are highest near the head of Hillsborough Bay, mile 36, and decrease toward the Gulf of Mexico. Such a distribution produces larger flushing by streamflow in Hillsborough Bay than in lower Tampa Bay (fig. 61).

For the example constituent, tide-induced flushing is generally low, between 2,000 and 6,000 lb/d in zones 1, 2, and 3 for all three levels of development (table 19). Zone 4 is an area of high tide-induced flushing followed by areas of progressively lower flushing in zones 5 and 6. Throughout the bay, tide-induced flushing for 1972 and 1985 conditions is generally greater than for 1880 conditions. Average flushing for each zone in the bay and percentage change between 1880, 1972, and 1985 are given in table 19.

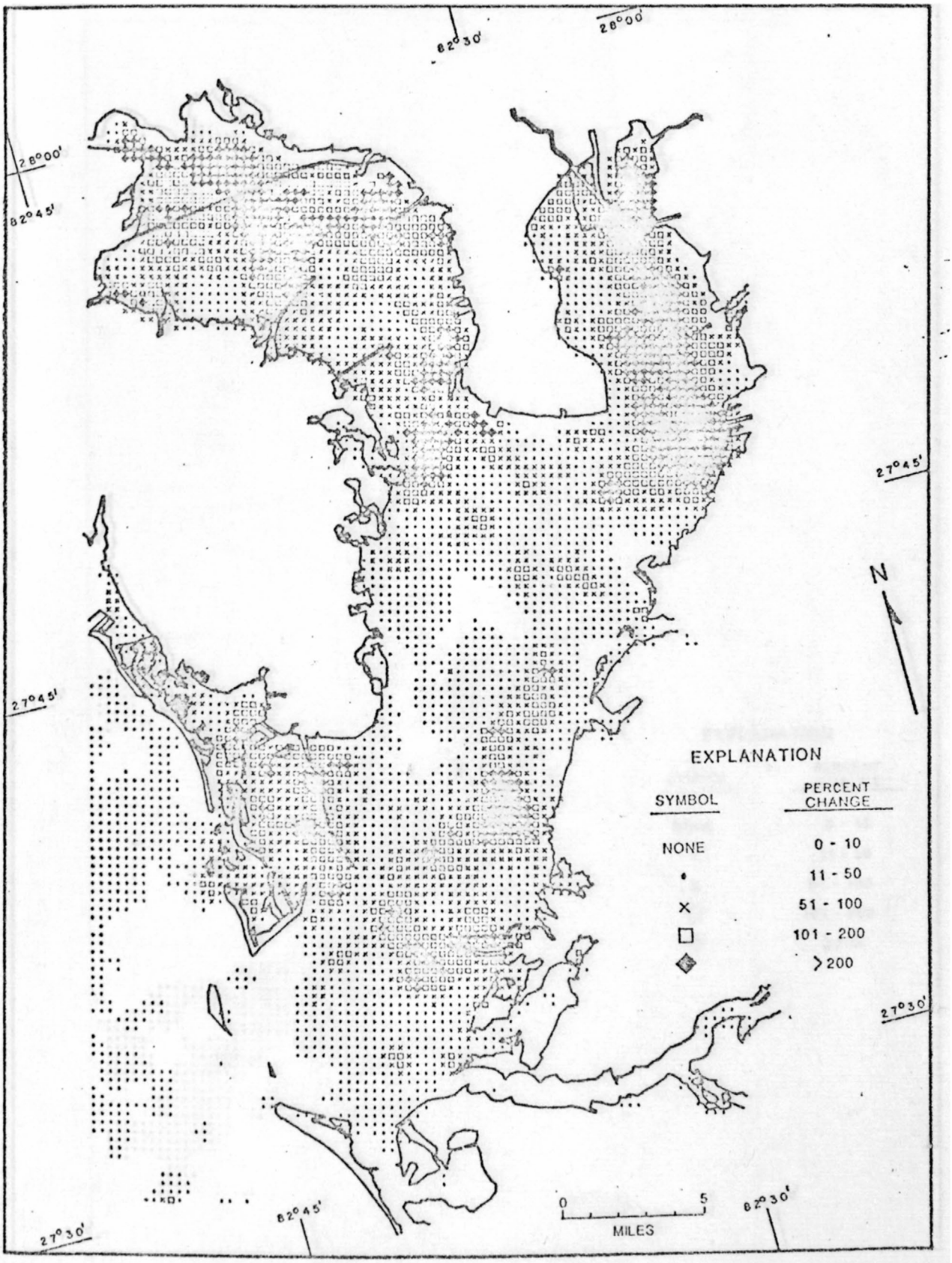

Figure 59.--Change in residual constituent transport between 1880 and 1972 levels of development.

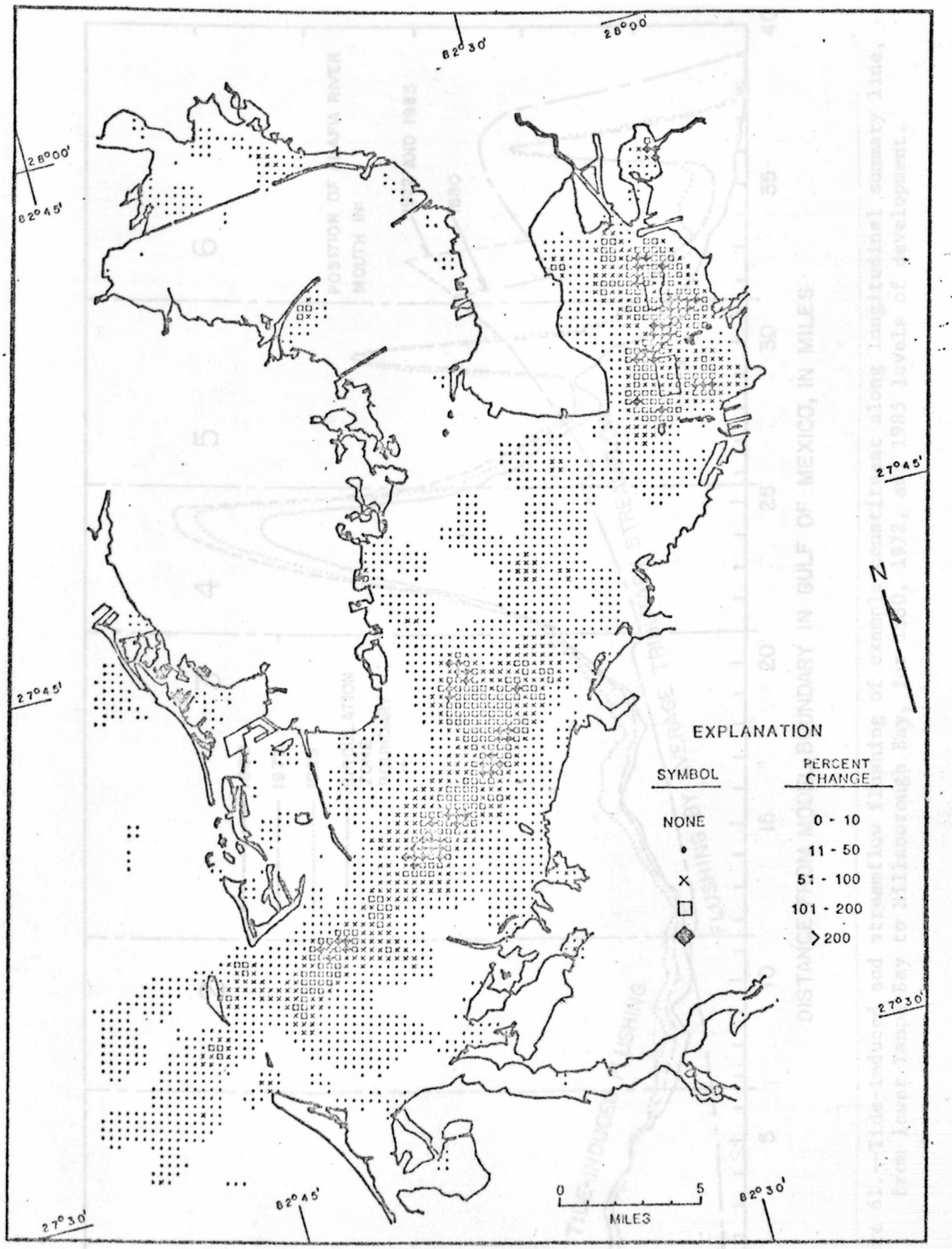

Figure 60.--Change in residual constituent transport between 1972 and 1985 levels of development.

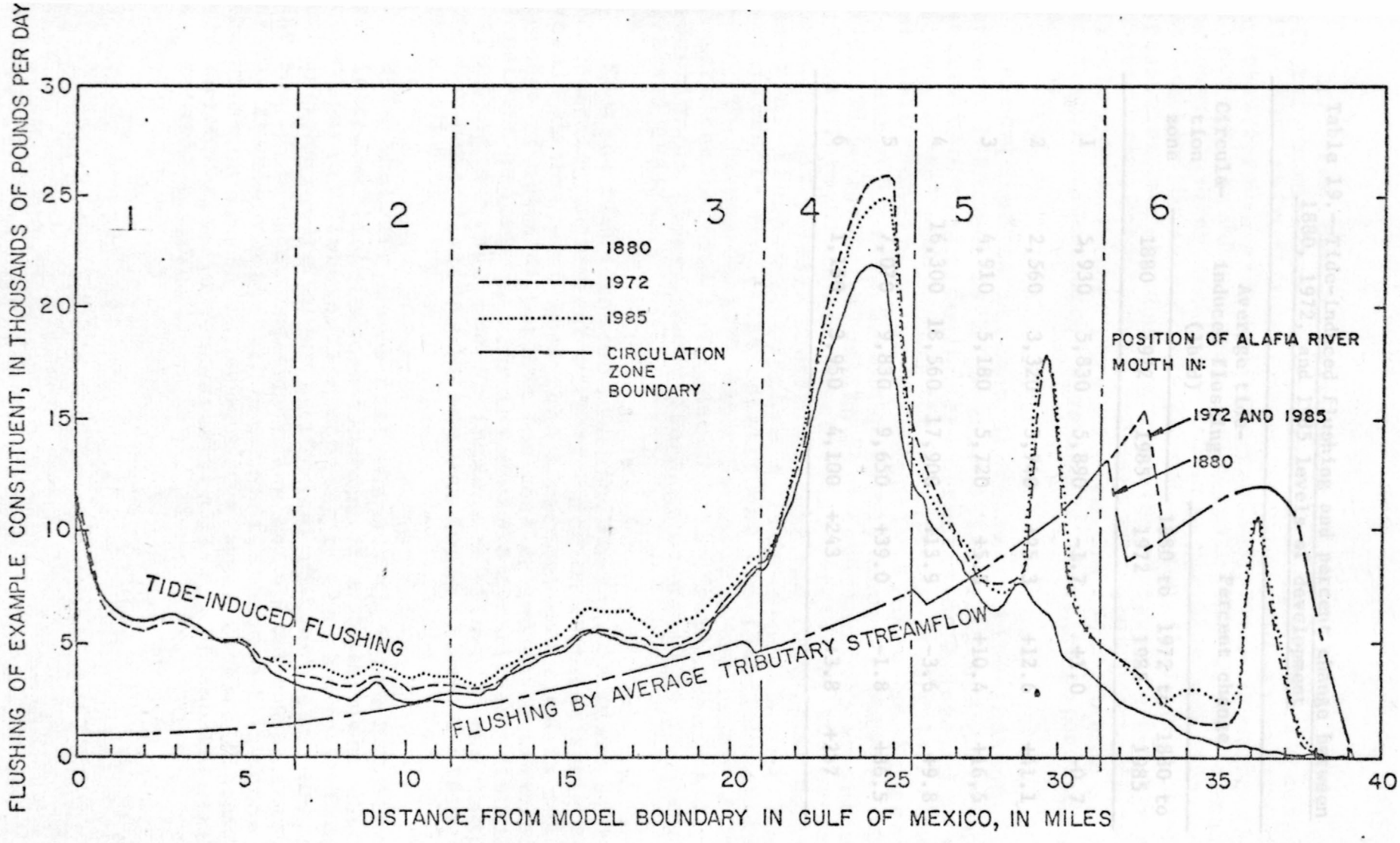

Figure 61.--Tide-induced and streamflow flushing of example constituent along longitudinal summary line, from lower Tampa Bay to Hillsborough Bay, for 1880, 1972, and 1985 levels of development.

Table 19.--Tide-induced flushing and percent change between 1880, 1972, and 1985 levels of development

Circulation zone	Average tide-induced flushing (lb/d)			Percent change		
	1880	1972	1985	1880 to 1972	1972 to 1985	1880 to 1985
1	5,930	5,830	5,890	-1.7	+1.0	-0.7
2	2,560	3,320	3,740	+25.3	+12.6	+41.1
3	4,910	5,180	5,720	+5.5	+10.4	+16.5
4	16,300	18,560	17,900	+13.9	-3.6	+9.8
5	7,070	9,830	9,650	+39.0	-1.8	+36.5
6	1,150	3,950	4,100	+243	+3.8	+257

In 1880, the primary flushing mechanism in zone 6 was tributary streamflow. Powerplant cooling-water circulation at mile 36, ship-channel construction, and shoreline filling expected through 1985 will cause tide-induced flushing increases of more than 250 percent. Streamflow, however, remains the dominant flushing mechanism computed for 1972 and 1985 levels of development in zone 6. In zone 5, streamflow and tide-induced circulation produce about equal rates of flushing for the example constituent. Computations indicate that powerplant cooling-water circulation and other physical changes will produce an overall increase in tide-induced flushing of about 36 percent by 1985 in zone 5.

A computed 14 percent increase in tide-induced flushing between 1880 and 1972 in zone 4 is difficult to comprehend because computed tide-induced circulation decreased by about 8 percent in the zone during the same period (table 14). The cause for this condition is apparently linked to increases in circulation in zone 5, and possibly zone 7, between 1880 and 1972. Tide-induced flushing is determined both by circulation and the distribution of constituent carried by the circulating water. It is likely, therefore, that the amounts of constituent material flushed into zone 4 from zones 5 and 7 caused significantly different constituent distributions in 1972 and 1880. The computed 1972 distribution was apparently sufficient to more than offset the reduced 1972 circulation. A 4 percent reduction in tide-induced flushing occurred in zone 4 between 1972 and 1985.

Average tide-induced flushing changes in zones 1, 2, and 3 are generally consistent with circulation changes (table 14). An overall decrease of less than 1 percent occurred in zone 1, an increase of about 41 percent for zone 2, and an increase of about 16 percent in zone 3. For the example constituent distribution, a flushing minimum occurs in zone 2 (fig. 61 and table 19), whereas a circulation minimum was found in zone 3 (fig. 44 and table 14).

This analysis shows that changes to Tampa Bay since 1880 have increased tide-induced flushing of a constituent that has a concentration distribution similar to that shown in figure 23. Most increases were caused by physical changes in the bay between 1880 and 1972. Assuming streamflow and upland source constituent inflow remain constant, greater flushing will cause lower concentration levels throughout the bay. Greater flushing also will cause a rise in concentration levels of constituents that have seaward sources.

SUMMARY

Changes in two-dimensional tidal flow, circulation, and flushing caused by dredge and fill construction in Tampa Bay are determined in this study using finite-difference computer simulation techniques. Three levels of development were chosen for comparison.

1. Conditions in 1880 prior to any significant manmade physical changes to the bay;
2. Conditions in 1972 after construction of numerous causeways, islands, shoreline fills, and a series of ship channels serving the Port of Tampa; and
3. Conditions projected for 1985 after completion of a Federal dredging project that requires excavation and deposition of about 70 million yd^3 of material.

Physical changes to Tampa Bay since 1880 have caused a progressive reduction in the quantity of water that enters and leaves the bay. Flow reductions that averaged about 5 percent from 1880 to 1972 and 1 percent from 1972 to 1985 are a result of reductions in intertidal water volume, or tidal prism, caused by filling of the bay. Hillsborough Bay has had the largest changes in tidal flows. Flow reductions in Hillsborough Bay were computed to be about 8 percent from 1880 to 1972 and about 6 percent from 1972 to 1985. Hillsborough Bay also had the largest percentage reduction in tidal prism.

Dredged and filled areas have changed the magnitude and direction of tidal flood and ebb flows in large parts of the bay. Areas near islands, causeways, channels, and shoreline fills have been affected most. Total flood and ebb transport were changed by more than 50 percent over about 58 mi^2 of the bay from 1880 to 1972. Similar changes from 1972 to 1985 were over less than 9 mi^2.

Residual water-transport maps for each development condition show a sequence of about 20 circulatory features, or gyres, that are thought to either control or have a large influence on the long-term interchange of water and constituents both within the bay and within the Gulf of Mexico. The overall circulation patterns in 1880, 1972, and 1985 are visually similar with some areas of obvious differences, mostly at and near areas of physical change. Gyre intensity can be reduced or increased, gyre location can be shifted, new gyres can be created, old gyres can be destroyed, and gyre shape can be distorted by these physical changes.

Areas of residual water-transport change are several times larger than those computed for tidal flood and ebb transport. Changes of more than 50 percent occurred in about 167 mi^2 from 1880 to 1972. About 58 mi^2 was changed by the same amount from 1972 to 1985. Between 1880 and 1972, large residual water-

transport changes occurred throughout most of Hillsborough and Old Tampa Bays due to dredge and fill activity. Another area of large residual change from 1880 to 1972 was in lower Tampa Bay due to residential, causeway, and ship-channel construction. Hillsborough and lower Tampa Bays also had large residual change from 1972 to 1985 as a result of ship-channel and island construction.

Tide-induced circulation was similar for all three levels of development. Circulation ranged from a high of about 45,000 ft^3/s at the entrance to Tampa Bay to about 5,000 ft^3/s in an area between middle and lower Tampa Bays, a zone of apparently constricted circulation. Circulation near the entrances to Hillsborough and Old Tampa Bays was about 8,000 ft^3/s. Circulation decreased to zero at the head of Hillsborough and Old Tampa Bays.

Eight zones have been identified that characterize tide-induced circulation characteristics in Tampa Bay. Three zonal sequences have been described that indicate a general similarity in circulation progression in the three bay subsystems within Tampa Bay. Tide-induced circulation progresses from zones of high circulation, through transition zones, to zones of low circulation.

Tide-induced circulation has increased throughout most of Tampa Bay in response to physical changes made since 1880. The greatest circulation increase, 225 percent, occurred in the upper part of Hillsborough Bay from 1880 to 1972. An additional 15 percent increase was computed for that area from 1972 to 1985. In the zone of circulation constriction, between middle and lower Tampa Bays, increases of 6 and 22 percent occurred from 1880 to 1972 and from 1972 to 1985, respectively. Large localized increases in circulation were caused by pumping for powerplant cooling-water systems. A reduction of about 4 percent in tide-induced circulation occurred near the mouth of Tampa Bay from 1880 to 1972. A reduction of about 6 percent occurred from 1972 to 1985.

Transport and flushing of a representative constituent was investigated in this study. The constituent distribution used in the model approximated that of phosphorus measured in July 1975. Highest concentrations of 1.5 to 2.5 mg/L were in Hillsborough Bay. Concentrations were nearly constant at 0.8 mg/L in Old Tampa Bay and decreased to less than 0.2 mg/L at the entrance to Tampa Bay.

Flood and ebb constituent transport reached maximum values of about 30 lb/s in the upper part of middle Tampa Bay and decreased toward the Gulf and toward the heads of Hillsborough and Old Tampa Bays. Physical changes since 1880 caused reductions in flood and ebb constituent transport, similar to those for flood and ebb water transport, because of reductions in tidal prism by manmade intertidal fills.

Residual constituent-transport maps show gyre features similar to those computed for residual water transport. Vector magnitudes are proportionately larger, however, for those gyres in regions of high constituent concentration and proportionately smaller in regions of low concentration. Areas of computed change in flood, ebb, and residual constituent transport are in all respects very similar to the corresponding changes computed for flood, ebb, and residual water transport.

Constituent flushing from Hillsborough Bay was dominated by inflow from streams for all three development conditions. Total flushing was about 10,000 lb/d. Tide-induced flushing was between 2,000 and 8,000 lb/d, about one to two times that of streamflow flushing, for a large part of middle and lower Tampa Bays. The highest tide-induced flushing, about 24,000 lb/d, occurred in the upper third of middle Tampa Bay.

As with tide-induced circulation, tide-induced constituent flushing increased throughout the bay in response to physical changes that have been made since 1880. The greatest flushing increase, 243 percent, occurred in Hillsborough Bay from 1880 to 1972. A 4-percent increase occurred in Hillsborough Bay from 1972 to 1985. In a zone of apparent flushing constriction in the middle of lower Tampa Bay, tide-induced flushing increased 25 percent from 1880 to 1972 and 13 percent from 1972 to 1985. Large local increases in flushing were caused by pumping for powerplant cooling-water systems.

As a result of increases in tide-induced circulation and flushing due to physical changes to Tampa Bay made since 1880, the bay can now more rapidly transfer waterborne constituents that have landward sources to the Gulf of Mexico. Conversely, the bay can also more rapidly transfer constituents that have their source in the Gulf into the upper parts of the bay.

REFERENCES

April, G. C., Hill, D. O., and Liu, Hua-An, 1975, Hydrodynamic and material transport model for Mobile Bay, Alabama: in Symposium on modeling techniques, Proceedings of the American Society of Civil Engineers Conference, San Francisco, Calif., September 3-5, 1975, p. 764-782.

Beauchamp, C. H., and Spaulding, M. F., 1978, Tidal circulation in coastal seas, in Verification of mathematical and physical models in hydraulic engineering: Proceedings of the American Society of Civil Engineers Specialty Conference, College Park, Md., August 9-11, 1978, p. 518-528.

Buchanan, T. J., and Somers, W. P., 1965, Discharge measurements at gaging stations: U.S. Geological Survey Surface-Water Techniques, Book 1, Chap. 11, 67 p.

Cheng, R. T., and Casulli, Vincenzo, 1982, On Lagrangian residual currents with applications in south San Francisco Bay, California: Water Resources Research, v. 18, no. 6, p. 1652-1662.

Cheng, R. T., and Gartner, J. W., in press, Harmonic analysis of tides and tidal currents in South San Francisco Bay, California: Estuarine, Coastal, and Shelf Science, London, Academic Press.

Dinardi, D. A., 1978, Tampa Bay circulatory survey 1963: National Ocean Survey Oceanographic Circulatory Survey Report No. 2, National Oceanic and Atmospheric Administration, 39 p.

Dronkers, J. J., 1964, Tidal computations: Amsterdam, North Holland Publishing Company, 518 p.

Elder, J. W., 1959, The dispersion of marked fluid in turbulent shear flow: Journal of Fluid Mechanics, v. 5, p. 544-560.

Fischer, H. B., List, J. E., Imberger, Jorg, and Brooks, N. H., 1979, Mixing in inland and coastal waters: New York, Academic Press, 483 p.

Giovannelli, R. F., 1981, Relation between freshwater flow and salinity distributions in the Alafia River, Bullfrog Creek, and Hillsborough Bay, Florida: U.S. Geological Survey Water-Resources Investigations 80-102, 62 p.

Goetz, C. L., and Goodwin, C. R., 1980, Water quality of Tampa Bay, Florida: June 1972-May 1976: U.S. Geological Survey Water-Resources Investigations 80-12, 55 p.

Goodwin, C. R., 1977, Circulation patterns for historical, existing, and proposed channel configurations in Hillsborough Bay, Florida: Proceedings of the 24th International Navigation Congress, subject 4, sec. 4, p. 167-179.

_____ 1980, Preliminary simulated tidal flow and circulation patterns in Hillsborough Bay, Florida: U.S. Geological Survey Open-File Report 80-1021, 25 p.

Goodwin, C. R., and Michaelis, D. M., 1976, Tides in Tampa Bay, Florida: June 1971 to December 1973: U.S. Geological Survey open-file report FL-75004, 338 p.

_____ 1981, Appearance and water quality of turbidity plumes created by dredging in Tampa Bay, Florida: U.S. Geological Survey Open-File Report 81-541, 147 p.

Goodwin, C. R., Rosenshein, J. S., and Michaelis, D. M., 1974, Water quality of Tampa Bay, Florida: dry weather conditions, June 1971: U.S. Geological Survey open-file report FL-74026, 85 p.

Goodwin, C. R., Rosenshein, J. S., and Michaelis, D. M., 1975, Water quality of Tampa Bay, Florida: wet-weather conditions, October 1971: U.S. Geological Survey open-file report FL-75005, 88 p.

Gren, G. G., 1976, Hydraulic dredges, including boosters in Dredging and its environmental effects: Proceedings of the American Society of Civil Engineers Specialty Conference, Mobile, Alabama, January 26-28, 1976, p. 115-124.

Heath, R. C., and Conover, C. S., 1981, Hydrologic almanac of Florida: U.S. Geological Survey Open-File Report 81-11-7, 239 p.

Holley, E. R., 1969, Unified view of diffusion and dispersion: Proceedings of the American Society of Civil Engineers, v. 95, no. HY2, p. 621-631.

Leendertse, J. J., 1970, A water-quality simulation model for well-mixed estuaries and coastal seas: Volume I, Principles of computation: Santa Monica, Calif., The Rand Corporation, RM-6230-RC, 71 p.

_____ 1972, A water-quality simulation model for well-mixed estuaries and coastal seas: Volume IV, Jamaica Bay tidal flows: New York, The New York City Rand Institute, R-1009-NYC, 48 p.

Leendertse, J. J., and Gritton, E. C., 1971, A water-quality simulation model for well-mixed estuaries and coastal seas: Volume II, Computation procedures: New York, The New York City Rand Institute, R-708-NYC, 48 p.

Leendertse, J. J., and Liu, Shiao-Kung, 1974, A water-qualit simulation model for well-mixed estuaries and coastal seas: Volume VI, Simulation observation and state estimation: New York, The New York City Rand Institute, R-1586-NYC, 103 p.

Lewis, R. R., and Whitman, R. L., 198_, A new geographic description of the boundaries and subdivisions of Tampa Bay: Proceedings of the Tampa Bay Area Scientific Information Symposium, 1983, Tampa, Fla. (in press).

Masch, F. D., and Brandes, R. J., 1975, Simulation of tidal hydrodynamics--Masonboro Inlet, in Symposium on modeling techniques: Proceedings of the American Society of Civil Engineers Conference, San Francisco, Calif., September 3-5, 1975, p. 220-239.

Prandle, David, and Crookshank, N. L., 1974, Numerical model of St. Lawrence River estuary: Journal of the Hydraulics Division, American Society of Civil Engineers, v. 100, no. HY4, p. 517-529.

Reid, R. O., and Bodine, B. R., 1968, Numerical model for storm surges in Galveston Bay: Journal of the Waterways and Harbors Division, American Society of Civil Engineers, v. 94, no. WWI, p. 33-57.

Rosenshein, J. S., Goodwin, C. R., and Jurado, Antonio, 1977, Bottom configuration and environment of Tampa Bay: Photogrammetric Engineering and Remote Sensing, v. 43, no. 6, p. 693-699.

Ross, B. E., 1973, The hydrology and flushing of the bays, estuaries, and nearshore areas of the eastern Gulf of Mexico, in A summary of knowledge of the eastern Gulf of Mexico: St. Petersburg, Fla., Florida Institute of Oceanography, p. IID-1 to IID-45.

Ross, B. E., and Anderson, M. W., 1972, Courtney-Campbell Causeway tidal flushing study: Report to the Florida Department of Transportation, Tampa Bay Regional Planning Council, St. Petersburg, Fla., 16 p.

Saloman, C. H., Finucane, J. H., and Kelly, J. A., Jr., 1964, Hydrographic observations of Tampa Bay, Florida, and adjacent waters, August 1961 through December 1962: U.S. Fish and Wildlife Service, Bureau of Commercial Fisheries Data Report 4, 112 p.

Schaffranek, R. W., and Baltzer, R. A., 1975, Compiling bathymetry for flow simulation models, in Symposium on modeling techniques: Proceedings of the American Society of Civil Engineers Conference, San Francisco, Calif., September 3-5, 1975, p. 1329-1346.

Thompson, R. B., ed., 1980, Florida statistical abstract: Gainesville, The University Presses of Florida, 695 p.

U.S. Department of Commerce, 1951, Tidal current charts--Tampa Bay: Coast and Geodetic Survey, 12 p.

_____ 1971, Tide tables 1972--high and low water predictions--east coast of North and South America including Greenland: National Oceanic and Atmospheric Administration, National Ocean Service, 290 p.

_____ 1982a, Tide tables 1983--High and low water predictions--east coast of North and South America including Greenland: National Oceanic and Atmospheric Administration, National Ocean Service, 285 p.

_____ 1982b, Tidal current tables 1983--Atlantic Coast of North America: National Oceanic and Atmospheric Administration, National Ocean Service, 234 p.

U.S. Department of the Interior, 1969, Problems and management of water quality in Hillsborough Bay, Florida: Federal Water Pollution Control Administration, 88 p.

U.S. Geological Survey, 1977, Water resources data for Florida, water year 1976: U.S. Geological Survey Water-Data Report FL-76-3, v. 3, Southwest Florida, 1,070 p.

Van der Ree, W. J., Voogt, J., and Leendertse, J. J., 1978, A tidal survey for a model of an offshore area, in Proceedings of the Sixteenth Coastal Engineering Conference: New York, American Society of Civil Engineers, ___ p.

Wang, J. D., 1978, Verification of finite element hydrodynamic model cafe, in Verification of mathematical and physical models in hydraulic engineering: Proceedings of the American Society of Civil Engineers Specialty Conference, College Park, Md., August 9-11, 1978, p. 500-508.

Woodward-Clyde Consultants, 1979, Egmont Channel, Tampa, Florida tidal height study: Final report contract DACW17-79-C-0020 to U.S. Army Corps of Engineers, Jacksonville, Fla., 17 p.